

**Analysis of Neuronal Diseases**  
**in the Model Organism *Aspergillus nidulans***

Dissertation  
zur Erlangung des Doktorgrades der  
Mathematisch-Naturwissenschaftlichen Fakultäten  
der Georg-August-Universität zu Göttingen

vorgelegt von  
Karen Laubinger  
aus Rendsburg

Göttingen 2008

Die vorliegende Arbeit wurde in der Arbeitsgruppe von Prof. Dr. Gerhard H. Braus in der Abteilung Molekulare Mikrobiologie und Genetik des Instituts für Mikrobiologie und Genetik der Georg-August-Universität Göttingen angefertigt.

Teile dieser Arbeit wurden veröffentlicht in:

Helmstaedt, K., Laubinger, K., Vosskuhl, K., Bayram, Ö., Busch, S., Hoppert, M., Valerius, O., Seiler, S., and Braus, G.H. (2008) The nuclear migration protein NUDF/LIS1 forms a complex with NUDC and BNFA at spindle pole bodies. *Eukaryot Cell* 7: 1041-1052.

Laubinger, K., Helmstaedt., K., Harting, R., Fichtner, L., and Braus, G.H. Sumoylation in *Aspergillus nidulans* prevents degradation and aggregation of the human protein  $\alpha$ -synuclein. Manuscript in preparation.

D7

Referent: Prof. Dr. Gerhard H. Braus

Korreferentin: Prof. Dr. Stefanie Pöggeler

Tag der mündlichen Prüfung:

Für meinen Ehemann, meine  
Mutter und meine Schwestern

## Acknowledgements

First of all I would like to thank Prof. Dr. Gerhard Braus for giving me the opportunity to conduct this research study in his department. I highly appreciate his time, his advice and direction, the optimal working conditions and his support to participate in national and international conferences.

Furthermore, I would like to thank Prof. Dr. Stefanie Pöggeler for being the co-referent of this thesis.

I am very grateful to Dr. Kerstin Helmstaedt for her support, her time for open discussions of scientific questions and her assistance to find my way through the different topics of this thesis.

I also wish to thank Gaby Heinrich for her fantastic technical assistance during the experiments for this work.

Furthermore, I am very thankful for the excellent work of Rebekka Harting during her diploma thesis, the results of which contributed to the outcome of this study.

In addition, I thank Dr. Lars Fichtner for the teamwork with the  $\alpha$ -synuclein project.

I would like to thank PD Dr. Michael Hoppert for his great help with the electron microscopy experiments.

I also wish to thank Prof. Dr. Fred Wouters for providing the  $\alpha$ -synuclein plasmids.

Special thanks go to the present and former members of the *Aspergillus* lab 102: Verena Große, Marc Dumkow, Naimeh Taheri-Talesh, Christian Timpner, Oliver Draht, Anna Bergmann, and Thomas Hartmann. I want to thank them for the great atmosphere in the lab and for the support through all this time. In this context, special thanks go to Dr. Christoph Sasse, who accompanied me through the study of biology, the diploma thesis, and the Ph.D. thesis, for his great assistance and support. Furthermore, I would like to thank PD Dr. Sven Krappmann for providing plasmids and his support in experimental questions. In this regard, I wish to thank Dr. Özgür Bayram for the retrieval of plasmids and primers.

I would like to thank all other present and former members of the group for the extraordinary helpfulness and the great working atmosphere through all these years.

Furthermore, I thank all my friends for their support.

I also wish to thank my godfather Jan Martens and his companion Gudrun Hinrichs for their help during my diploma thesis and the Ph.D. thesis.

My deepest thanks go to my husband Rudolf, who always encouraged and strengthened me with his advice and his love.

Sincere thanks are given to my mother as well as to my sisters and their families for their guidance and support.

# Table of contents

<b>Acknowledgements</b> .....	<b>I</b>
<b>Table of contents</b> .....	<b>III</b>
<b>Abbreviations</b> .....	<b>VII</b>
<b>Summary</b> .....	<b>XI</b>
<b>Zusammenfassung</b> .....	<b>XIII</b>
<b>1 Introduction</b> .....	<b>1</b>
1.1 Neuronal diseases .....	1
1.2 Parkinson's disease .....	2
1.2.1 $\alpha$ -synuclein .....	3
1.2.2 $\alpha$ Syn mutants .....	6
1.2.3 Toxicity of $\alpha$ Syn .....	8
1.2.4 Degradation of $\alpha$ Syn .....	9
1.2.5 SUMO and sumoylation of $\alpha$ Syn .....	12
1.2.6 $\alpha$ Syn in model organisms .....	15
1.3 Implication of neuronal and nuclear migration in lissencephaly .....	16
1.3.1 Lissencephaly and neuronal migration .....	16
1.3.2 The LIS1 protein .....	18
1.3.3 Nuclear migration in <i>A. nidulans</i> .....	19
1.3.4 <i>nud</i> genes in <i>A. nidulans</i> .....	21
1.3.5 NUDF, the regulator of dynein .....	23
1.3.6 The regulator protein NUDC .....	25
1.4 The model organism <i>A. nidulans</i> .....	26
1.4.1 Vegetative growth .....	26
1.4.2 The asexual and sexual life cycle .....	28
1.4.3 Regulation of asexual and sexual development .....	30
1.5 Aim of this work .....	32
<b>2 Materials and Methods</b> .....	<b>34</b>
2.1 Growth media and growth conditions .....	34
2.2 Strains, plasmids, and primers .....	35

2.2.1	<i>Escherichia coli</i> strains .....	35
2.2.2	<i>Saccharomyces cerevisiae</i> strains .....	35
2.2.2.1	Plasmid construction for yeast two-hybrid analyses .....	35
2.2.3	Primers and plasmids .....	36
2.2.4	<i>Aspergillus nidulans</i> strains .....	42
2.2.4.1	Plasmid and strain construction for <i>sumO</i> deletion and reconstitution in <i>A. nidulans</i> .....	44
2.2.4.2	Plasmid and strain construction for expression of human $\zeta$ Syn and respective <i>egfp</i> fusion constructs in <i>A. nidulans</i> .....	45
2.2.4.3	Plasmid and strain construction for bimolecular fluorescence complementation experiments with $\zeta$ SynWT and SUMO .....	46
2.2.4.4	Plasmid and strain constructions for NUDC localization experiments....	47
2.3	Genetic manipulations.....	48
2.3.1	Transformation procedures .....	48
2.3.2	Sequence analysis.....	48
2.3.3	Recombinant DNA methods .....	48
2.3.4	DNA isolation and hybridization .....	49
2.4	RNA isolation and hybridization.....	49
2.5	Protein methods.....	50
2.5.1	Protein isolation and analysis.....	50
2.5.2	Yeast two-hybrid analysis .....	51
2.6	Microscopic analysis.....	51
<b>3</b>	<b>Results .....</b>	<b>53</b>
3.1	Deletion of <i>sumO</i> affects asexual and sexual spore production in <i>A. nidulans</i> .....	53
3.1.1	Deletion and reconstitution of the <i>sumO</i> gene in <i>A. nidulans</i> .....	53
3.1.2	Deletion of <i>sumO</i> results in reduced conidiospore production and altered conidiophore morphology in <i>A. nidulans</i> .....	55
3.1.3	The $\Delta$ <i>sumO</i> mutant exhibits higher sensitivity to DNA-damaging agents and oxidative stress .....	57
3.1.4	Sumoylation is essential for ascospore production and normally sized cleistothecia in <i>A. nidulans</i> .....	58

3.1.5	The light-dependent repression of sexual development is impaired in the $\Delta sumO$ strain .....	60
3.2	Expression of human $\zeta$ Syn in <i>A. nidulans</i> with and without an intact <i>sumO</i> gene.....	61
3.2.1	$\zeta$ SynWT is sumoylated <i>in vivo</i> in <i>A. nidulans</i> .....	61
3.2.2	Expression of $\zeta$ Syn in a wild type strain and the $\Delta sumO$ mutant of <i>A. nidulans</i> .....	63
3.2.3	Expression of three copies of $\zeta$ SynA30P in the $\Delta sumO$ mutant leads to a one-third growth reduction in <i>A. nidulans</i> .....	65
3.2.4	Expression of three copies of <i>egfp::</i> $\zeta$ SynA30P in the $\Delta sumO$ mutant confirms growth reduction in <i>A. nidulans</i> .....	67
3.2.5	Sumoylation stabilizes GFP- $\zeta$ SynWT and GFP- $\zeta$ SynA53T in <i>A. nidulans</i> .....	70
3.2.6	Aggregation of GFP- $\zeta$ SynA53T in the $\Delta sumO$ mutant of <i>A. nidulans</i> .....	74
3.3	Localization studies on NUDC in <i>A. nidulans</i> .....	77
3.3.1	NUDC is localized to immobile dots at the cell cortex .....	77
3.3.2	NUDF associates with NUDC at spindle pole bodies and at the cortex.....	78
<b>4</b>	<b>Discussion .....</b>	<b>83</b>
4.1	Deletion of the <i>sumO</i> gene in <i>A. nidulans</i> shows pleiotrophic effects.....	83
4.1.1	SUMO protects cells from DNA-damaging agents and oxidative stress .....	84
4.1.2	Involvement of SUMO in conidiation .....	84
4.1.3	The $\Delta sumO$ mutant displays self-sterility.....	86
4.1.4	Light-dependent development is disturbed in the <i>sumO</i> deletion strain .....	87
4.2	Sumoylation stabilizes $\alpha$ Syn and prevents aggregation in <i>A. nidulans</i> .....	92
4.2.1	Human $\alpha$ Syn is a substrate for sumoylation in <i>A. nidulans</i> .....	92
4.2.2	Growth impairment provoked by higher levels of unsumoylated $\alpha$ SynA30P in <i>A. nidulans</i> .....	93
4.2.3	SUMO conjugation antagonizes degradation of $\zeta$ Syn and mediates solubility of the human protein in <i>A. nidulans</i> .....	94
4.3	NUDC localizes to the cell cortex and to spindle pole bodies in <i>A. nidulans</i> .....	99
4.3.1	Cortical localization of NUDC .....	99
4.3.2	Colocalization of NUDF and NUDC in <i>A. nidulans</i> .....	100

4.4 Outlook.....	102
<b>5 References .....</b>	<b>106</b>
<i>Curriculum vitae</i> .....	<b>127</b>

## Abbreviations

A	.....	alanine
aa	.....	amino acid
<i>amp<sup>R</sup></i>	.....	ampicillin resistance
$\alpha$ Syn	.....	$\alpha$ -synuclein
$\alpha$ Syn $\Delta$ C	.....	C-terminally truncated form of $\alpha$ -synuclein
AD	.....	Alzheimer's disease
BiFC	.....	bimolecular fluorescence complementation
b, bp	.....	base (pairs)
CD	.....	cytoplasmic dynein
CIS	.....	cisplatin
CPT	.....	camptothecin
C-terminus	.....	carboxyterminus
DAPI	.....	4'-6'-Diamino-2'phenylindol
DHC(s)	.....	dynein heavy chain(s)
DIC	.....	differential interference contrast
DIC(s)	.....	dynein intermediate chain(s)
DLC(s)	.....	dynein light chain(s)
DLIC(s)	.....	dynein light intermediate chain(s)
DMSO	.....	dimethyl sulfoxide
DNA	.....	deoxyribonucleic acid
E	.....	glutamic acid
ECL	.....	enhanced chemiluminescence
EDTA	.....	ethylene-diamintetraacetate
Fig.	.....	Figure
GFP	.....	green fluorescent protein
eGFP	.....	enhanced GFP
sGFP	.....	synthetic GFP
IgG	.....	immunoglobuline G
hNUDC	.....	human NUDC
HRP	.....	horseradish peroxidase

ILS	.....	isolated lissencephaly sequency
K	.....	lysine
<i>kan<sup>R</sup></i>	.....	kanamycin resistance
kb	.....	kilobase pairs
kDa	.....	Kilodalton
LB	.....	Lysogeny Broth
MDS	.....	Miller-Dieker syndrome
MENA	.....	menadione
MM	.....	minimal media
MTOC	.....	microtubule organization center
MTs	.....	microtubules
<i>nat<sup>R</sup></i>	.....	nourseothricin resistance
4-NQO	.....	4-nitroquinoline 1-oxide
<i>nud</i>	.....	nuclear distribution
N-terminus	.....	aminotermimus
OD	.....	optical density
ORF	.....	open reading frame
P	.....	proline
PAGE	.....	polyacrylamide gel electrophoresis
PCR	.....	polymerase chain reaction
PIM	.....	protease inhibitor mix
PD	.....	Parkinson's disease
<i>ptrA<sup>R</sup></i>	.....	pyrithiamine resistance
RFP	.....	red fluoescent protein
mRFP	.....	monomeric RFP
RNA	.....	ribonucleic acid
rpm	.....	revolutions per minute
SC	.....	synthetic complete
SDS	.....	sodium dodecyl sulfate
SNpc	.....	substantia nigra pars compacta
SPB	.....	spindle pole body
T	.....	threonine

Tris	.....	tris(hydroxymethyl)aminomethane
UTR	.....	untranslated region
UVA light	.....	ultraviolet A light (black light)
X-Gal	.....	5-bromo-4-chloro-3-indolyl- $\beta$ -D-galactopyranoside
YFP	.....	yellow fluorescent protein
eYFP	.....	enhanced YFP
(C)eYFP	.....	C-terminal half of eYFP
(N)eYFP	.....	N-terminal half of eYFP



## Summary

Neuronal diseases can include abnormal aggregation of key proteins or the dysfunction of transport processes during the development of nerve cells. Parkinson's disease (PD) is a neurodegenerative disorder affecting numerous elderly people, whereas lissencephaly type 1 especially affects children. In PD, the human protein  $\alpha$ -synuclein ( $\alpha$ Syn) can be highly enriched resulting in protein aggregates, whereas lissencephaly affects the migration of neurons in human embryogenesis due to defects in the human *Lis1* gene.

Cells of the filamentous fungal model *Aspergillus nidulans* were used to address unsolved questions concerning both diseases. Wild type  $\alpha$ Syn as well as patient-derived mutant alleles were heterologously expressed in the fungus, but did not affect fungal growth significantly. *sumO*, the gene for the small ubiquitin like modifier SUMO1, was deleted to address the question whether SUMO1 affects  $\alpha$ Syn stability or aggregation. The  $\Delta$ *sumO* mutant (without  $\alpha$ Syn) revealed that sumoylation is essential for sexual ascospore production and normally sized fruit bodies (cleistothecia) in *A. nidulans*. Deletion of *sumO* also resulted in a fungus which is unresponsive to light and exhibits reduced production of asexual spores (conidia) and altered conidiophore morphology. In addition, the  $\Delta$ *sumO* strain exhibited higher sensitivity to DNA-damaging agents and oxidative stress. After heterologous expression it could be shown that  $\alpha$ SynWT is sumoylated *in vivo* in the fungus which had been only shown *in vitro* before. Expression of three copies of the  $\alpha$ SynA30P variant significantly reduced growth of the  $\Delta$ *sumO* mutant. Without sumoylation, the GFP- $\alpha$ SynWT fusion protein is less stable and GFP- $\alpha$ SynA53T forms aggregates. This suggests that in fungal wild type cells sumoylation counteracts the degradation of  $\alpha$ SynWT and prevents the formation of aggregates of  $\alpha$ SynA53T. Furthermore, sumoylation protects the fungus from growth impairment caused by higher levels of  $\alpha$ SynA30P in the  $\Delta$ *sumO* mutant.

Mutations of the *nudF* gene of *A. nidulans*, which is the homolog of human *Lis1*, lead to disturbed nuclear distribution in the fungus. NUDF is regulated by NUDC in a yet not fully understood mechanism. In this study it could be shown that NUDC is present at the cell cortex, in the cytoplasm and at spindle pole bodies of *A. nidulans*. The interaction of

NUDC and NUDF was monitored in the cytoplasm near the cortex and at spindle pole bodies and is mediated by the WD40 domain of NUDF.

## Zusammenfassung

Bei neuronalen Krankheiten kann es zu abnormalen Aggregaten von Schlüsselproteinen oder zur Fehlfunktion von Transportvorgängen während der Entwicklung von Nervenzellen kommen. Während die neurodegenerative Krankheit Parkinson viele ältere Menschen betrifft, leiden insbesondere Kinder unter der Krankheit Lissenzephalie Typ 1. Bei der Parkinson Krankheit kann das menschliche Protein  $\alpha$ -synuclein in hohem Maße angereichert sein, was zur Aggregation desselben führt, wogegen bei Lissenzephalie die Neuronenwanderung durch Mutationen im menschlichen *Lis1*-Gen während der Embryogenese beim Menschen beeinträchtigt ist.

Zellen des filamentösen Pilzmodells *Aspergillus nidulans* wurden verwendet, um sich mit ungelösten Fragen beider Krankheiten zu beschäftigen. Sowohl Wildtyp  $\alpha$ Syn als auch im Patienten gefundene mutierte Allele wurden heterolog im Pilz expremiert, haben das Pilzwachstum aber nicht signifikant beeinflusst. Das den „small ubiquitin like modifier“ SUMO1 kodierende *sumO*-Gen wurde deletiert, um sich mit der Frage zu beschäftigen, ob SUMO1 die Stabilität oder die Aggregation von  $\alpha$ Syn beeinflusst. Die  $\Delta$ *sumO*-Mutante (ohne  $\alpha$ Syn) zeigte, dass Sumoylierung essentiell für die Produktion von sexuellen Ascosporen und normal großen Fruchtkörpern (Kleistothecien) in *A. nidulans* ist. Durch die Deletion von *sumO* wies der Pilz zudem eine fehlende Reaktion auf Licht, eine reduzierte Produktion von asexuellen Sporen (Konidien) sowie veränderte Konidiophorenmorphologie auf. Zusätzlich zeigte der  $\Delta$ *sumO*-Stamm eine stärkere Empfindlichkeit gegenüber DNA-schädigenden Agenzien und oxidativem Stress. Nach der heterologen Expression konnte die Sumoylierung von  $\alpha$ SynWT *in vivo* im Pilz gezeigt werden, was bisher nur *in vitro* gelang. Die Expression von drei Kopien von  *$\alpha$ SynA30P* führte zu einem beträchtlichen Wachstumsrückgang der  $\Delta$ *sumO*-Mutante. Fehlende Sumoylierung führt zu geringerer Stabilität des GFP- $\alpha$ SynWT Fusionsproteins und zu Aggregaten von GFP- $\alpha$ SynA53T. Dies lässt vermuten, dass in Zellen des Wildtyp-Pilzes Sumoylierung der Degradation von  $\alpha$ SynWT entgegenwirkt und die Bildung von  $\alpha$ SynA53T-Aggregaten verhindert. Des Weiteren schützt Sumoylierung den Pilz vor einer

durch gesteigerte Mengen an  $\alpha$ SynA30P in der  $\Delta sumO$ -Mutante hervorgerufenen Wachstumsbeeinträchtigung.

Mutationen im zum menschlichen *Lis1* homologen *nudF*-Gen von *A. nidulans* führt zu gestörter Kernwanderung im Pilz. NUDF wird durch NUDC im Rahmen eines bisher nicht völlig verstandenen Mechanismus reguliert. In dieser Arbeit wurde gezeigt, dass NUDC am Zellkortex, im Cytoplasma und an den Spindelpolen in *A. nidulans* vorhanden ist. Außerdem konnte herausgefunden werden, dass eine Interaktion von NUDC und NUDF durch die WD40-Domäne von NUDF vermittelt wird und im Cytoplasma nahe dem Kortex und an den Spindelpolen stattfindet.

# 1 Introduction

## 1.1 Neuronal diseases

The cerebral cortex in mammals is developed during embryogenesis and consists of six highly structured neuronal layers generated by neurogenesis and neuronal migration. The majority of neurons in the cortex (Fig. 1) are formed by radial glial or neuroepithelial cells (Anthony *et al.*, 2004; Hanashima *et al.*, 2004; Malatesta *et al.*, 2003; Noctor *et al.*, 2001; Rakic, 2003).

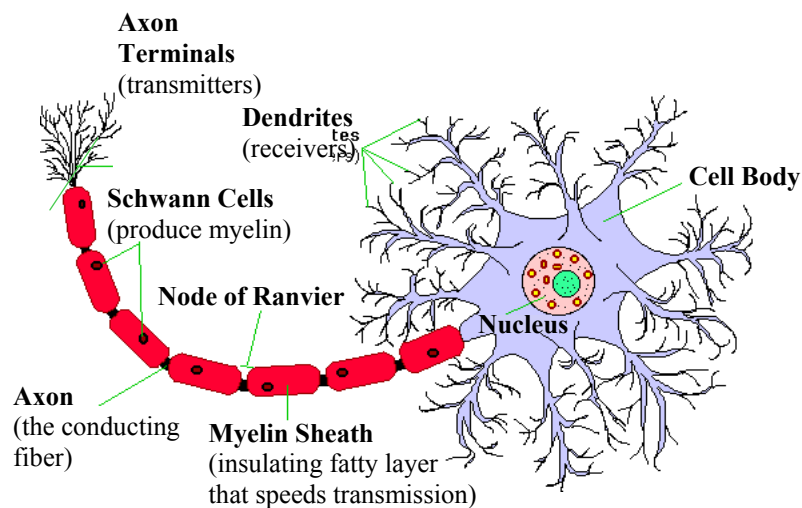


**Fig. 1: The nerve cell (neuron).**

A neuron comprises a cell body with branches of dendrites, which serve as signal receivers and a projection named axon transmitting the nerve signal. The myelin layer generated by Schwann cells surrounds the axons to enhance the speed of transmitted impulses. The gaps formed between myelin sheath cells along axons are termed nodes of Ranvier. The axon terminals transfer the electro-chemical signal to a receiving cell (<http://www.enchantedlearning.com/subjects/anatomy/brain/Neuron.shtml>).

Various physical as well as psychiatric diseases evolve from neuronal dysfunction, which can be due to other neurodevelopmental disorders or the degeneration of neurons. Examples for neurodevelopmental diseases include autosomal-dominant lissencephaly type 1 (Jellinger and Rett, 1976; Stewart *et al.*, 1975), autism (Santangelo and Tsatsanis, 2005),

fragile X syndrome (Castro-Volio and Cuenca-Berger, 2005), schizophrenia (Anckarsäter, 2006) or Rett syndrome (Percy and Lane, 2005). Common impairments like Alzheimer's disease (AD), multiple system atrophy, and Parkinson's disease belong to the group of neurodegenerative diseases (Trojanowski and Lee, 2003).

In this study, proteins implicated in Parkinson's disease and lissencephaly type 1 were analyzed in the model organism *Aspergillus nidulans* to gain insights into the pathology of these impairments on a molecular level.

## **1.2 Parkinson's disease**

The most common movement disorder is Parkinson's disease (PD), which was first described in the essay entitled 'An Essay of the Shaking Palsy' by James Parkinson in 1817. The clinical features of PD include motor impairments like resting tremor, bradykinesia (slowness of movement), rigidity and postural instability as well as non-motoric symptoms involving autonomic, cognitive and psychiatric problems (Goedert, 2001). Neuropathologically, PD is characterized by the loss of dopaminergic neurons in the portion of the midbrain called substantia nigra pars compacta (SNpc) (Fig. 2A) (Forno, 1996). The neurons in this part of the brain produce the pigment neuromelanin, and therefore the SNpc appears as a black stripe in a brain section. Due to the loss of nerve cells, the black colour vanishes in PD cases (Fig. 2B). Along with the loss of nerve cells in the SNpc, a vast neurodegeneration in the central nervous system was observed (Braak *et al.*, 2003).

Furthermore, the presence of intracytoplasmic, proteinaceous inclusions was noted in the SNpc. These were detected in 1912 and termed Lewy bodies and Lewy neurites, which are composed of abnormal filamentous material (Forno, 1996) and are immunoreactive to anti-ubiquitin antibodies (Kuzuhara *et al.*, 1988; Probst-Cousin *et al.*, 1996).

Although the origins of PD remain unclear, it is assumed that pathogenic mutations, environmental factors or a combination of the two are implicated in this pathological progress (reviewed by Thomas and Beal, 2007). The idiopathic form is the most common type of PD, and only less than 10% of PD cases have a familial background. In general, PD affects 1-2% of the world population older than 50 years (reviewed by Thomas and Beal, 2007).

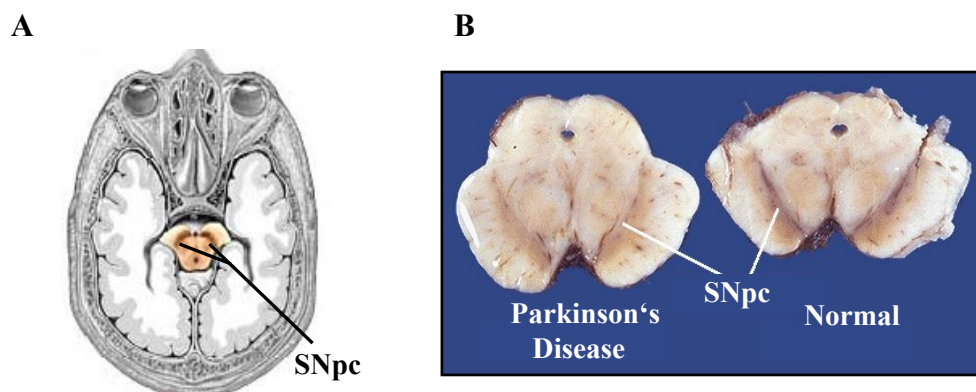


**Fig. 2: The substantia nigra pars compacta.**

(A) The substantia nigra pars compacta (SNpc) is a heterogeneous portion of the midbrain (<http://www.nlm.nih.gov/medlineplus/ency/imagepages/19515.htm>). (B) Due to the loss of neuromelanin-containing dopaminergic neurons, the black colour characteristic for the SNpc disappears in the brains of PD patients (<http://www.gwc.maricopa.edu/class/bio201/parkn/parkn1.jpg>).

### 1.2.1 $\alpha$ -synuclein

A neuropathological hallmark of PD is the presence of inclusion bodies so-called Lewy bodies (LBs), which are large intraneuronal protein aggregates localized near the nucleus (Forno, 1996; Spillantini *et al.*, 1997). In 1997,  $\alpha$ -synuclein ( $\alpha$ Syn) was identified as the main component of LBs in sporadic cases of PD (Tofaris and Spillantini, 2005). Along with PD,  $\alpha$ -synuclein inclusions were identified in other diseases including Multiple System Atrophy, neurodegeneration with brain iron accumulation, Gerstmann-Straussler-Scheinker disease, pure autonomic failure, some cases of Parkinsonism-Dementia complex of Guam, and AD (Arai *et al.*, 2000; Arawaka *et al.*, 1998; Kotzbauer *et al.*, 2001; Lippa *et al.*, 1999; Spillantini *et al.*, 1998a; Tofaris *et al.*, 2007; Wakabayashi *et al.*, 1999; Yamazaki *et al.*, 2000). Neurodegenerative disorders with filamentous aggregates of  $\alpha$ Syn in LBs have been referred to as  $\alpha$ -synucleinopathies.

Human  $\alpha$ Syn is a 140-amino acid (aa) protein with a mass of 17 kDa. The  $\alpha$ Syn gene is homologous to the respective gene in rats and the zebra finch synelfin gene and was first described in the Pacific electric ray *Torpedo californica* (George *et al.*, 1995; Maroteaux and Scheller, 1991; Tofaris and Spillantini, 2005).  $\alpha$ Syn belongs to the synuclein family including  $\beta$ - and  $\gamma$ -synuclein (George *et al.*, 1995; Maroteaux and Scheller, 1991) and is

highly expressed in the brain in comparison to other tissue (Ueda *et al.*, 1993). The synuclein family members belong to a group of proteins referred to as ‘natively unfolded’ due to the fact that such proteins assume no stable tertiary structure and change their conformation during their existence (Lansbury, 1999; Wright and Dyson, 1999). All synucleins have in common that they share a series of imperfect repeats (Fig. 3A) including the amino acid motif KTKEGV in their N-terminus and a variable C-terminal tail. In case of  $\alpha$ Syn, the C-terminal part is highly acidic (Fig. 3A) and is supposed to be involved in protein-protein interactions (Cookson, 2005; Tsigelny *et al.*, 2007).  $\alpha$ Syn has the tendency to bind to lipid membranes mediated by a central hydrophobic region (aa 71-82) (Fig. 3A). This interaction leads to a conformational change of  $\alpha$ Syn by forming two helical domains connected by a short non-helical linker (Fig. 3A, B) (Chandra *et al.*, 2003; Davidson *et al.*, 1998; Kamp and Beyer, 2006; Ulmer *et al.*, 2005). It has been proposed that this conformational change leads to the generation of  $\alpha$ Syn oligomers through the interaction of hydrophobic residues of the  $\alpha$ -helices (Zhu *et al.*, 2003). Furthermore, it was shown that the central hydrophobic region per se causes self-association, thereby enhancing the aggregation of  $\alpha$ Syn (Bodles *et al.*, 2001; Giasson *et al.*, 2001). In contrast, the highly acidic tail of  $\alpha$ Syn was reported to inhibit aggregation (Murray *et al.*, 2003).

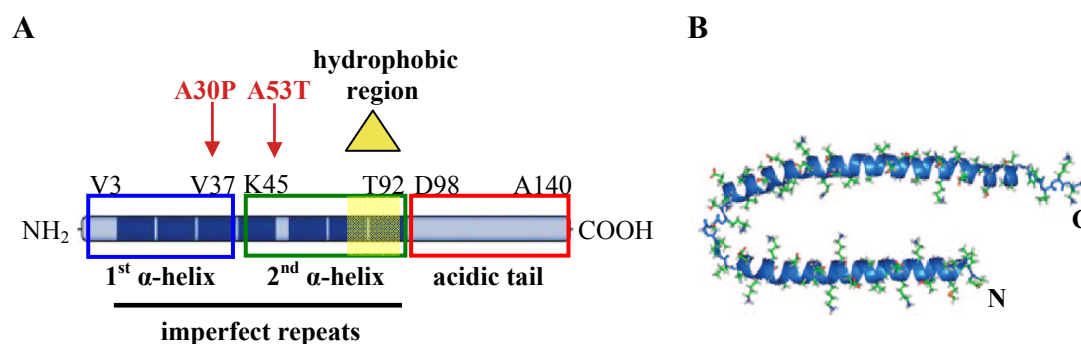


**Fig. 3: Motifs and conformational changes of human  $\alpha$ Syn.**

(A) The  $\alpha$ Syn protein is displayed in its natively unfolded form. The N-terminal part bears the imperfect repeats, which reach to the central hydrophobic region (yellow box, yellow arrowhead). This central region mediates self-aggregation and binding to lipid membranes. The interaction with membranes causes a conformational change of the protein leading to the generation of two  $\alpha$ -helices, illustrated in form of boxes (blue- and green-framed) to show the respective regions in the protein. Furthermore, the acidic C-terminus (red-framed region) and the positions of the two point mutations A30P and A53T involved in familial PD are

shown (modified from Cookson, 2005). (B) The average structure of membrane-bound  $\alpha$ Syn. The unstructured tail has been left out (Ulmer *et al.*, 2005).

$\beta$ Syn lacks part of the hydrophobic region (aa 60-95) that  $\alpha$ Syn bears, which could be an explanation for the diminished ability of  $\beta$ Syn to self aggregate (Hashimoto *et al.*, 2001; Uversky *et al.*, 2002a). Previous studies showed that  $\alpha$ Syn forms homodimers with self-propagating properties that interact with membranes, which allows the incorporation of additional  $\alpha$ Syn molecules resulting in the formation of pore-like structures. The generation of multimeric structures can be avoided by the binding of  $\beta$ Syn to  $\alpha$ Syn aggregates (Tsigelny *et al.*, 2007).

In general, it is assumed that the aggregation pathway of  $\alpha$ Syn starts with the formation of soluble so-called oligomers or protofibrils with  $\alpha$ - and  $\beta$ -sheet conformations, which are a rather unstable species (Fig. 4). This aggregation is promoted by the initial binding to lipid membranes and stabilized by catechols like dopamine.

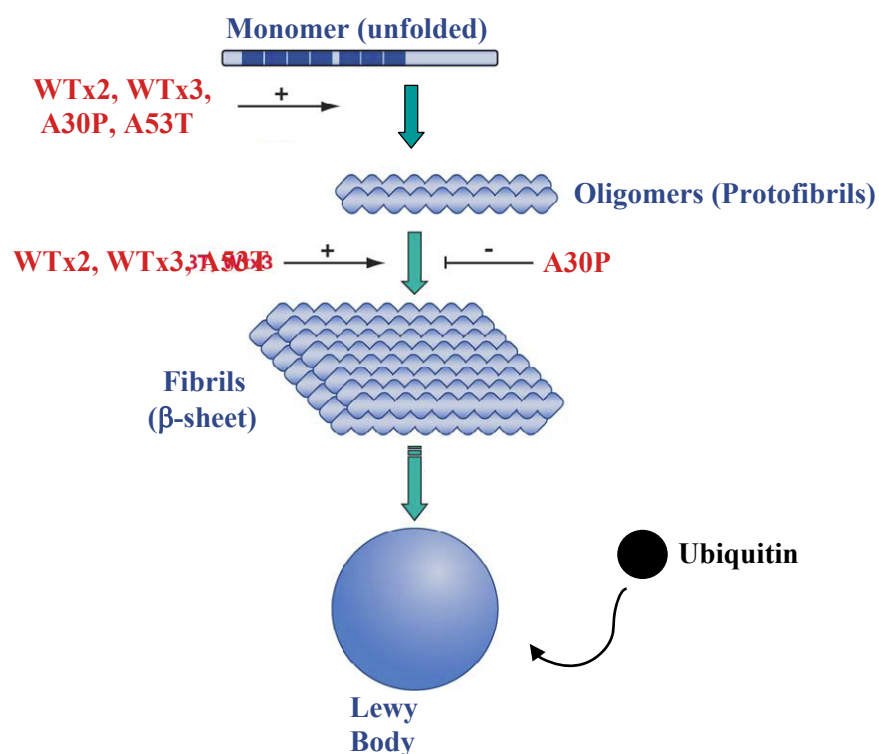


**Fig. 4: Aggregation pathway of  $\alpha$ Syn.**

Natively,  $\alpha$ Syn exists as an unfolded monomer. All mutations promote the accumulation of  $\alpha$ Syn, which begins with the formation of oligomers (protofibrils). This soluble, rather transient species proceeds to aggregate to mature, highly insoluble fibrils stabilized by  $\beta$ -sheet-like interactions. The production of fibrils is not performed by the mutant form  $\alpha$ SynA30P, which is likely due to its Alanin to Proline substitution. Finally, enhanced fibril formation leads to the generation of Lewy bodies, which were found to be ubiquitinated (modified from Cookson, 2005).

It was described that these type of aggregates can form pore-like annular structures, which might damage the membrane (Lashuel *et al.*, 2002; Volles and Lansbury, 2002). However, these oligomers can continue to form highly insoluble mature fibrils, which are stabilized by  $\beta$ -sheet-like interactions. The generation of Lewy bodies is supposed to be a consequence of fibrillation followed by attachment of ubiquitin (Fig. 4) (Conway *et al.*, 2001; Cookson, 2005).

The precise function of the  $\alpha$ Syn protein is still unknown but it has been implicated in several cellular processes. It was reported that  $\alpha$ Syn might be important for synaptic membrane biogenesis processes at the presynaptic terminals since the  $\alpha$ Syn levels resemble those of other proteins involved in synaptogenesis and development (Hsu *et al.*, 1998; Jenco *et al.*, 1998).

Furthermore, a neuroprotective role of  $\alpha$ Syn has been proposed as overexpression of wild type  $\alpha$ Syn ( $\alpha$ SynWT) led to the protection of neuronal cells from apoptotic stimuli (da Costa *et al.*, 2000).

### 1.2.2 $\alpha$ Syn mutants

The involvement of  $\alpha$ Syn in neurodegenerative diseases is based on two observations: the discovery that autosomal-dominant mutations and gene duplication as well as triplication are implicated in rare familial cases of PD and that  $\alpha$ Syn is the main component of LBs in idiopathic forms of PD (Spillantini *et al.*, 1997; Spillantini *et al.*, 1998b).

The first  $\alpha$ Syn point mutation (A53T) was discovered in an Italian and Greek kinship implicated in early-onset PD (Polymeropoulos *et al.*, 1997). Interestingly, this amino acid substitution is part of the natural  $\alpha$ Syn sequence of rodents and zebra finch (Hamilton, 2004). Subsequently, more mutations were identified: A30P in a German familial case of PD (Krüger *et al.*, 1998), E46K in a Spanish kindred (Zarranz *et al.*, 2004), and triplication of  $\alpha$ SynWT in a large family from Iowa (Singleton *et al.*, 2003). Furthermore, the duplication of the wild type locus was found to cause familial PD (Chartier-Harlin *et al.*, 2004).

Of all the above listed  $\alpha$ Syn variants, the wild type protein as well as the mutant forms A30P and A53T have been studied most intensively. All three  $\alpha$ Syn forms WT, A30P and A53T have the ability to form protofibrils (Fig. 4) whereby this initial aggregation is elevated for the  $\alpha$ SynA53T mutant compared to  $\alpha$ SynWT and A30P. A slight acceleration was also observed for  $\alpha$ SynA30P in comparison to the  $\alpha$ SynWT monomer suggesting that the increase in fibril generation is a shared property of both mutations (Conway *et al.*, 2000a).

The subsequent formation of insoluble mature fibrils is promoted by  $\alpha$ SynWT and A53T, but not by  $\alpha$ SynA30P (Fig. 4), which therefore increases the generation of oligomers. Furthermore,  $\alpha$ SynA30P disfavours the binding to membranes like brain vesicles accomplished by  $\alpha$ SynWT and A53T, thereby enhancing the availability of the protein for aberrant interactions and neuropathology causing some forms of familial PD (Conway *et al.*, 2000b; Giasson *et al.*, 1999). Except for mice overexpressing  $\alpha$ SynA30P, where intracellular inclusions have been reported (Frasier *et al.*, 2005), the inability of  $\alpha$ SynA30P to form mature fibrils, is likely due to the substitution of alanine to proline, which disfavours the  $\beta$ -sheet structure stabilizing the insoluble aggregates, because its Ramachandran angle is not compatible with standard  $\beta$ -sheets (Li *et al.*, 1996).

Since all  $\alpha$ Syn variants are involved in familial or idiopathic cases of PD, it was proposed that the initially produced protofibrils generated by all  $\alpha$ Syn forms, are the toxic species in the pathway of this neurodegenerative disorder. Therefore, it was speculated that the formation of LBs and the attachment of ubiquitin seemed to be a last attempt of the cell to degrade this misfolded and aggregated protein (Lashuel *et al.*, 2002; Tofaris and Spillantini, 2007).

The general properties of  $\alpha$ Syn leading to the damage of neurons, are not specific to the mutant forms, but are a propensity of the wild type protein. Instead, the  $\alpha$ Syn mutants enhance special features of the pathogenic pathway of  $\alpha$ Syn leading to neurodegenerative diseases like PD (Cookson, 2005).

### 1.2.3 Toxicity of $\alpha$ Syn

So far it is still elusive, which factors contribute to the toxicity of  $\alpha$ Syn causing neurodegeneration in PD. Numerous factors including metals, pesticides, mitochondrial dysfunction, oxidative stress, degradation disturbances or posttranslational modification have been linked to  $\alpha$ Syn aggregation (Bence *et al.*, 2001; Betarbet *et al.*, 2000; Di Monte, 2003; Fujiwara *et al.*, 2002; Hodara *et al.*, 2004; Venkatraman *et al.*, 2004).

In this context, it was reported that the overexpression of  $\alpha$ Syn in a murine tumour cell line caused mitochondrial dysfunction (Hsu *et al.*, 2000). Furthermore, it was shown that expression of  $\alpha$ SynA30P, A53T, and C-terminally truncated  $\alpha$ Syn in human cell lines caused enhanced vulnerability to oxidative stress in dopaminergic neurons (Kanda *et al.*, 2000).

The C-terminally truncated form of  $\alpha$ Syn ( $\alpha$ Syn $\Delta$ C) was described to be naturally formed *in vivo* and is enriched in aggregates of human cases with  $\alpha$ Syn lesions (Li *et al.*, 2005b). Given the importance of the highly acidic C-terminal tail of  $\alpha$ Syn which inhibits aggregation, the removal of this part facilitates fibrillation confirmed by the fact that  $\alpha$ Syn $\Delta$ C generates filaments at a faster rate than the full-length protein (Crowther *et al.*, 1998; Murray *et al.*, 2003).

Furthermore, the C-terminal part of  $\alpha$ Syn is of high relevance since several posttranslational modifications are conducted in this region, and thus may influence the propensity of  $\alpha$ Syn to form aggregates.

Accordingly, the hyperphosphorylation of filamentous  $\alpha$ Syn at Ser129 in  $\alpha$ -synucleinopathies was reported and phosphorylation at this residue has been described to enhance fibril formation of  $\alpha$ Syn *in vitro* (Fujiwara *et al.*, 2002; Nishie *et al.*, 2004; Saito *et al.*, 2003; Smith *et al.*, 2005). However, latest reports show that phosphorylation at Ser129 rather inhibits than promotes  $\alpha$ Syn fibril generation *in vitro* (Paleologou *et al.*, 2008).

Additionally, tyrosine nitrated  $\alpha$ Syn forms were found in the majority of LB pathology (Giasson *et al.*, 2000) enhancing fibrillation of the wild type protein (Hodara *et al.*, 2004). Besides, this modification was reported to interfere with the degradation of monomeric  $\alpha$ Syn<sup>WT</sup> (Hodara *et al.*, 2004) leading to partially degraded, C-terminally truncated  $\alpha$ Syn (Liu *et al.*, 2003).

Furthermore, methionine oxidation has been described for  $\alpha$ Syn inhibiting fibrillation proportional to the number of oxidized methionines *in vitro* (Hokenson *et al.*, 2004; Uversky *et al.*, 2002b).

In general, posttranslational modifications, the interaction with other cell components or missense mutations may influence the folding properties and/or the cellular localization of wild type  $\alpha$ Syn. Thereby, the function of  $\alpha$ Syn can be altered or its degeneration might be blocked, which leads to the accumulation of  $\alpha$ Syn and to the generation of toxic species.

#### 1.2.4 Degradation of $\alpha$ Syn

Another pathway implicated in the generation of LBs, is aberrant protein degradation.

As described above,  $\alpha$ Syn adopts different conformational stages and the impairment of degradation in neurons is believed to lead to the generation of toxic aggregates and subsequent LBs (Stefanis *et al.*, 2001; Tanaka *et al.*, 2001; Webb *et al.*, 2003; Wilson *et al.*, 2004).

In earlier studies, it was reported that  $\alpha$ Syn is mainly degraded by the proteasome and by lysosomes (autophagy) (Cuervo *et al.*, 2004; Stefanis *et al.*, 2001; Webb *et al.*, 2003).

Degradation of proteins by the lysosome requires mono-ubiquitination (Tofaris and Spillantini, 2007) and altered species of  $\alpha$ Syn of 22-24 kDa in LB disorders were shown to be preferentially mono- or di-ubiquitinated (Tofaris *et al.*, 2003).

The degradation of  $\alpha$ Syn by the lysosome via chaperone-mediated autophagy (CMA) (Cuervo *et al.*, 2004) requires the recognition of the substrate by a cytosolic chaperone followed by the interaction with a lysosomal-associated membrane protein type 2A (LAMP-2A). This protein represents a CMA receptor at the lysosomal membrane (Cuervo and Dice, 1996; Dice, 2007) (Fig. 5). The mutant forms of  $\alpha$ Syn, A30P and A53T were shown to be poorly degraded by the lysosome.

Latest reports show that only monomers and dimers, but not oligomers, are removed by CMA, and while oxidation and nitration slightly impair procession by this pathway, phosphorylation and exposure to dopamine entirely inhibited protein degradation by CMA (Martinez-Vicente *et al.*, 2008).

Besides CMA,  $\alpha$ Syn can also be degraded by macroautophagy in the lysosomes (Webb *et al.*, 2003), which was reported to be an alternative pathway in case the CMA or the ubiquitin-dependent degradation are impaired (Iwata *et al.*, 2005).

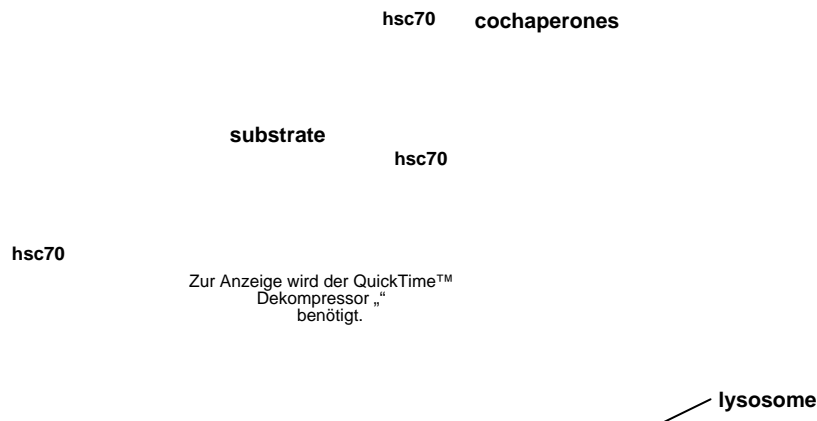


**Fig. 5: A model for chaperone-mediated autophagy (CMA).**

(1) Assisted by cochaperones, the cytosolic chaperone hsc70 binds to the target substrate via recognition of a specific region in the protein. (2) This complex interacts with the lysosomal membrane-associated multisubunit form of the CMA receptor LAMP-2A. (3) The substrate protein is unfolded before crossing the lysosomal membrane. (4) The translocation across the membrane is assisted by the luminal chaperone hsc70 (ly-hsc70). (5) Inside the lysosome, the substrate protein is rapidly degraded by proteases in the lysosomal lumen. (6, 7) The cytosolic chaperone hsc70 is released from the membrane and available for the recognition of further target proteins for CMA (Dice, 2007).

However, Martinez-Vicente *et al.* showed recently that macroautophagy cannot replace CMA under dopamine-induced stress conditions due to increased cellular sensibility to stressors, which leads to apoptosis and cell death (Martinez-Vicente *et al.*, 2008).

Basically, monomeric wild type  $\alpha$ Syn is not ubiquitinated in transfected cells and can therefore be degraded by the 20S proteasome in an ubiquitin-independent way (Tofaris *et al.*, 2001). This pathway is negatively affected by nitration of  $\alpha$ Syn as mentioned above (Hodara *et al.*, 2004).

Along with the removal of  $\alpha$ Syn by lysosomes, degradation in a ubiquitin-dependent way (Fig. 6) was shown through an increase of the  $\alpha$ Syn protein level after cell treatment with the proteasome inhibitor  $\beta$ -lactone (Bennett *et al.*, 1999). Besides, the detection of ubiquitin-immunoreactive LBs in PD cases (Kuzuhara *et al.*, 1988; Probst-Cousin *et al.*, 1996), the ubiquitination of the protein itself was shown *in vivo* (Nonaka *et al.*, 2005).

In general, dysfunction of the ubiquitin-dependent degradation pathway has been directly implicated in familial PD due to the identification of mutations in the E3 ubiquitin ligase parkin (Hattori and Mizuno, 2004; Kitada *et al.*, 1998; Lücking *et al.*, 2000). Parkin was shown to polyubiquitinate O-glycosylated  $\alpha$ Syn, which represents a rare form of the protein (Fig. 6A) (Shimura *et al.*, 2001).

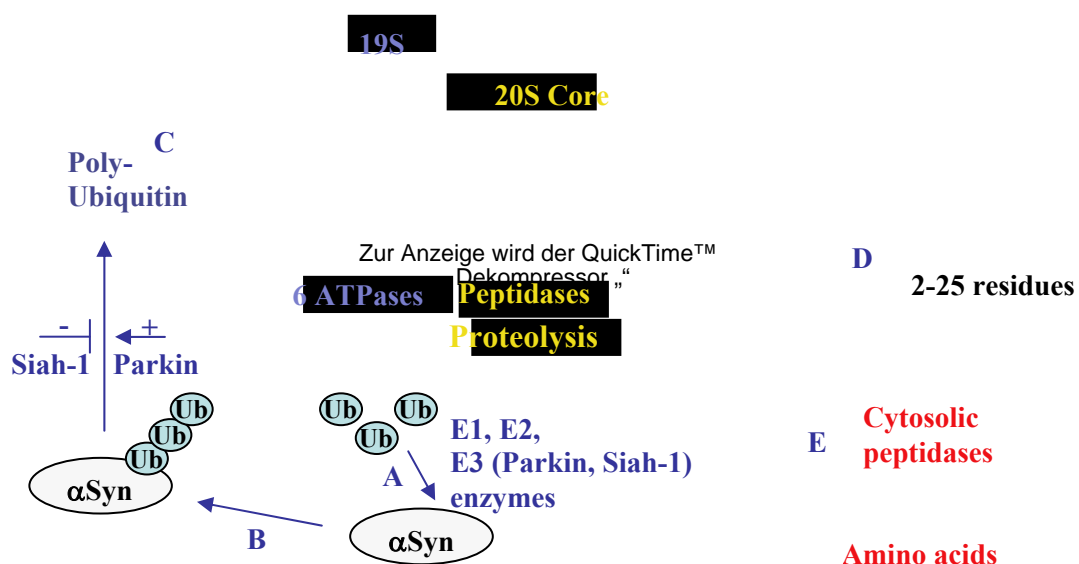


**Fig. 6: The ubiquitin-dependent degradation by the 26S proteasome.**

(A, B) Conjugation of ubiquitin to a target protein like  $\alpha$ Syn requires an enzyme cascade consisting of E1, E2, and E3 enzymes. Two E3 ligases, Parkin and Siah-1 were shown be involved in the ubiquitination of  $\alpha$ Syn, but only Parkin mediates degradation, whereas Siah-1-mediated modification stimulates aggregation. (C) The 26S proteasome associates with the poly-ubiquitin chain, which marks the substrate protein for degradation. ATP is required to unfold and transfer the target proteins from the 19S regulator complex into the 20S core, which represents a multicatalytic proteinase. (D) Once in the 20S proteasome, the substrate is proteolyzed into residues of variable sizes. (E) Cytosolic peptidases proceed degradation into amino acids (modified from Goldberg, 2005).

Recent studies reported that the E3 ubiquitin-protein ligase Siah-1, which is also a component of LBs (Liani *et al.*, 2004), mono- and di-ubiquitinates  $\alpha$ Syn *in vivo*

(Fig. 6A). Along with  $\alpha$ Syn<sup>WT</sup>, A53T was also shown to be modified by Siah-1 but not the mutant form  $\alpha$ Syn<sup>A30P</sup> (Lee *et al.*, 2007). Surprisingly, the Siah-1-mediated modifications of wild type  $\alpha$ Syn and the mutant variant A53T do not mark the proteins for degradation, but promote aggregation and increase toxicity, thus being possibly implicated in PD pathogenesis (Lee *et al.*, 2007).

In addition to ubiquitination,  $\alpha$ Syn was shown to be a target for sumoylation *in vitro* (Dorval and Fraser, 2006; Pountney *et al.*, 2005). Aside from other consequences, sumoylation can effect the lifespan of proteins by counteracting ubiquitination, thus preventing the substrates from degradation (Desterro *et al.*, 1998).

### **1.2.5 SUMO and sumoylation of $\alpha$ Syn**

A protein can be modified by the attachment of numerous small groups like phosphates, methyl groups or sugars, thereby modulating and controlling the protein's function (Bossis and Melchior, 2006a). Another possibility to modify a protein is through the covalent attachment of another, mostly smaller protein (Jentsch and Pyrowolakis, 2000; Schwartz and Hochstrasser, 2003; Welchman *et al.*, 2005). The most prominent representative of the group of small peptidic modifiers is ubiquitin (Glickman and Ciechanover, 2002; Hershko and Ciechanover, 1992; Hicke and Dunn, 2003; Pickart, 2004). Similar proteins are referred to as ubiquitin-related modifiers like SUMO (small ubiquitin-related modifier), NEDD8, ISG15 or FAT10 (Melchior, 2000; Welchman *et al.*, 2005).

Like ubiquitin, SUMO is attached to the target substrates via an enzyme cascade (Fig. 7). In a first step, SUMO needs to be converted from an immature precursor to the mature protein by a C-terminal hydrolase (reviewed by Melchior *et al.*, 2003). After processing, the SUMO protein bears a diglycine motif at its C-terminus necessary for the conjugation to target substrates. Subsequently, the mature protein is activated in an ATP-dependent process by an E1 SUMO-activating enzyme (the heterodimer Aos-Uba2) (Desterro *et al.*, 1999). Once activated, SUMO is transferred to the conjugating enzyme E2 (Ubc9) (Desterro *et al.*, 1997). The final step is the attachment of the small modifier to the target protein. This process is usually facilitated by one of several SUMO E3 ligases (Johnson and Gupta, 2001; Kagey *et al.*, 2003; Kahyo *et al.*, 2001; Pichler *et al.*, 2002), but in some cases the E1 and E2 enzymes are sufficient to conduct sumoylation of target substrates

(Okuma *et al.*, 1999; Rodriguez *et al.*, 1999). The conjugation is achieved by the generation of an isopeptide bond between the C-terminal diglycine of SUMO and the free amino group of a lysine residue on its target substrate.

Sumoylation is a highly dynamic and reversible process and many proteins go through rapid cycles of sumoylation and SUMO deconjugation (reviewed by Melchior *et al.* 2003), conducted by specific isopeptidases belonging to the ubiquitin-like protein-specific protease (Ulp) family in yeast or to the SENP family in mammals (Mukhopadhyay and Dasso, 2007). The C-terminal hydrolases processing newly synthesized SUMO proteins are also members of the SENP/Ulp family.

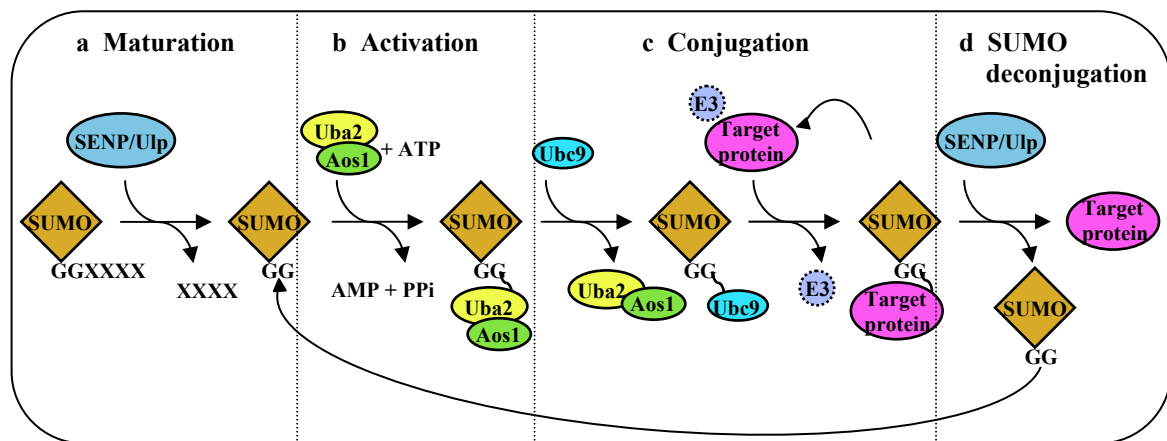


**Fig. 7: The SUMO conjugation and deconjugation pathway.**

(a) The expression of SUMO genes results in immature proteins, which need to be processed by specific proteases (SENP/Ulp) to cleave off C-terminal residues (shown as XXXX). After the removal, two glycine residues (GG) are present at the C-terminus of the SUMO proteins, which are essential for the conjugation to target substrates. (b) The mature SUMO protein is activated in an ATP-dependent step by the E1 activating enzyme Aos1-Uba2, (c) followed by the transfer to the E2 conjugation enzyme Ubc9. The final step is the formation of an isopeptide bond between the two glycine residues of the C-terminus of SUMO and a lysine residue of the target substrate. The conjugation step is usually alleviated by E3 ligases. (d) Sumoylation is a reversible process since proteases of the SENP/Ulp family can rapidly remove SUMO from its target proteins, releasing the modifier and the substrate for further modification cycles (modified from Meulmeester and Melchior, 2008).

In addition to the covalent binding of SUMO, a SUMO-interacting motif (SIM) has been identified, which generally bears a hydrophobic core flanked by acidic amino acid residues. These motifs support low-affinity, non-covalent interactions between proteins lacking a covalent SUMO-binding site and free SUMO. Besides target substrates, SIMs have been identified in the enzymes of the SUMO conjugation cascade and in proteins

implicated in SUMO-dependent repression of gene transcription (Meulmeester and Melchior, 2008).

The sumoylation of proteins can have several consequences for the target substrates depending on their function. In higher eukaryotes it was shown that sumoylation is implicated in signal transduction, transcription regulation, genome stability, DNA repair, or cell cycle progression (Gill, 2004; Johnson, 2004; Verger *et al.*, 2003).

There are three possible ways how SUMO can influence the target proteins. First, the antagonizing mechanism caused by the conjugation of SUMO to the substrate, thereby blocking the access for other putative interaction partners. Second, once conjugated, SUMO could serve as binding interface alleviating the association with other proteins or DNA. At last, SUMO conjugation could affect the target protein's conformation by binding to a second non-covalent SUMO site at the same substrate enhancing for example its activity (Meulmeester and Melchior, 2008).

Several control mechanisms for sumoylation exist. Phosphorylation might act as positive or negative signal for sumoylation while acetylation or ubiquitination can be conducted at the same lysine residue representing examples for competitive modifications (Bossis and Melchior, 2006b).

In the human genome, four SUMO isoforms exist: SUMO1, the twins SUMO2 and SUMO3, and SUMO4 (Marx, 2005). In case of SUMO4, which is highly homologous to SUMO3 (Bohren *et al.*, 2004), it remains unclear if it can associate with other proteins (Meulmeester and Melchior, 2008). Independent of the developmental stages, SUMO1, 2 and 3 are evenly expressed in all tissues, while SUMO4 appears to be restricted to the kidney and the spleen (Bohren *et al.*, 2004; Meulmeester and Melchior, 2008). SUMO1 is predominantly localized at the nuclear membrane (Su and Li, 2002), whereas SUMO2 and SUMO3, whose expression levels are much higher compared to SUMO1 (Saitoh and Hinchey, 2000), are mainly found in the nucleus and in the cytoplasm, respectively (Su and Li, 2002). SUMO2 and SUMO3 are capable of forming SUMO chains by bearing a SUMO consensus motif in their N-terminal part recognized by the SUMO conjugating enzyme E2, whereas SUMO1 lacking such a motif might serve as a capping protein of SUMO2/3 chains (Chung *et al.*, 2004; Tatham *et al.*, 2001; Vertegaal *et al.*, 2004; Zhao *et al.*, 2004).

SUMO is expressed by mainly all eukaryotes like fungi, plants and animals (Meulmeester and Melchior, 2008). Four SUMO proteins were identified in vertebrates, while eight

SUMO genes have been found in *Arabidopsis thaliana* (Bohren *et al.*, 2004; Kurepa *et al.*, 2003; Su and Li, 2002). In contrast, model organisms like *Drosophila melanogaster* (Long and Griffith, 2000), *Caenorhabditis elegans* (Harris *et al.*, 2004), *Saccharomyces cerevisiae* (Giaever *et al.*, 2002; Johnson *et al.*, 1997), *Schizosaccharomyces pombe* (Tanaka *et al.*, 1999) and the filamentous fungus *Aspergillus nidulans* (Wong *et al.*, 2008) possess only one gene, which is similar to the SUMO1 encoding gene in mammals, referred to as *DmSUMO-1*, *SMO-1*, *SMT3*, *pmt3*, and *sumO*, respectively. Accordingly to mammalian SUMO1 (Meulmeester and Melchior, 2008), the sumoylation pathway in *Drosophila* (Long and Griffith, 2000), *C. elegans* (Jones *et al.*, 2002), and *S. cerevisiae* (Giaever *et al.*, 2002; Johnson *et al.*, 1997) is essential. In contrast, *SUMO* deletions mutants of *S. pombe* (*pmt3* $\Delta$ ) (Tanaka *et al.*, 1999) or *A. nidulans* ( $\Delta$ *sumO*) (Wong *et al.*, 2008) are viable.

Sumoylation has also been implicated in neurodegenerative diseases (reviewed by Dorval and Fraser, 2007). It was reported that  $\alpha$ Syn is exclusively monosumoylated by SUMO1 *in vitro*, but the functional consequences remain unclear. The precise modification site could not be clearly identified indicating that more than one recognition site contributes to the sumoylation of  $\alpha$ Syn (Dorval and Fraser, 2006).

### 1.2.6 $\alpha$ Syn in model organisms

Numerous model organisms have been used to study the properties of human  $\alpha$ Syn or the respective mutants. Besides rodent models, the protein was also analyzed in eukaryotic organisms lacking a homologous protein like *D. melanogaster* or *S. cerevisiae*. In *Drosophila*, the phosphorylation of Ser129 of soluble  $\alpha$ Syn was analyzed (Chen and Feany, 2005). Expression and localization studies of  $\alpha$ Syn<sup>WT</sup> and the respective mutant forms A30P and A53T were conducted in *S. cerevisiae*, revealing that more than one copy of  $\alpha$ Syn<sup>WT</sup> or A53T led to toxicity and growth inhibition, whereas  $\alpha$ Syn<sup>A30P</sup> expression showed no significant effect. Furthermore, the localization pattern of the respective GFP fusion constructs was observed, demonstrating cytoplasmic inclusions in case more than one copy of  $\alpha$ Syn<sup>WT</sup> or A53T was expressed. In contrast, the mutant form  $\alpha$ Syn<sup>A30P</sup> was dispersed throughout the cytoplasm (Outeiro and Lindquist, 2003).

The human protein  $\alpha$ Syn has not been analyzed in a filamentous fungus like *A. nidulans* yet. This fungal model represents not only a higher eukaryotic organism compared to *S. cerevisiae*, but was also shown to be a useful tool to gain more insights into the accomplishment of neuronal migration in humans (reviewed by Wynshaw-Boris and Gambello, 2001).

To elucidate the importance of sumoylation for  $\alpha$ Syn, an organism like *A. nidulans* bearing a non-essential SUMO1-like protein would be suitable compared to, e.g., *S. cerevisiae* (Giaever *et al.*, 2002; Johnson *et al.*, 1997) or mice (Meulmeester and Melchior, 2008), in which the deletion of the respective homolog is lethal.

### 1.3 Implication of neuronal and nuclear migration in lissencephaly

#### 1.3.1 Lissencephaly and neuronal migration

The second neuronal disorder for which *A. nidulans* served as a model organism in this thesis was lissencephaly type 1. Lissencephaly (from the Greek “lissos” for smooth and “enkefalos” for brain) is a term describing the smooth surface of the cortex in severe brain developmental diseases characterized by mental deficiency and epilepsy (reviewed by Hatten, 2005; reviewed by Wynshaw-Boris, 2007).



**Fig. 8: Magnetic resonance imaging (MRI) of normal and LIS1 human brain.**

(A) MRI of a normal developed human brain. (B) The image shows the brain of a lissencephaly patient displaying the characteristic features namely reduced gyration of the cerebral surface and enhanced thickness of the cortex (Hatten, 2005).

Furthermore, lissencephaly can be defined as pachygyria meaning a reduction in the number of gyri, which are cortical grooves characteristic for the external cerebral surface and an unusual thickness of these convolutions of the cortex (Fig. 8) (reviewed by Hatten, 2005). Classic lissencephaly disorders include ‘isolated lissencephaly sequency’ (ILS), a disease involved in brain lesion without other major malformations, the Miller-Dieker syndrome (MDS), which is generally more severe than ILS, and X-linked lissencephaly (Dobyns *et al.*, 1991; Lo Nigro *et al.*, 1997; Wynshaw-Boris and Gambello, 2001). Classical features of MDS are craniofacial anomalies (for instance, microcephaly with bitemporal narrowing, a high forehead, and a small nose with anteverted nares) and other deformities (Dobyns *et al.*, 1984). Classic lissencephaly in ILS and MDS patients is characterized by the mislocalization of cortical neurons due to point mutations or deletions of the human *Lis1* gene (reviewed by Wynshaw-Boris, 2007). Normally, neurons migrate from the paraventricular proliferative region to the cerebral cortex (Morris *et al.*, 1998a).

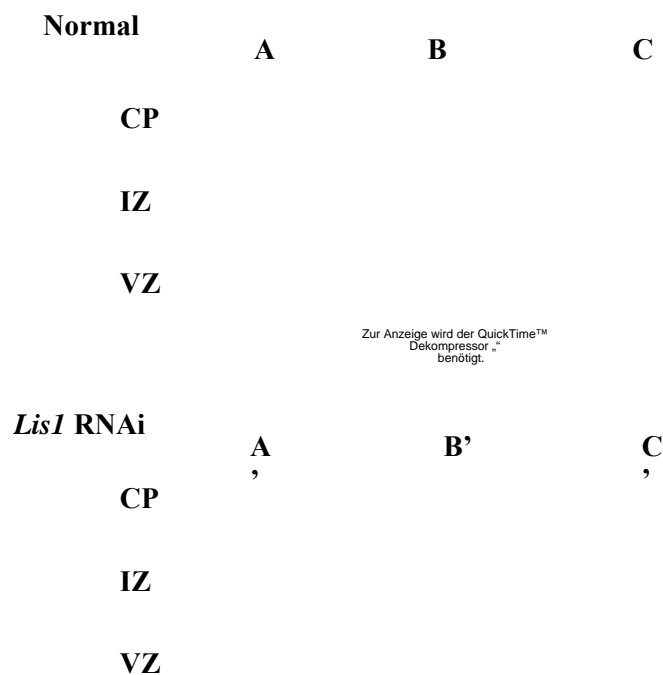


**Fig. 9: Neural progenitor cell morphogenesis and migration in the human fetal neocortex.**

Radial glial cells (yellow) show interkinetic nuclear migration and move to the basis of the ventricular zone to conduct mitosis (A). Young neurons (green) are generated after asymmetric division and migrate to the subventricular zone to remain there as multipolar cells with axonal extensions (B). After transformation into bipolar cells, the neurons migrate along radial glial fibers to the pial surface of the developing cortex (C).

Cells with LIS1 depletion display a block in the interkinetic nuclear oscillation characteristic for neuronal progenitor cells (A'). Additionally, the young neurons exhibit a modified bimolecular morphology and impaired axonal extension (B'). Although the migration of the extensions along the radial glial fibers persists, the movement of the cell soma is inhibited (C'). (VZ) Ventricular zone; (IZ) intermediate zone; (CP) cortical plate (Vallee and Tsai, 2006).

Therefore, neuronal progenitor cells proliferate in the ventricular zone. During migration, cell cycle-dependent nuclear translocation is performed as progenitor cells move back to the basal surface of the ventricular zone for division. Assymetric divisions lead to the generation of neurons, which become bipolar at the subventricular zone and move along glial fibers to the pial surface (Fig. 9A, B, C). Depletion of LIS1 leads to a block of the interkinetic nuclear migration of the progenitor cells and impaired extension of the axon.

Furthermore, the radial migration of the cell soma of the young neurons is inhibited, although the extension of their migratory processes remains unaffected (Fig. 9A', B', C').

The consequences of disturbed neuronal migration are severe as children with ILS or MDS usually die early in childhood (reviewed by Wynshaw-Boris and Gambello 2001; Dobyns *et al.*, 1984).

### **1.3.2 The LIS1 protein**

It was shown that sporadic mutations in the autosomal gene *Lis1* cause type 1 lissencephaly in patients (Reiner *et al.*, 1993). The LIS1 protein is a highly conserved protein with homologs in mouse, *D. melanogaster*, *C. elegans* and fungi (Morris *et al.*, 1998a). LIS1 was shown to be a 45 kD protein with seven WD40 repeats that interacts with microtubules (MTs) (reviewed by Hatten, 2005). In earlier studies it was reported that LIS1 is needed for nuclear movement by tethering the nucleus to the centrosome during neuronal migration (Tanaka *et al.*, 2004). This regulation is believed to be accomplished by the binding of LIS1 to the motor protein dynein thereby controlling its function (reviewed by Wynshaw-Boris, 2007).

The regulation of nuclear migration is a mechanism highly conserved from fungi to mammals (reviewed by Wynshaw-Boris and Gambello, 2001). The *Lis1* homologous *nudF* gene of *A. nidulans* was shown to be involved in the signalling pathway controlling the movement of nuclei involving MTs. The analysis of other mutants impaired in nuclear

migration in *A. nidulans* has led to a better understanding of LIS1-dependent pathways. Numerous proteins have been identified, which are implicated in the nuclear distribution process in *A. nidulans*.

### **1.3.3 Nuclear migration in *A. nidulans***

The process of nuclear motility seems to be required for proper growth and development for all eukaryotes. Nuclear migration is a precisely controlled mechanism and is, for instance, involved in the translocation of nuclei to the egg cortex during embryogenesis in *D. melanogaster* or in the movement of daughter nuclei into the bud in *S. cerevisiae* (reviewed by Morris, 2000).

In the elongated hyphae of filamentous fungi, multiple nuclei are evenly distributed in the cytoplasm and migrate toward the growing tip to achieve regular spacing referred to as nucleokinesis (Oakley and Morris, 1980; Xiang and Morris, 1999). In the filamentous fungus *A. nidulans*, nuclear translocation appears at several developmental stages including vegetative hyphal growth and asexual spore production (reviewed by Xiang and Fischer, 2004). Furthermore, the nucleus-to-cytoplasm ratio is believed to be important for the fungus to achieve relatively high growth rates. Due to the fact that hyphal tips are multinucleate, the cell has several copies of the same gene at one place. This allows the fast supply of material required for growth, which shows the significance of nuclear translocation to the tips of fungal cells (Horio and Oakley, 2005; Horio, 2007).

The precise mechanism of nuclear migration in *A. nidulans* has not been elucidated to date, but it is known that many factors are involved in this process including MTs and the motor protein dynein together with the multisubunit complex dynactin (Fig. 10) (reviewed by Morris, 2000).

In eukaryotic cells, microtubules are hollow tubes composed of 13 protofilaments (reviewed by Xiang and Fischer, 2004). The basic building unit of assembling microtubules is a heterodimer termed tubulin, which consists of two closely related proteins known as  $\alpha$ - and  $\beta$ -tubulin (reviewed by Oakley, 2004). The heterodimers are arranged in a head-to-tail way in a protofilament with  $\beta$ -tubulins at its plus-end and  $\alpha$ -tubulins at its minus-end (Nogales *et al.*, 1999). The respective genes of  $\alpha$ - and  $\beta$ -tubulin in *A. nidulans* are *tubA/tubB* and *benA*, respectively (Kirk and Morris, 1991; reviewed by

Oakley, 2004). In general, MTs emanate from a microtubule organization center (MTOC), which is referred to as spindle pole body (SPB) in *A. nidulans*. SPBs are located in the nuclear envelope and at septa (Veith *et al.*, 2005). A third form of tubulins was found in 1989 termed  $\gamma$ -tubulin encoded by the *mipA* gene in *A. nidulans*, which is predominantly localized at the SPBs. The  $\gamma$ -subunit is needed for the generation of the mitotic spindle and for the nucleation of MT polymerization (reviewed by Oakley, 2004; reviewed by Xiang and Fischer, 2004). Microtubules are dynamic structures as they grow and shrink periodically. The fast growing ends of MTs are termed plus-ends, which face the cell periphery, whereas the slow growing ends at the MTOC are called minus-ends (Adames and Cooper, 2000; reviewed by Xiang and Fischer, 2004; Yeh *et al.*, 2000).

Cytoplasmic dynein (CD) is a minus-end directed microtubule motor present in all eukaryotic cells (Yamamoto and Hiraoka, 2003), which accomplishes the movement along MTs by ATP hydrolysis (Paschal and Vallee, 1987; Vallee *et al.*, 1988). CD is a multisubunit complex with two heavy chains (DHCs), numerous intermediate chains (DICs), four light intermediate chains (DLICs), and several light chains (DLCs) (Fig. 10A) (Bowman *et al.*, 1999; reviewed by Holzbaaur and Vallee, 1994; King *et al.*, 1998).

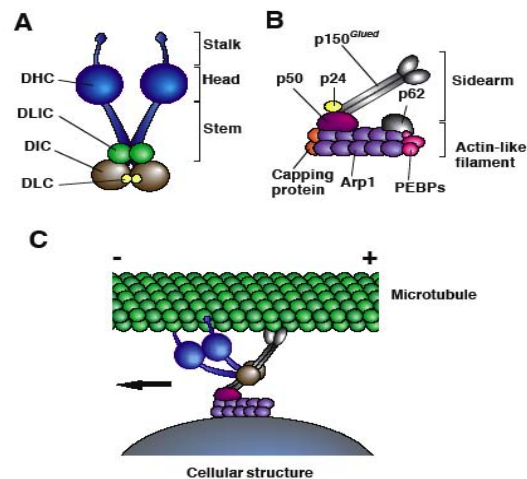


**Fig. 10: Assembly of dynein and dynactin and their association with a microtubule and another cellular structure.**

(A) Dynein organization, displaying only two molecules of DIC, DLIC and DLC. (B) Dynactin assembly. The Capping protein and pointed-end-binding proteins (PEBPs) including p62 are components of the actin-like filament together with the Arp1 polymer. The sidearm is presumably associated with the actin-like filament protein together with a p24 protein through dynamitin (p50). (C) Model for dynein/dynactin interaction with a microtubule and a cellular structure (Holleran *et al.*, 1996; Karki and Holzbaaur, 1995) displaying only DHC, DIC, p150<sup>Glued</sup>, p50 and Arp1. Dynactin is connected to Dynein via interaction of a

middle part of p150<sup>Glued</sup> with DICs. Dynein binds to a microtubule with the tip of the DHC stalk, while dynactin associates with the microtubule at an N-terminal domain of p150<sup>Glued</sup>. An Arp1 filament mediates the interaction of dynein/dynactin with a cellular structure. The minus (-) and (+) ends of the microtubule are indicated as well as the minus-end directed movement (arrow) of the dynein/dynein motor (Yamamoto and Hiraoka, 2003).

The motor protein is implicated in numerous processes like vesicle transport, perinuclear localization of the Golgi apparatus, nuclear positioning, and spindle assembly (reviewed by Hirokawa *et al.*, 1998; reviewed by Karcher *et al.*, 2002; reviewed by Karki and Holzbaur, 1999). The heavy chains represent the motor unit (reviewed by King, 2000), while the other chains are involved in binding of the motor to various cargoes (Fig. 10A, C) (Yamamoto and Hiraoka, 2003). To conduct its function, CD requires dynactin, which represents another multisubunit complex. Dynactin mediates the interaction of CD with membranous cargo and increases the processivity of the motor on MTs (Fig. 10B, C) (Holleran *et al.*, 1998; King and Schroer, 2000; Schroer, 2004).

Dynactin consists of a short, actin-like filament formed by a polymer of the actin-related protein Arp1 and several attached proteins as well as of a projecting sidearm, which comprises of a dimer of p150<sup>Glued</sup>. The sidearm bears special binding sites for MTs, the intermediate chains of CD and Arp1 (Fig. 10B, C) (Eckley *et al.*, 1999; Karki and Holzbaur, 1995; Schafer *et al.*, 1994).

Many genes that encode for the subunits of CD and dynactin have been identified in *A. nidulans* (Table 1) and were shown to be involved in the nuclear migration process. Therefore, these genes have been termed ‘*nud*’ for nuclear distribution (Beckwith *et al.*, 1998; Xiang *et al.*, 1994). In addition, other proteins have been found to be involved in the translocation of nuclei that are not part of the dynein or dynactin complex, but are also well conserved in higher eukaryotes (Yamamoto and Hiraoka, 2003).

### 1.3.4 *nud* genes in *A. nidulans*

It has been shown that the model organism *A. nidulans* is very useful to study the regulation of cytoplasmic dynein (Morris, 1975; Xiang *et al.*, 1994).

In a screen for nuclear migration mutants, several genes were discovered and were shown to be components of the CD/dynactin complex or are involved in its regulation pathway



**Fig. 11: The direct and genetic interactions between NUD proteins.**

Solid green arrows display direct interactions between proteins, while the dashed red arrow shows the genetic interaction between NUDF and NUDC. The orientation of the arrows indicates the supposed direction of the information transfer (modified from Wynshaw-Boris and Gambello, 2001).

Furthermore, the colonies appear brownish due to the lack of coloured asexual spores and their size is decreased in mutant strains (Morris, 1975; Xiang *et al.*, 1994; Xiang *et al.*, 1995a). The dynein components in *A. nidulans* include *nudA* (heavy chain), *nudG* (light chain), and *nudI* (intermediate chain) (Beckwith *et al.*, 1998; Xiang *et al.*, 1994; Zhang *et al.*, 2002a).

The actin-related protein Arp1 and the p150<sup>Glued</sup> subunit, which both participate in the dynactin complex are encoded by *nudK* and *nudM*, respectively (Xiang *et al.*, 1999; Zhang *et al.*, 2003).

Besides, three other proteins have been identified namely NUDC (Osmani *et al.*, 1990), NUDF (Xiang *et al.*, 1995a), and NUDE (Efimov and Morris, 2000), which are not components of the dynein or dynactin complexes.

**1.3.5 NUDF, the regulator of dynein**

NUDF is a protein implicated in nuclear migration in *A. nidulans* through the regulation of cytoplasmic dynein. Originally, the *nudF* gene was identified as a multicopy-suppressor of the temperature-sensitive *nudC3* mutant (Xiang *et al.*, 1995a). It was shown that *nudF* is a homolog to the human *Lis1* gene, the haploinsufficiency of which causes autosomal-dominant lissencephaly type 1. Since NUDF and LIS1 have amino acid identities of 42% (Reiner *et al.*, 1995; Xiang *et al.*, 1995a) it was proposed that neuronal migration and nuclear translocation are related (Morris *et al.*, 1998a). Both proteins have been shown to contain an N-terminal  $\alpha$ -helical LisH (LIS1-homology) dimerization motif, followed by a coiled-coil region, and a C-terminal WD40 domain, which is a  $\beta$ -propeller (Kim *et al.*, 2004; Tarricone *et al.*, 2004). Furthermore, both, NUDF and LIS1 function as a homodimer (Ahn and Morris, 2001; Mateja *et al.*, 2006). First evidence for the regulation of dynein through NUDF was the isolation of dynein heavy-chain mutations as extragenic suppressors of a temperature-sensitive *nudF* mutation (Willins *et al.*, 1997). Along with this observation, it was shown that the *nudF/nudA* double mutant phenotype was

undistinguishable from that of the single mutants, which suggested that NUDA and NUDF belong to the same pathway (Willins *et al.*, 1997). The interaction of NUDF with the ATPase domain of the dynein heavy chain was demonstrated in a yeast two-hybrid assay (Sasaki *et al.*, 2000) and it had been proposed that NUDF is required for the activation of the dynein's retrograde transport (Zhang *et al.*, 2003). This is supported by the fact that NUDA and NUDF colocalize at the MT plus-ends. Mutations in *nudF* or *nudA*, led to a decrease in the depolymerization of MTs indicating that both proteins influence the stability of MTs by their availability at the plus-ends (Han *et al.*, 2001a). In addition, the attachment of MT plus-ends to the cell cortex implicates dynein and NUDF, since NUDF was shown to interact with APSA (anucleate primary stigmata A), a cortical landmark protein. This process is assumed to fix dividing nuclei attached to the MT minus-ends at specific cellular positions (Efimov, 2003; Veith *et al.*, 2005). The colocalization of NUDF and NUDA was additionally observed at the spindle poles, whereby the positioning of NUDA depends on NUDF (Li *et al.*, 2005a).

The colocalization of dynein and NUDF was also observed for LIS1 and dynein, which were found together at the cell cortex, the centrosome, and mitotic kinetochores (Faulkner *et al.*, 2000; Tanaka *et al.*, 2004).

It has been described, that various other *nud* mutants regulate the function of NUDF itself. NUDE is a multicopy suppressor of the *nudF7* temperature-sensitive mutation and has been shown to interact with the NUDF's coiled-coil helix via its own N-terminal coiled-coil domain (Efimov and Morris, 2000). Its C-terminal domain directs NUDE to MT plus ends, but NUDE also forms immobile specks along hyphae suggesting additional cortical functions of NUDE (Efimov *et al.*, 2006). NUDE is also implicated in the neuronal migration pathway since two mammalian homologs, NDE1 and NDEL1, exist in higher eukaryotes that have been demonstrated to interact with LIS1 (Feng *et al.*, 2000; Kitagawa *et al.*, 2000; Niethammer *et al.*, 2000; Sasaki *et al.*, 2000; Sweeney *et al.*, 2001).

It has been shown that NUDF is recruited to MT plus-ends by NUDE and CLIPA, which belongs to the group of plus-end tracking proteins. The mammalian homolog CLIP-170 also regulates MT dynamics and mediates MT capture at cortical sites (Fukata *et al.*, 2002; Komarova *et al.*, 2002).

Another protein described to be implicated in the control of NUDF is NUDC, which was shown to be a putative upstream regulator of NUDF (Fig. 11) (Xiang *et al.*, 1995a).

### 1.3.6 The regulator protein NUDC

The first *nud* gene that was cloned in *A. nidulans* was *nudC*, which encodes a protein of 22 kDa (Osmani *et al.*, 1990). The *nudC* gene is highly conserved with homologs in man (Matsumoto and Ledbetter, 1999), rat (Morris *et al.*, 1997), mouse (Hirotsume *et al.*, 1998), *D. melanogaster* (Cunniff *et al.*, 1997), and *C. elegans* (Dawe *et al.*, 2001). All respective proteins show in their C-terminal halves about 50% identities to NUDC in *A. nidulans*, but possess an additional 15 kDa N-terminal part, which is missing in the filamentous fungus protein (Morris *et al.*, 1998a). The function and intracellular localization of NUDC, which was shown to be an essential protein in *A. nidulans*, are still unknown (Chiu *et al.*, 1997). Besides its role in nuclear migration, NUDC seems to have additional essential functions as *nudC* deletion resulted in the loss of polar growth, abnormal cell walls, and the lysis of cells (Chiu *et al.*, 1997). As stated above the fungal *nudF* gene was identified as an extracopy suppressor of the temperature-sensitive *nudC3* mutation (Xiang *et al.*, 1995a). This mutant shows the typical *nud* phenotype at restrictive temperature with defective nuclear migration defects, irregular shaped conidiophores, impaired production of coloured conidia and reduced colony size (Osmani *et al.*, 1990; Xiang *et al.*, 1995b). Interestingly, whereas the protein concentration of NUDC is unaffected by the *nudC3* mutation a decrease in the level of NUDF was observed, indicating that NUDC acts upstream of NUDF (Xiang *et al.*, 1995a).

Murine NUDC interacts biochemically with LIS1 and copurifies with the dynein heavy and intermediate chains. Similarly, the colocalization of murine NUDC, LIS1, and dynein at MT-organizing centers near the nucleus indicate that NUDC exerts its function at least partly via the regulation of the dynein/LIS1 complex (Morris *et al.*, 1998b). In addition, murine NUDC was found at discrete foci at the cortical cytoskeleton. In different rat cell types, NUDC is localized at the region of the Golgi apparatus (Morris and Yu-Lee, 1998). Human NUDC (hNUDC), is essential for bipolar spindle formation, indicating a function in MT organization at spindle poles (Zhang *et al.*, 2002b). hNUDC is also localized to the kinetochore and regulates MT attachment to chromosomes (Nishino *et al.*, 2006). Besides, hNUDC is a substrate for the polo-like kinase 1 (Plk1) (Nishino *et al.*, 2006). During late mitosis, hNUDC is found at midzone MTs and the midbody in HeLa cells, which

emphasizes its role for cytokinesis (Aumais *et al.*, 2003). Thus, NUDC plays a broad role during mitosis in mammalian cells.

#### **1.4 The model organism *A. nidulans***

Fungi that belong to the genus *Aspergillus* are of significant importance, as this group comprises organisms, which are of industrial, pharmaceutical, pathological, and scientific relevance. In general, *Aspergilli* are a ubiquitous group of filamentous ascomycetes, which consists of at least 186 species. Mostly all species are non-pathogenic and saprophytes, that can be isolated from soil. As a result of the saprophytic life cycle, the fungus is obliged to utilize a wide range of materials as sources of nutrition.

The first published genome sequences from a related filamentous fungus group have been the genomes of *A. nidulans*, *A. fumigatus*, *A. oryzae*, *A. clavatus*, *A. flavus*, *A. niger*, *A. parasiticus*, *A. terreus*, and *Neosartorya fischeri*, which represents a gain for genomic approaches (reviewed by Jones, 2007).

*A. nidulans* is a key model organism for genetics and cell biology first described by Eidam in 1883, but the study of this fungus was started later by the Italian Guido Pontecorvo in 1953. It's genome was sequenced by the Broad Institute and was published by Galagan *et al.* in 2005. The size of the genome is about 31 Mb distributed among eight chromosomes. *A. nidulans* belongs to the group of homothallic (self-fertile) fungi and is a well characterized genetic system, allowing classical genetic analysis.

##### **1.4.1 Vegetative growth**

*A. nidulans* develops vegetatively from a dormant conidiospore or ascospore that contain one or two nuclei, respectively, which are arrested in the G1 phase of the cell cycle (Bergen and Morris, 1983). Prior to the outgrowing germ tube, the spore swells and performs a nuclear division (Harris, 1999). The emerging hypha grows in a polarized manner by apical extension, and therefore cell wall deposition is mainly restricted to the tip region. Along with elongation, nuclear division proceeds in a parasynchronous way (Rosenberger and Kessel, 1967).

Once a hypha has reached a definite length (about 80  $\mu\text{m}$ ), the generation of a septum at its base is provoked by the next nuclear division cycle (Wolkow *et al.*, 1996). Septum

formation is achieved via invagination of the plasma membrane. Inside the septum, a small pore is retained, which allows the passage of organelles, thus cytoplasmic continuity along the entire hypha is achieved.

Subsequent to septation and further rounds of nuclear division, lateral branches are formed and usually the spore produces a secondary germ tube in a bipolar manner (Harris, 2001). The complete network of multinuclear, branched filaments or hyphae is referred to as mycelium. After approximately 18-20 hours of vegetative growth, the fungus has reached developmental competence and has the ability to differentiate either asexually or sexually (Fig. 12) (Axelrod *et al.*, 1973), which depends on the microenvironmental conditions (reviewed by Ugalde, 2006).

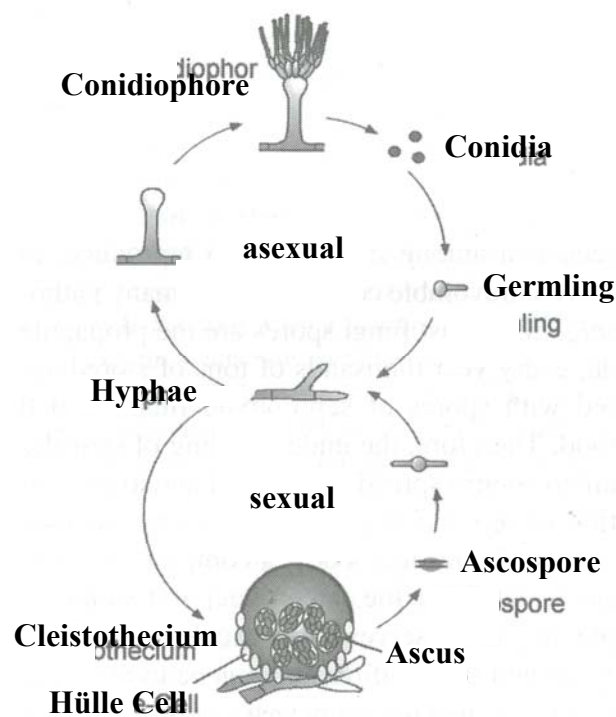


**Fig. 12: Life cycle of *A. nidulans*.**

The germination of conidia leads to the formation of branched hyphae. Competent mycelium can differentiate asexually to form conidiospores or enter the sexual cycle to generate cleistotheceum with red-pigmented ascospores (Fischer, 2002).

### 1.4.2 The asexual and sexual life cycle

The asexual reproduction of *A. nidulans* can be separated into five morphologically distinct stages (Fig. 13) (reviewed by Timberlake, 1990). The development is initiated from a thick-walled hyphal cell, the foot, from which a stalk arises. The stalk grows as an areal hypha (Fig. 13A) until a length of approximately 70  $\mu\text{m}$  is reached and swells terminally to generate the conidiophore vesicle (Fig. 13B). On the vesicle surface, several buds are synchronously formed, which develop to uninuclear cells called primary sterigmata or metulae (Fig. 13C). Subsequently, budding is performed at the distal tips of metulae due to the formation of uninuclear, sporogenous secondary sterigmata called phialides (Fig. 13D). Metulae and phialides are separated by septa, which allow cytoplasmic communication. The first row of isogenic haploid asexual spores develops by constriction from the tips of the phialides. Thereby, the phialide nucleus reaches the neck region and divides mitotically, followed by the translocation of one daughter nucleus into the differentiating conidium, whereas the second nucleus returns to the neck of the phialide. The development of a septum in the phialide neck separates the conidium from the phialide. As a result of repeated nuclear division, long clonal chains of conidia are generated (Fig. 13E) with the youngest conidium near the sterigmatum and the oldest at the tip.

Interestingly, the two gene products required for the characteristic green pigmentation of conidia in *A. nidulans*, *wA* and *yA*, have been shown to be transcribed in the phialide cells and not in differentiated spores. This indicates that the phialides secrete enzymes required for cell wall synthesis, since the gene product of *yA*, conidial laccase, is concentrated in the spore wall (Mayorga and Timberlake, 1990; O'Hara and Timberlake, 1989).

Zur Anzeige wird der QuickTime™  
Dekompressor „  
benötigt.



**Fig. 13: Conidiophore development in *A. nidulans*.**

(A) The thick-walled stalk. (B) Swelling of the stalk tip to the conidiophore vesicle. (C) The buds of initial metulae. (D) Developing phialides indicated by yellow arrowheads. (E) View on the tip of a mature conidiophore with several chains of conidia (modified from Timberlake, 1990).

As a homothallic (self-fertile) ascomycete, *A. nidulans* is capable of performing the sexual cycle without a mating partner and has a sexual stage name: *Emericella nidulans* (Braus *et al.*, 2002; Pontecorvo *et al.*, 1953). The sexual pathway is, amongst other factors, triggered in the absence of light and under low oxygen conditions. In general, sexual development begins subsequent to conidiophore differentiation about 50 h after spore germination. At this time point, two ascogonial hyphae fuse to generate a dikaryon. Growing mycelium that produces a nest-like structure encloses the fused hyphae and develops to multinucleate globose Hülle cells. The species name *nidulans*, which means “nest-former” is derived from these closely packed structures (Pontecorvo *et al.*, 1953). The Hülle or nurse cells, are believed to support the development of the cleistothecia, by providing many tissue-specific proteins (Zonneveld, 1977). Inside the nests, a cleistothecial primordium forms, which later develops into a cleistothecium. The fruit body wall is produced by the surrounding mycelium, which differentiates to generate a network, which is glued by an uncharacterized substance, cleistin, to form the mature envelope. Within the developing cleistothecium, asci formation is initiated with the generation of croiziers. Croiziers, which resemble hook-like structures, are a result of the simultaneous division of two nuclei in a terminal cell of a binuclear ascogenous hypha. Nuclear fusion or karyogamie within the croizier leads to the formation of a diploid zygote about 70-80 h after spore germination. Subsequently, meiosis is conducted generating four nuclei followed by a mitotic division, which results into eight nuclei. Developing membranes depart the nuclei and give rise to eight ascospores. The nuclei undergo another round of mitosis, which leads to the formation of eight mature, binuclear ascospores within the ascus. The red colour of the ascospores is due to a red pigment called asperthecin that is accumulated in the ascus wall during sporogenesis. Generally, mature cleistothecia harbour up to 80.000 viable ascospores (reviewed by Braus *et al.*, 2002; Champe *et al.*, 1994).

### 1.4.3 Regulation of asexual and sexual development

Numerous regulators have been described to control the developmental pathways of *A. nidulans*, of which a few are listed in Fig. 14. One essential factor for the differentiation in asexual or sexual structures is the exposure to an air interphase as cultivation of *A. nidulans* in liquid medium allows only vegetative growth (Axelrod *et al.*, 1973; Skromne *et al.*, 1995). The second main regulator of asexual development is illumination. Light was shown to play a significant role in the development of *A. nidulans* as the exposure is indispensable for conidiation and acts as a negative regulator for fruiting body formation (Mooney and Yager, 1990). In 2005, Blumenstein *et al.* demonstrated that a phytochrome red light receptor encoded by the *fphA* gene led to the induction of asexual sporulation. Furthermore, the photolyase-like CryA was shown to have a regulatory function during light-dependent development in *A. nidulans*, as the sexual development is repressed under UVA light (350-370 nm) (Bayram *et al.*, 2008a). With regard to the light detection, one gene has been identified several year ago, the velvet (*veA*) gene, which is suggested to play a major role in light sensing or transduction (Käfer, 1965). Since mutations in this gene result into light-independent asexual development, the *veA* gene product was defined as negative regulator of asexual development (Champe *et al.*, 1981; Mooney and Yager, 1990; Timberlake, 1990; Yager, 1992).

Another main restrictive factor is the availability of nutrients. As organic nutrients are not evenly distributed in the natural environment of *A. nidulans*, the fungus responds to nutrient fluctuations by inducing, e.g., airborne spore production to colonize new substrates (Bussink and Osmani, 1998; Pöggeler *et al.*, 2006).

For the sexual development of *A. nidulans*, aeration and elevated partial CO<sub>2</sub> pressure are of high significance as well as the absence of light (Braus *et al.*, 2002; Pöggeler *et al.*, 2006). Furthermore, signal transduction pathways have also been discovered for the asexual as well as for sexual life cycle of *A. nidulans* including, e.g., the transcription factors BrlA or AbaA (Fischer, 2002; Timberlake, 1990) for asexual and SteA or NsdD for sexual development (Han *et al.*, 2001b; Vallim *et al.*, 2000).

Besides, proteins involved in the ubiquitin-dependent degradation pathway have been reported to take part in the regulation of the sexual development. The constitutive photomorphogenesis complex 9 (COP9) called COP9 signalosome (CSN), directly associates with E3 ligases (Schwechheimer *et al.*, 2001; Suzuki *et al.*, 2002). The CSN

complex consists of eight subunits, which are highly conserved in higher eukaryotes as well as in the filamentous fungus *A. nidulans* (Busch *et al.*, 2003; Kapelari *et al.*, 2000). Two components, *csnD* and *csnE*, were found to act as regulators of sexual development. The deletion of *csnD* or *csnE* resulted in a developmental arrest at the stage of cleistothecial primordia. Furthermore, the  $\Delta$ *csnD* mutant was shown to be ‘blind’ which means that the sexual cycle was induced independent of light (Busch *et al.*, 2003).

In addition, the F-box protein GrrA was shown to be necessary for ascosporeogenesis in *A. nidulans* (Krappmann *et al.*, 2006). F-box proteins mediate substrate specificity in cullin-ring ubiquitin ligases or more precisely in SKP1, CUL1, F-box (SCF) proteins (reviewed by Cardozo and Pagano, 2004). Whereas deletion of *grrA* did not affect the formation of Hülle cells or cleistothecia, the ascospore generation was completely impaired (Krappmann *et al.*, 2006). A similar phenotype was observed for the *tubB* deletion mutant encoding  $\alpha$ -tubulin (Kirk and Morris, 1991).

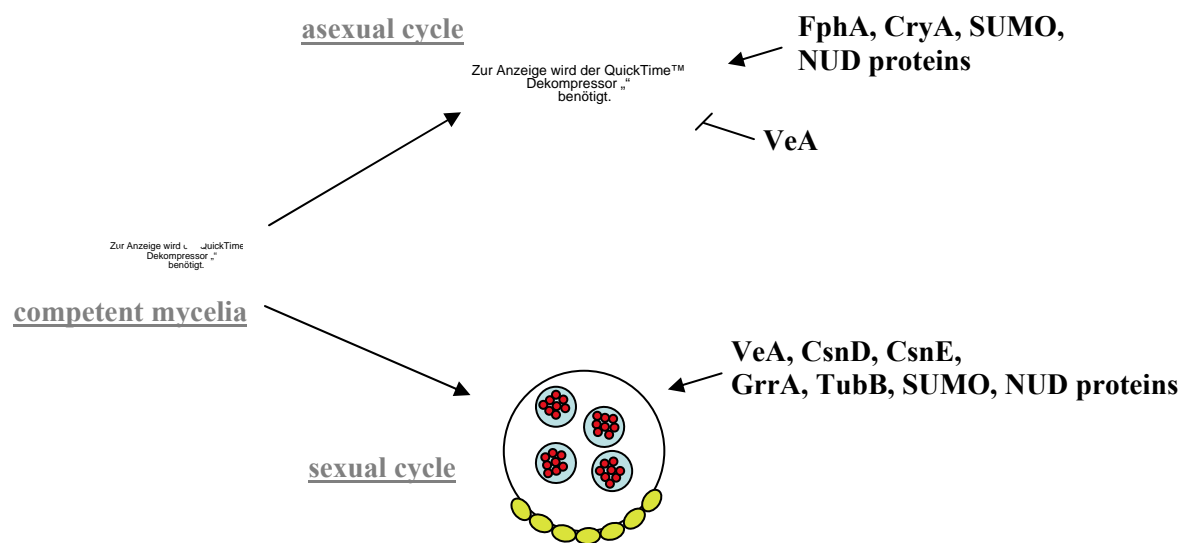


**Fig. 14: Regulators of sexual and asexual development in *A. nidulans*.**

As the mycelium reaches competence, it can differentiate either asexually or sexually dependent on specific conditions and regulators. Regulatory proteins shown to be needed for the accomplishment of the sexual cycle are VeA, CsnD, CsnE, GrrA, TubB, SUMO and NUD proteins. Additionally, VeA, SUMO, and NUD proteins are also implicated in the asexual differentiation as well as FphA and CryA (parts of the model have been adopted from Casselton and Zolan, 2002).

Just recently, deletion of the SUMO1 related gene, *sumO* of *A. nidulans* was described to affect asexual and sexual development (Wong *et al.*, 2008). The  $\Delta$ *sumO* strain revealed a reduced number of conidiospores, but the conidiophore morphology remained unaltered. In the *sumO* deletion strain, the production of Hülle cells was not affected, but the size of cleistothecia was significantly reduced. Furthermore, ascosporeogenesis was completely inhibited. The deletion strain revealed an enhanced sensitivity to DNA-damaging agents. In addition, the SUMO protein was localized in the nuclei during interphase, but as the cells entered mitosis the signal disappeared until telophase. Interestingly, overexpression of the *sumO* gene, which led to a strong increase of sumoylated proteins, did not affect normal growth (Wong *et al.*, 2008).

Another group of proteins was shown to be involved the sexual and asexual cycle. Since both developmental processes require the translocation of nuclei, strains defective in nuclear migration like the *nudF6* mutant display anucleate sterigmata and a reduction in the production of conidia and ascospores (Fischer, 2002; Xiang *et al.*, 1995a).

## **1.5 Aim of this work**

This work focused on two neuronal disorders, Parkinson's disease and lissencephaly type 1 with respect to the two proteins  $\alpha$ -synuclein and NUDC, respectively, which are implicated in the pathogenesis of these disorders.

The very abundant human protein  $\alpha$ Syn as well as the mutant forms, A30P and A53T were shown to be involved in idiopathic and inherited cases of Parkinson's disease (Tofaris and Spillantini, 2005). Protein modifications of  $\alpha$ Syn were reported to be important for the abnormal protein aggregation behaviour of  $\alpha$ Syn characteristic for PD pathogenesis (Hokenson *et al.*, 2004; Nishie *et al.*, 2004). Therefore, one aim of this thesis was to elucidate, whether sumoylation is important for the aggregation and toxicity properties of wild type and mutant  $\alpha$ Syn. In this context, the model organism *A. nidulans* which was lately shown to harbour a single non-essential SUMO1 related gene (Wong *et al.*, 2008), was used to analyze the sumoylation of  $\alpha$ Syn *in vivo*. Thus, a  $\Delta$ *sumO* strain was constructed and phenotypically characterized to express different  $\alpha$ Syn alleles for the purpose of elucidating the importance of this posttranslational modification for  $\alpha$ Syn pathology.

In addition, the nuclear migration protein, NUDC was analyzed in this work. NUDC belongs to a group of proteins with homologs in higher eukaryotes, which are implicated in the neuronal migration at early brain developmental stages (Efimov and Morris, 2000; Osmani *et al.*, 1990). NUDC is the upstream regulator of a second nuclear migration protein NUDF the homolog of which, LIS1 is directly implicated in lissencephaly type 1 (Reiner *et al.*, 1993; Xiang *et al.*, 1995a). Due to the fact that the biochemical function of NUDC is still unknown, the precise mechanism of NUDF regulation remains unclear. In this work, the localization of NUDC was analyzed in *A. nidulans*. Furthermore, the question was addressed whether NUDC interacts with NUDF and where this association takes place to decipher its role in nuclear migration.

## 2 Materials and Methods

### 2.1 Growth media and growth conditions

Chemicals used for the production of buffers, solutions, and media were received from CARL ROTH GMBH & CO KG (Karlsruhe, D), FLUKA (Neu-Olm, D), SIGMA-ALDRICH CHEMIE GMBH (Steinheim, D), INVITROGEN GMBH (Karlsruhe, D), MERCK (Darmstadt, D) and ROCHE GMBH (Mannheim, D).

*Escherichia coli* strains were grown in lysogeny broth (LB) medium (1% bacto-tryptone, 0.5% yeast extract, 1% NaCl) (Bertani, 1951) in the presence of 100 mg/ml ampicillin at 37°C.

*Saccharomyces cerevisiae* strains were grown on selective synthetic complete (SC) medium (0.15% yeast nitrogen base, 0.55% (NH<sub>4</sub>)<sub>2</sub>SO<sub>4</sub>, 0.1% (v/v) 200 mM myo-inositol, 0.2% amino acid mix-4, 2% glucose, 2% agar) lacking tryptophan, uracil, histidine and in case of growth assays also leucine (SC-3, SC-4) at 30°C. When needed, supplements were added according to Guthrie and Fink, 1991.

*Aspergillus nidulans* strains were cultivated in minimal medium (MM, 1% glucose, 2 mM MgSO<sub>4</sub>, 70 mM NaNO<sub>3</sub>, 7 mM KCl, 11.2 mM KH<sub>2</sub>PO<sub>4</sub>, 0.1% trace element solution pH 5.5, 2% agar) (Käfer, 1977), supplemented with the appropriate amounts of pyridoxine-HCl (0.1%), uridine (5 mM), uracil (5 mM), pyrithiamine (100 ng/ml), or nourseothricin (120 mg/l). Vegetative mycelia were obtained from liquid cultures inoculated with 10<sup>6</sup> spores/ml and grown on a rotary shaker for 20 hours at 30°C or 37°C. For developmental induction, an appropriate number of spores was spread on agar plates and asexual development was achieved by incubating the plates in the light. The sexual life cycle was induced under oxygen limiting conditions on tape-sealed plates in the dark (Clutterbuck, 1974). To analyze the vegetative growth behaviour of strains, 2 µl of the respective spore suspension containing 500 spores were spotted onto MM plates in triplicate and the colony size was measured every day over a time period of seven days. To determine the growth rate of the strains, the mean average of the growth span (d) at day three (t<sub>1</sub>=72 h) was subtracted from the respective mean average at day seven (t<sub>2</sub>=168 h). This factor was divided by 96, since this is the difference of hours between 72 h and 168 h and the resulting factor was compared to the corresponding factor of the control strain

$$(\mu=(d_{t_2}-d_{t_1})/(t_2-t_1)).$$

For stress tests, 25  $\mu$ M cisplatin, 50  $\mu$ M camptothecin, 1.3  $\mu$ M 4-nitroquinoline 1-oxide, and 50  $\mu$ M menadione, respectively, were added to MM containing the appropriate supplements and strains were incubated for three days at 37°C. For the quantification of conidiospores of *A. nidulans*, 4 ml of MM with 0.6% agar and about  $1 \times 10^6$  spores was poured on respective solid medium. After 48 h, spores were counted after excision of about 1 cm<sup>2</sup> of the top layer (Busch *et al.*, 2003).

## 2.2 Strains, plasmids, and primers

### 2.2.1 *Escherichia coli* strains

*Escherichia coli* strain DH5a [ $F^-$ ,  $\Phi$ 80 $d$ lacZ $\Delta$ M15,  $\Delta$ (lacZYA-argF), U169, *endA1*, *recA1*, *hsdR17* ( $r_K^-$ ,  $m_K^+$ ), *deoR*, *supE44*,  $\lambda^-$ , *thi-1*, *gyrA96*, *relA1*] (Woodcock *et al.*, 1989) was employed for preparation of plasmid DNA.

### 2.2.2 *Saccharomyces cerevisiae* strains

For two-hybrid experiments, *Saccharomyces cerevisiae* strain EGY48 (*MAT $\alpha$*  *trp1*, *his3*, *ura3*, *lexAops-LEU2*) harbouring pRB1840 (*URA3*, *amp<sup>R</sup>*, *lexAop-lacZ*,  $2\mu$ ) (Golemis *et al.*, 1999b) was used.

#### 2.2.2.1 Plasmid construction for yeast two-hybrid analyses

Plasmids pEG202 and pJG4-5 were used for the expression of open reading frames encoding bait and prey proteins. The complete open reading frame of *nudF* was PCR-amplified from the sexual cDNA library pCNS4 (Krappmann *et al.*, 2006) with specific primers containing flanking *NcoI* and *XhoI* sites and cloned into pEG202 (OLKH146, OLKH147, pME2938). *nudF* was also cloned into pJG4-5 as an *XhoI* fragment (OLKH226, OLKH147, pME3237). The *nudC* open reading frame was amplified using OLKH148 and OLKH149 and cloned into pJG4-5 and pEG202, respectively, as *EcoRI* fragment (pME3245, pME3246). As positive control, the first 585 bp encoding the coiled-coil region of NUDE were PCR-amplified and cloned as *EcoRI/XhoI* fragment into pJG4-5

(OLKH162, OLKH163, pME2939). As negative control, vector pME2938 was used in combination with the empty vector pJG4-5.

For the domain interaction analysis, the LisH motif/coiled-coil region of *nudF* (aa 1-100) was amplified with primers OLKM3 and OLKM15 and cloned into pJG4-5 and pEG202, respectively, via *XhoI* (pME3241, pME3242). The region encoding the WD40 domain of *nudF* (aa 99-445) was amplified using primers OLKM5 and OLKH147 and cloned as *XhoI* fragment into both vectors (pME3243, pME3244). The 5' part of *nudC* encoding amino acids 1-28 was amplified with OLKH148 and OLKM12 and cloned as *EcoRI* fragment (pME3247, pME3248). The region for the p23 domain (aa 29-116) was amplified using OLKM8 and OLKM13 and cloned as *EcoRI* fragment (pME3249, pME3250) and the C-terminal part (aa 117-199) was generated using OLKM10 and OLKM14 and also cloned as *EcoRI* fragment (pME3251, pME3252). The constructs were transformed in different combinations into EGY48 (pRB1840).

### **2.2.3 Primers and plasmids**

The plasmids and oligonucleotides used in this study are listed in Tables 2 and 3, respectively.

**Table 2: Plasmid constructs used in this work.**

Plasmid	Description and characteristics	Reference
---------	---------------------------------	-----------

pBluescript® II KS <sup>+</sup>	general cloning plasmid; <i>amp<sup>R</sup></i>	Stratagene, La Jolla, CA, USA
pBluescript® II SK <sup>+</sup>	general cloning plasmid; <i>amp<sup>R</sup></i>	Stratagene, La Jolla, CA, USA
PCDNA3SYNWT	∫ <i>SynWT</i> ( <i>HindIII/XhoI</i> ) ( <sup>P</sup> CMV, <sup>P</sup> SV40, <i>bla</i> , <i>neo<sup>R</sup></i> )	F. Wouters <sup>a</sup> , Göttingen, D
PCDNA3A30P	∫ <i>SynA30P</i> ( <i>HindIII/XhoI</i> ) ( <sup>P</sup> CMV, <sup>P</sup> SV40, <i>bla</i> , <i>neo<sup>R</sup></i> )	F. Wouters <sup>a</sup> , Göttingen, D
PCDNA3A53T	∫ <i>SynA53T</i> ( <i>HindIII/XhoI</i> ) ( <sup>P</sup> CMV, <sup>P</sup> SV40, <i>bla</i> , <i>neo<sup>R</sup></i> )	F. Wouters <sup>a</sup> , Göttingen, D
PCDNA3GFPSYNWT	<i>egfp::∫SynWT</i> ( <i>HindIII/XhoI</i> ) ( <sup>P</sup> CMV, <sup>P</sup> SV40, <i>bla</i> , <i>neo<sup>R</sup></i> )	F. Wouters <sup>a</sup> , Göttingen, D
PCDNA3GFPA30P	<i>egfp::∫SynA30P</i> ( <i>HindIII/XhoI</i> ) ( <sup>P</sup> CMV, <sup>P</sup> SV40, <i>bla</i> , <i>neo<sup>R</sup></i> )	F. Wouters <sup>a</sup> , Göttingen, D
PCDNA3GFPA53T	<i>egfp::∫SynA53T</i> ( <i>HindIII/XhoI</i> ) ( <sup>P</sup> CMV, <sup>P</sup> SV40, <i>bla</i> , <i>neo<sup>R</sup></i> )	F. Wouters <sup>a</sup> , Göttingen, D
pCR®-BluntII-TOPO®	general cloning plasmid ( <i>kan<sup>R</sup></i> )	Invitrogen, Karlsruhe, D
pEG202	2-hybrid bait vector ( <i>amp<sup>R</sup></i> , <sup>P</sup> <i>ADH::lexA::<sup>t</sup>ADH</i> , <i>HIS3</i> , 2 μm)	(Golemis <i>et al.</i> , 1999a)
pJG4-5	2-hybrid prey vector ( <i>amp<sup>R</sup></i> , <sup>P</sup> <i>GAL1::B42::<sup>t</sup>ADH</i> , <i>TRP1</i> , 2 μm)	(Golemis <i>et al.</i> , 1999a)
pMCB32	general <i>sgfp</i> expression plasmid ( <sup>P</sup> <i>alcA::sgfp</i> , <sup>t</sup> <i>his2B</i> , <i>bla</i> , <i>pyr-4</i> )	(Fernández-Ábalos <i>et al.</i> , 1998)
pMCB17apx	general <i>gfp2-5</i> expression plasmid ( <sup>P</sup> <i>alcA::gfp2-5</i> , <i>bla</i> , <i>pyr-4</i> )	(Efimov <i>et al.</i> , 2006)
pME2822	genomic region of <i>nudF</i> ( <i>BglII/BamHI</i> ) in pBluescript® II SK <sup>+</sup>	(Helmstaedt <i>et al.</i> , 2008)
pME2823	<i>nudC</i> (750 bp) ( <i>KpnI</i> ) in pMCB32	(Helmstaedt <i>et al.</i> , 2008)
pME2938	<i>nudF</i> ORF (1.35 kb) ( <i>NcoI/XhoI</i> ) in pEG202	(Helmstaedt <i>et al.</i> , 2008)
pME2939	585 bp fragment with coiled coil domain of <i>nudE</i> (aa1-195) ( <i>EcoRI/XhoI</i> ) in pJG4-5	(Helmstaedt <i>et al.</i> , 2008)
pME2984	( <i>GA</i> ) <sub>5</sub> :: <i>mrfp::<sup>P</sup>gpdA::nat<sup>R</sup></i> (2176 bp) ( <i>EcoRI/BamHI</i> ) in pBluescript® II SK <sup>+</sup>	(Helmstaedt <i>et al.</i> , 2008)
pME2985	<i>nudC</i> (750 bp) ( <i>KpnI</i> ) in pME3322	(Helmstaedt <i>et al.</i> , 2008)
pME3012	<i>neyfp</i> (462 bp) in pMCB17apx	(Blumenstein <i>et al.</i> , 2005)

Table 2: Plasmid constructs used in this work, continued.

Plasmid	Description and characteristics	Reference
pME3013	<i>ceyfp</i> (258 bp) in pMCB17apx	(Blumenstein <i>et al.</i> , 2005)
pME3024	<i>A. oryzae ptrA</i> resistance gene flanked by <i>SfiI</i> sites in pBluescript® II KS <sup>+</sup>	(Krappmann <i>et al.</i> , 2006)
pME3160	expression module <sup>t</sup> <i>niiA</i> - <sup>P</sup> <i>niiA</i> / <sup>P</sup> <i>niiA</i> D- <sup>t</sup> <i>niiA</i> D- <i>Af pyrG</i> , <i>bla</i>	(Bayram <i>et al.</i> , 2008b)
pME3173	<sup>P</sup> <i>gpdA</i> :: <i>intron</i> :: <i>mrfp</i> :: <i>h2A</i> ( <i>EcoRV</i> ) and <sup>P</sup> <i>gpdA</i> :: <i>nat</i> <sup>R</sup> ( <i>SmaI</i> ) in pBluescript® II KS <sup>+</sup>	(Bayram <i>et al.</i> , 2008b)
pME3237	<i>nudF</i> ORF (1.35 kb) ( <i>XhoI</i> ) in pJG4-5	(Helmstaedt <i>et al.</i> , 2008)
pME3238	<i>nudC</i> :: <i>ceyfp</i> (1059 bp) ( <i>SwaI</i> ) and <i>nudF</i> (1927 bp):: <i>neyfp</i> ( <i>PmeI</i> ) in pME3160	(Helmstaedt <i>et al.</i> , 2008)
pME3241	300 bp fragment with coiled coil domain of NUDF (aa 1-100) ( <i>XhoI</i> ) in pJG4-5	(Helmstaedt <i>et al.</i> , 2008)
pME3242	300 bp fragment with coiled coil domain of NUDF (aa 1-100) ( <i>XhoI</i> ) in pEG202	(Helmstaedt <i>et al.</i> , 2008)
pME3243	1 kb fragment with WD40 domain of NUDF (aa 99-445) ( <i>XhoI</i> ) in pJG4-5	(Helmstaedt <i>et al.</i> , 2008)
pME3244	1 kb fragment with WD40 domain of NUDF (aa 99-445) ( <i>XhoI</i> ) in pEG202	(Helmstaedt <i>et al.</i> , 2008)
pME3245	<i>nudC</i> ORF (596 bp) ( <i>EcoRI</i> ) in pJG4-5	(Helmstaedt <i>et al.</i> , 2008)
pME3246	<i>nudC</i> ORF (596 bp) ( <i>EcoRI</i> ) in pEG202	(Helmstaedt <i>et al.</i> , 2008)
pME3247	87 bp fragment with coiled coil domain of NUDC (aa 1-28) ( <i>EcoRI</i> ) in pJG4-5	(Helmstaedt <i>et al.</i> , 2008)
pME3248	87 bp fragment with coiled coil domain of NUDC (aa 1-28) ( <i>EcoRI</i> ) in pEG202	(Helmstaedt <i>et al.</i> , 2008)
pME3249	264 bp fragment with pp23 domain of NUDC (aa 29-116) ( <i>EcoRI</i> ) in pJG4-5	(Helmstaedt <i>et al.</i> , 2008)
pME3250	264 bp fragment with pp23 domain of NUDC (aa 29-116) ( <i>EcoRI</i> ) in pEG202	(Helmstaedt <i>et al.</i> , 2008)
pME3251	249 bp fragment with C-terminal part of NUDC (aa 117-198) ( <i>EcoRI</i> ) in pJG4-5	(Helmstaedt <i>et al.</i> , 2008)
pME3252	249 bp fragment with C-terminal part of NUDC (aa 117-198) ( <i>EcoRI</i> ) in pEG202	(Helmstaedt <i>et al.</i> , 2008)
pME3313	∇ <i>SynWT</i> ORF (422 bp) ( <i>HindIII/XhoI</i> , Klenow) in pME3321 ( <i>SmaI</i> )	this study
pME3314	∇ <i>SynA53T</i> ORF (422 bp) ( <i>HindIII/XhoI</i> , Klenow) in pME3321 ( <i>SmaI</i> )	this study
pME3315	∇ <i>SynA30P</i> ORF (422 bp) ( <i>HindIII/XhoI</i> , Klenow) in pME3321 ( <i>SmaI</i> )	this study

Table 2: Plasmid constructs used in this work, continued.

Plasmid	Description and characteristics	Reference
pME3316	<i>egfp::SynWT</i> (1152 bp) ( <i>HindIII/XhoI</i> , Klenow) in pME3321 ( <i>SmaI</i> )	this study
pME3317	<i>egfp::SynA53T</i> (1152 bp) ( <i>HindIII/XhoI</i> , Klenow) in pME3321 ( <i>SmaI</i> )	this study
pME3318	<i>egfp::SynA30P</i> (1152 bp) ( <i>HindIII/XhoI</i> , Klenow) in pME3321 ( <i>SmaI</i> )	this study
pME3319	genomic <i>ApaI</i> fragment of <i>sumO</i> (3.3 kb) in pNV1	this study
pME3320	<i>A. oryzae ptrA</i> resistance cassette flanked by 5' and 3' UTRs of <i>sumO</i> (8.0 kb) in pCR®-BluntII-TOPO®	this study
pME3321	General expression plasmid ( <i>P<sub>alcA</sub></i> , <i>his2B</i> , <i>bla</i> , <i>pyr-4</i> )	this study
pME3322	general <i>gfp2-5</i> expression plasmid ( <i>P<sub>alcA</sub>::gfp2-5</i> , <i>bla</i> , <i>pyr-4</i> ) (pMCB17apx derivate)	(Helmstaedt <i>et al.</i> , 2008)
pME3489	<i>ceyfp::sumO</i> (591 bp) ( <i>SwaI</i> ) in pME3160	this study
pME3490	<i>neyfp::SynWT</i> (897 bp)( <i>PmeI</i> ) in pME3489	this study
pNV1	general cloning plasmid carrying nourseothricin ( <i>nat</i> ) resistance cassette ( <i>bla</i> , <i>P<sub>gpdA</sub>::nat<sup>R</sup></i> )	(Seiler <i>et al.</i> , 2006)

a. Kindly provided by Prof. Dr. Fred S. Wouters, □Laboratory for Molecular and Cellular Systems, □Dept. of Neuro- and Sensory Physiology□Centre II, Physiology and Pathophysiology, University of Göttingen, D.

**Table 3: Primers used in this study.**

Primer	Size	Sequence
OLKH115	28mer	5'- AAG GTA CCA TGT CGG AAC AAG AAC CGT C -3'
OLKH116	29mer	5'- AAG GTA CCC CAA TCT TCG CAT TCG AAA AG -3'
OLKH146	31mer	5'- CAT CCA TGG ATG AGC CAA ATA TTG ACA GCT C -3'
OLKH147	30mer	5'- CCC CTC GAG TTA GCT GAA CAC CCG TAC AGA -3'
OLKH148	28mer	5'- CGG AAT TCA TGT CGG AAC AAG AAC CGT C -3'
OLKH149	28mer	5'- CGG AAT TCC TAA CCA ATC TTC GCA TTC G -3'
OLKH162	27mer	5'- CGG AAT TCA TGC CTT CCG CCG ATG AGC -3'
OLKH163	30mer	5'- CCC CTC GAG GTT ATT GTT CCT GAG CCT CTC -3'
OLKH226	29mer	5'- CGC CTC GAG AGC CAA ATA TTG ACA GCT CC -3'
OLKH258	20mer	5'- ATG TCG GAA CAA GAA CCG TC -3'
OLKH259	75mer	5'- GTG GTT CAT GAC CTT CTG TTT CAG GTC GTT CGG GAT CTT GCA GGC CGG GCG ACC AAT CTT CGC ATT CGA AAA GTC -3'
OLKH260	78mer	5'- CGC CCG GCC TGC AAG ATC CCG AAC GAC CTG AAA CAG AAG GTC ATG AAC CAC GCC GAC AAG CAG AAG AAC GGC ATC AAG -3'
OLKH261	36mer	5'- TTA CTT GTA CAG CTC GTC CAT GCC GAG AGT GAT CCC -3'
OLKH262	22mer	5'- ATG AGC CAA ATA TTG ACA GCT C -3'
OLKH263	52mer	5'- CTC CTC GCC CTT GCT CAC CGT GGC GAT GGA GCG GCT GAA CAC CCG TAC AGA G -3'
OLKH264	55mer	5'- CTC TGT ACG GGT GTT CAG CCG CTC CAT CGC CAC GGT GAG CAA GGG CGA GGA GCT G -3'
OLKH265	28mer	5'- TTA GAT ATA GAC GTT GTG GCT GTT GTA G -3'
OLKH301	55mer	5'- GGA ATT CGG AGC TGG TGC AGG CGC TGG AGC CGG TGC CGC CTC CTC CGA GGA CGT C -3'
OLKH302	47mer	5'- ACC GGT CAC TGT ACA GAG CTG CGG CCG CTT AGG CGC CGG TGG AGT GG -3'
OLKH303	47mer	5'- CCA CTC CAC CGG CGC CTA AGC GGC CGC AGC TCT GTA CAG TGA CCG GT -3'
OLKH304	27mer	5'- CGG GAT CCT CAG GGG CAG GGC ATG CTC -3'
OLKH306	19mer	5'- GGA GCT GGT GCA GGC GCT G -3'
OLKH307	19mer	5'- TCA GGG GCA GGG CAT GCT C -3'
OLKH308	20mer	5'- GCA TGA ACG ACC GAT TTC CG -3'
OLKH309	19mer	5'- GCA GAT GTC GTG GTC AAC C -3'
OLKH310	42mer	5'- TCC AGC GCC TGC ACC AGC TCC TAC TCC AAC TTC ATC CTT TCC -3'
OLKH311	42mer	5'- GAG CAT GCC CTG CCC CTG AAT TCA GCC TAG ATA TAA TGT ACC -3'
OLKH312	20mer	5'- CCC AAT CCC CTG GTT GAG AC -3'
OLKH313	23mer	5'- CAT TGA TAG GAA CAG GTG ACT TG -3'
OLKM3	31mer	5'- CCC CTC GAG ATG AGC CAA ATA TTG ACA GCT C -3'
OLKM5	29mer	5'- CCC CTC GAG AAT TGG CTT CCT AAA CCG TC -3'

Table 3: Primers used in this study, continued.

Primer	Size	Sequence
OLKM8	26mer	5'- CGG AAT TCC AGG CGA CCC TCC CCT AC -3'
OLKM10	25mer	5'- CGG AAT TCC AGA TGG AGT GGT GGG C -3'
OLKM12	29mer	5'- CGG AAT TCT TAC TCA GCT TCT TCG GCG GC -3'
OLKM13	33mer	5'- CGG AAT TCT TAG TTG ACT TTG TCA AGG TGG ATG -3'
OLKM14	33mer	5'- CGG AAT TCT TAA CCA ATC TTC GCA TTC GAA AAG -3'
OLKM15	31mer	5'- CCC CTC GAG TTA CCA ATT GGT CGG ATC TTG G -3'
OLKM20	21mer	5'- ATG GAT GTA TTC ATG AAA GGA -3'
OLKM21	21mer	5'- TTA GGC TTC AGG TTC GTA GTC -3'
OLKM31	19mer	5'- CGG TGG CAG ATC TGC GAT G -3'
OLKM32	21mer	5'- GTT GAT TGT TGG TTG ATG ATG -3'
OLKM34	23mer	5'- CAT TTC ATA ATA ATC ACG CAT TC -3'
OLKM35	39mer	5'- TAG GCC TGA GTG GCC TGT TGA AAC TAT TTG GGA GTT ATC -3'
OLKM36	35mer	5'- TAG GCC ATC TAG GCC TCC ACC AGA GTC CGG TTT CC -3'
OLKM37	19mer	5'- CTT TTC TGG CCT CCG AAG G -3'
OLKM42	23mer	5'- CAA TCA AGA ATG AAT TGA CTG AC -3'
OLKM44	29mer	5'- AAA GGG CCC ATC CCT TCA CCA ACT GGT AG -3'
OLKM45	30mer	5'- TTT GGG CCC ACG AGC TAG GTT CAC CAA ATG -3'
OLKM47	29mer	5'- TTT GGT ACC TAG AGA CCA CCG CCG ATT TG -3'
OLKM67	21mer	5'- CCA TAA CCC TAT TGC CAC TAG -3'
OLKM68	24mer	5'- GTA TGG GAT AGG AAA ATA ATA TAG -3'
OLKM86	21mer	5'- ATG GCC GAC AAG CAG AAG AAC -3'
OLKM87	70mer	5'- GTG GTT CAT GAC CTT CTG TTT CAG GTC GTT CGG GAT CTT GCA GGC CGG GCG CTT GTA CAG CTC GTC CAT G -3'
OLKM88	69mer	5'- CGC CCG GCC TGC AAG ATC CCG AAC GAC CTG AAA CAG AAG GTC ATG AAC CAC TCT GAT CCA TCT GCT CCC -3'
OLKM89	21mer	5'- TTA GAG ACC ACC GCC GAT TTG -3'
OLKM91	19mer	5'- ATG GTG AGC AAG GGC GAG G -3'
OLKM92	56mer	5'- GTC CTT TCA TGA ATA CAT CCG TGG CGA TGG AGC GCA TGA TAT AGA CGT TGT GGC TG -3'
OLKM93	60mer	5'- CAG CCA CAA CGT CTA TAT CAT GCG CTC CAT CGC CAC GGA TGT ATT CAT GAA AGG ACT TTC -3'
OLKM94	21mer	5'- TTA GGC TTC AGG TTC GTA GTC -3'

## 2.2.4 *Aspergillus nidulans* strains

The *Aspergillus nidulans* strains used and constructed in this study are listed in Table 4.

**Table 4: *Aspergillus nidulans* strains used in this study.**

Strain	Genotype	Reference
A1149	<i>pyroA4; pyrG89; ΔnkuA::argB</i>	(Nayak <i>et al.</i> , 2006)
A779	<i>nudC3; wA2; nicA2; pabaA1; pyrG89</i>	FGSC (Kansas City, MO, USA)
UI224	<i>pyrG89; yA2; argB2</i>	FGSC (Kansas City, MO, USA)
XX20	<i>nudF6; pyrG89</i>	(Xiang <i>et al.</i> , 1995a)
AGB152	<i>pyroA4; pyrG89</i>	(Busch <i>et al.</i> , 2003)
AGB190	<i>pyroA4 pyrG89/pyr-4<sup>P</sup>alcA::sgfp::<sup>t</sup>his2B</i>	(Busch <i>et al.</i> , 2007)
AGB241	<i>pabaA1; nicA2; wA2; pyrG89/pyr-4; nudC3; <sup>P</sup>alcA::nudC::sgfp</i>	(Helmstaedt <i>et al.</i> , 2008)
AGB302	<i>pabaA1; nicA2; wA2; pyrG89/Afp<sub>pyrG</sub>; nudC3; <sup>P</sup>niiA::nudF::neyfp; <sup>P</sup>niaD::nudC::ceyfp</i>	(Helmstaedt <i>et al.</i> , 2008)
AGB303	<i>pyrG89/Afp<sub>pyrG</sub>; nudF6; <sup>P</sup>gpdA::nat<sup>R</sup>; <sup>P</sup>niiA::nudF::neyfp; <sup>P</sup>niaD::nudC::ceyfp; <sup>P</sup>gpdA::mrfp::h2A</i>	(Helmstaedt <i>et al.</i> , 2008)
AGB334	<i>pyrG89/Afp<sub>pyrG</sub>; nudF6; <sup>P</sup>niiA::nudF::neyfp; <sup>P</sup>niaD::nudC::ceyfp</i>	(Helmstaedt <i>et al.</i> , 2008)
AGB335	<i>pyrG89/Afp<sub>pyrG</sub>; nudF6; <sup>P</sup>niiA::nudF::neyfp; <sup>P</sup>niaD::nudC::ceyfp; mipA::mrfp::<sup>P</sup>gpdA::nat<sup>R</sup></i>	(Helmstaedt <i>et al.</i> , 2008)
AGB336	<i>pyroA4; pyrG89; ΔnkuA::argB; mipA::mrfp::<sup>P</sup>gpdA::nat<sup>R</sup></i>	(Helmstaedt <i>et al.</i> , 2008)
AGB338	<i>pyroA4; pyrG89/pyr-4; ΔnkuA::argB; mipA::mrfp::<sup>P</sup>gpdA::nat<sup>R</sup>; <sup>P</sup>nudC::nudC::gfp2-5::<sup>P</sup>alcA::nudC</i>	(Helmstaedt <i>et al.</i> , 2008)
AGB339	<i>pyrG89; yA2; ΔsumO::<sup>P</sup>ptrA::ptrA<sup>R</sup></i>	this study
AGB340	<i>yA2, ΔsumO::<sup>P</sup>ptrA::ptrA<sup>R</sup>; pyrG89/pyr-4; <sup>P</sup>alcA::⟨SynWT::<sup>t</sup>his2B (1x)⟩</i>	this study
AGB341	<i>yA2, ΔsumO::<sup>P</sup>ptrA::ptrA<sup>R</sup>; pyrG89/pyr-4; <sup>P</sup>alcA::⟨SynWT::<sup>t</sup>his2B (2x)⟩</i>	this study
AGB342	<i>yA2, ΔsumO::<sup>P</sup>ptrA::ptrA<sup>R</sup>; pyrG89/pyr-4; <sup>P</sup>alcA::⟨SynWT::<sup>t</sup>his2B (3x)⟩</i>	this study
AGB343	<i>yA2; ΔsumO::<sup>P</sup>ptrA::ptrA<sup>R</sup>; pyrG89/pyr-4; <sup>P</sup>alcA::⟨SynA53T::<sup>t</sup>his2B (1x)⟩</i>	this study
AGB344	<i>yA2; ΔsumO::<sup>P</sup>ptrA::ptrA<sup>R</sup>; pyrG89/pyr-4; <sup>P</sup>alcA::⟨SynA53T::<sup>t</sup>his2B (2x)⟩</i>	this study
AGB345	<i>yA2; ΔsumO::<sup>P</sup>ptrA::ptrA<sup>R</sup>; pyrG89/pyr-4; <sup>P</sup>alcA::⟨SynA53T::<sup>t</sup>his2B (3x)⟩</i>	this study
AGB346	<i>yA2; ΔsumO::<sup>P</sup>ptrA::ptrA<sup>R</sup>; pyrG89/pyr-4; <sup>P</sup>alcA::⟨SynA30P::<sup>t</sup>his2B (1x)⟩</i>	this study

Table 4: *Aspergillus nidulans* strains used in this study, continued.

Strain	Genotype	Reference
AGB347	<i>yA2; ΔsumO::<sup>p</sup>ptrA::ptrA<sup>R</sup>; pyrG89/pyr-4;</i> <i><sup>p</sup>alcA::⟨SynA30P::<sup>t</sup>his2B (2x)</i>	this study
AGB348	<i>yA2; ΔsumO::<sup>p</sup>ptrA::ptrA<sup>R</sup>; pyrG89/pyr-4;</i> <i><sup>p</sup>alcA::⟨SynA30P::<sup>t</sup>his2B (3x)</i>	this study
AGB349	<i>yA2; ΔsumO::<sup>p</sup>ptrA::ptrA<sup>R</sup>; pyrG89/pyr-4;</i> <i><sup>p</sup>alcA::<sup>t</sup>his2B</i>	this study
AGB350	<i>pyrG89; yA2; ΔsumO::<sup>p</sup>ptrA::ptrA<sup>R</sup>/<sup>p</sup>sumO::sumO::</i> <i><sup>t</sup>sumO; <sup>p</sup>gpdA::nat<sup>R</sup></i>	this study
AGB351	<i>yA2; ΔsumO::<sup>p</sup>ptrA::ptrA<sup>R</sup>; pyrG89/pyr-4;</i> <i><sup>p</sup>alcA::egfp::⟨SynWT::<sup>t</sup>his2B (1x)</i>	this study
AGB352	<i>yA2; ΔsumO::<sup>p</sup>ptrA::ptrA<sup>R</sup>; pyrG89/pyr-4;</i> <i><sup>p</sup>alcA::egfp::⟨SynWT::<sup>t</sup>his2B (2x)</i>	this study
AGB353	<i>yA2; ΔsumO::<sup>p</sup>ptrA::ptrA<sup>R</sup>; pyrG89/pyr-4;</i> <i><sup>p</sup>alcA::egfp::⟨SynWT::<sup>t</sup>his2B (3x)</i>	this study
AGB354	<i>yA2; ΔsumO::<sup>p</sup>ptrA::ptrA<sup>R</sup>; pyrG89/pyr-4;</i> <i><sup>p</sup>alcA::egfp::⟨SynA53T::<sup>t</sup>his2B (1x)</i>	this study
AGB355	<i>yA2; ΔsumO::<sup>p</sup>ptrA::ptrA<sup>R</sup>; pyrG89/pyr-4;</i> <i><sup>p</sup>alcA::egfp::⟨SynA53T::<sup>t</sup>his2B (2x)</i>	this study
AGB356	<i>yA2; ΔsumO::<sup>p</sup>ptrA::ptrA<sup>R</sup>; pyrG89/pyr-4;</i> <i><sup>p</sup>alcA::egfp::⟨SynA53T::<sup>t</sup>his2B (3x)</i>	this study
AGB357	<i>yA2; ΔsumO::<sup>p</sup>ptrA::ptrA<sup>R</sup>; pyrG89/pyr-4;</i> <i><sup>p</sup>alcA::egfp::⟨SynA30P::<sup>t</sup>his2B (3x)</i>	this study
AGB358	<i>yA2; ΔsumO::<sup>p</sup>ptrA::ptrA<sup>R</sup>; pyrG89/pyr-4;</i> <i><sup>p</sup>alcA::egfp::⟨SynA30P::<sup>t</sup>his2B (3x)</i>	this study
AGB359	<i>yA2; ΔsumO::<sup>p</sup>ptrA::ptrA<sup>R</sup>; pyrG89/pyr-4;</i> <i><sup>p</sup>alcA::egfp::⟨SynA30P::<sup>t</sup>his2B (3x)</i>	this study
AGB361	<i>pyroA4; pyrG89/pyr-4; <sup>p</sup>alcA::⟨SynWT::<sup>t</sup>his2B (1x)</i>	this study
AGB362	<i>pyroA4; pyrG89/pyr-4; <sup>p</sup>alcA::⟨SynWT::<sup>t</sup>his2B (2x)</i>	this study
AGB363	<i>pyroA4; pyrG89/pyr-4; <sup>p</sup>alcA::⟨SynWT::<sup>t</sup>his2B (3x)</i>	this study
AGB364	<i>pyroA4; pyrG89/pyr-4; <sup>p</sup>alcA::⟨SynA53T::<sup>t</sup>his2B (1x)</i>	this study
AGB365	<i>pyroA4; pyrG89/pyr-4; <sup>p</sup>alcA::⟨SynA53T::<sup>t</sup>his2B (2x)</i>	this study
AGB366	<i>pyroA4; pyrG89/pyr-4; <sup>p</sup>alcA::⟨SynA53T::<sup>t</sup>his2B (3x)</i>	this study
AGB367	<i>pyroA4; pyrG89/pyr-4; <sup>p</sup>alcA::⟨SynA30P::<sup>t</sup>his2B (1x)</i>	this study
AGB368	<i>pyroA4; pyrG89/pyr-4; <sup>p</sup>alcA::⟨SynA30P::<sup>t</sup>his2B (2x)</i>	this study
AGB369	<i>pyroA4; pyrG89/pyr-4; <sup>p</sup>alcA::⟨SynA30P::<sup>t</sup>his2B (3x)</i>	this study
AGB370	<i>pyroA4; pyrG89/pyr-4;</i> <i><sup>p</sup>alcA::egfp::⟨SynWT::<sup>t</sup>his2B (1x)</i>	this study
AGB371	<i>pyroA4; pyrG89/pyr-4;</i> <i><sup>p</sup>alcA::egfp::⟨SynWT::<sup>t</sup>his2B (2x)</i>	this study
AGB372	<i>pyroA4; pyrG89/pyr-4;</i> <i><sup>p</sup>alcA::egfp::⟨SynWT::<sup>t</sup>his2B (3x)</i>	this study

**Table 4: *Aspergillus nidulans* strains used in this study, continued.**

Strain	Genotype	Reference
AGB373	<i>pyroA4</i> ; <i>pyrG89/pyr-4</i> ; <i>P<sub>alcA</sub>::egfp::(SynA53T)::<sup>t</sup>his2B</i> (1x)	this study
AGB374	<i>pyroA4</i> ; <i>pyrG89/pyr-4</i> ; <i>P<sub>alcA</sub>::egfp::(SynA53T)::<sup>t</sup>his2B</i> (2x)	this study
AGB375	<i>pyroA4</i> ; <i>pyrG89/pyr-4</i> ; <i>P<sub>alcA</sub>::egfp::(SynA53T)::<sup>t</sup>his2B</i> (3x)	this study
AGB376	<i>pyroA4</i> ; <i>pyrG89/pyr-4</i> ; <i>P<sub>alcA</sub>::egfp::(SynA30P)::<sup>t</sup>his2B</i> (1x)	this study
AGB377	<i>pyroA4</i> ; <i>pyrG89/pyr-4</i> ; <i>P<sub>alcA</sub>::egfp::(SynA30P)::<sup>t</sup>his2B</i> (2x)	this study
AGB378	<i>pyroA4</i> ; <i>pyrG89/pyr-4</i> ; <i>P<sub>alcA</sub>::egfp::(SynA30P)::<sup>t</sup>his2B</i> (3x)	this study
AGB379	<i>pyroA4</i> ; <i>pyrG89/pyr-4</i> ; <i>P<sub>alcA</sub>::<sup>t</sup>his2A</i>	this study
AGB380	<i>pyroA4</i> ; <i>pyrG89</i> ; $\Delta$ <i>nkuaA::argB</i> ; $\Delta$ <i>sumO::P<sub>ptrA</sub>::ptrA<sup>R</sup></i>	this study
AGB387	<i>yA2</i> ; $\Delta$ <i>sumO::P<sub>ptrA</sub>::ptrA<sup>R</sup></i> ; <i>pyrG89/pyr-4</i> ; <i>P<sub>alcA</sub>::gfp2-5</i> (3x)	this study
AGB397	<i>pyrG89/pyr4</i> ; <i>yA2</i> ; $\Delta$ <i>sumO::P<sub>ptrA</sub>::ptrA<sup>R</sup>/P<sub>sumO</sub>::sumO</i> ; <i>P<sub>gpdA</sub>::nat<sup>R</sup></i> ; <i>P<sub>alcA</sub>::(SynA30Pt)::<sup>t</sup>his2B</i> (3x)	this study
AGB398	<i>pyrG89/pyr4</i> ; <i>yA2</i> ; $\Delta$ <i>sumO::P<sub>ptrA</sub>::ptrA<sup>R</sup>/P<sub>sumO</sub>::sumO</i> ; <i>P<sub>gpdA</sub>::nat<sup>R</sup></i> ; <i>P<sub>alcA</sub>::egfp::(SynWT)::<sup>t</sup>his2B</i> (3x)	this study
AGB399	<i>pyrG89/pyr4</i> ; <i>yA2</i> ; $\Delta$ <i>sumO::P<sub>ptrA</sub>::ptrA<sup>R</sup>/P<sub>sumO</sub>::sumO</i> ; <i>P<sub>gpdA</sub>::nat<sup>R</sup></i> ; <i>P<sub>alcA</sub>::egfp::(SynA53T)::<sup>t</sup>his2B</i> (3x)	this study
AGB400	<i>pyrG89/pyr4</i> ; <i>yA2</i> ; $\Delta$ <i>sumO::P<sub>ptrA</sub>::ptrA<sup>R</sup></i> ; <i>P<sub>niiA</sub>::neyfp::(SynWT; P<sub>niiA</sub>D::ceyfp::sumO</i>	this study
AGB401	<i>pyrG89/pyr4</i> ; <i>yA2</i> ; $\Delta$ <i>sumO::P<sub>ptrA</sub>::ptrA<sup>R</sup></i> ; <i>P<sub>niiA</sub>D::ceyfp::sumO</i>	this study

#### 2.2.4.1 Plasmid and strain construction for *sumO* deletion and reconstitution in

##### *A. nidulans*

For the purpose of deleting *sumO*, a deletion cassette containing 2.3 kb of the 5' and 3.3 kb of the 3' untranslated region (UTR) of *sumO* was generated. The UTRs were amplified from genomic DNA using specific primers containing flanking *SfiI* sites (OLKM34, OLKM35, OLKM36, OLKM37). The PCR product was ligated with the pyrithiamine (*ptrA*) deletion cassette (for targeted gene replacement) (Krappmann *et al.*, 2006), which was cut out of pME3024 using *SfiI* restriction sites. The ligation product was cloned into pCR®-BluntII-TOPO® yielding plasmid pME3320 and the entire deletion cassette with a

size of 7.6 kb was obtained by digestion of pME3320 with *ScaI* and transformed into the  $\Delta nkuA$  strain A1149 (AGB380). Southern hybridization analysis was conducted to confirm homologous recombination of the *ptrA* knockout cassette at the *sumO* locus using a PCR-amplified 5' UTR *sumO* probe (OLKM35, OLKM42). AGB380 was backcrossed with the strain UI224 resulting in strain AGB339.

For reconstitution of *sumO*, the plasmid pME3319 was transformed into AGB339 yielding strain AGB350. pME3319 was created by cloning a genomic PCR fragment with the size of 3.3 kb containing 2 kb of the 5' UTR and 300 bp of the 3' UTR of *sumO* as well as the respective ORF (OLKM44, OLKM45) into the *ApaI* restriction site of pNV1 (Seiler *et al.*, 2006). Ectopical integration was confirmed by PCR using primers OLKM42 and OLKM47.

#### 2.2.4.2 Plasmid and strain construction for expression of human $\zeta$ Syn and respective *egfp* fusion constructs in *A. nidulans*

For expression of human  $\zeta$ Syn and the respective *egfp* fusion constructs in *A. nidulans*, the plasmid pME3321 was used carrying the inducible *alcA* promoter. The  $\zeta$ Syn alleles *WT*, *A30P* and *A53T* as well as respective *egfp* fusion constructs were obtained by cutting the plasmids PCDNA3SYNWT, PCDNA3A30P, PCDNA3A53T, PCDNA3GFPSYNWT, PCDNA3GFPA30P, and PCDNA3GFPA53T, respectively, with *HindIII/XhoI*. Subsequently, Klenow reaction was conducted for cloning into expression plasmid pME3321 (*SmaI*) yielding plasmids pME3313, pME3314, pME3315, pME3316, pME3317 and pME3318, respectively, which were transformed into strain AGB152. Southern hybridization analysis was performed using a PCR-amplified *alcA* promoter probe (OLKM31, OLKM32) to obtain strains that have inserted one, two and three copies of each plasmid referred to as AGB361 (1x $\zeta$ SynWT), AGB362 (2x $\zeta$ SynWT), AGB363 (3x $\zeta$ SynWT), AGB364 (1x $\zeta$ SynA53T), AGB365 (2x $\zeta$ SynA53T), AGB366 (3x $\zeta$ SynA53T), AGB367 (1x $\zeta$ SynA30P), AGB368 (2x $\zeta$ SynA30P), AGB369 (3x $\zeta$ SynA30P), AGB370 (1xGFP- $\zeta$ SynWT), AGB371 (2xGFP- $\zeta$ SynWT), AGB372 (3xGFP- $\zeta$ SynWT), AGB373 (1xGFP- $\zeta$ SynA53T), AGB374 (2xGFP- $\zeta$ SynA53T), AGB375 (3xGFP- $\zeta$ SynA53T), AGB376 (1xGFP- $\zeta$ SynA30P), AGB377 (2xGFP- $\zeta$ SynA30P), AGB378 (3xGFP- $\zeta$ SynA30P). Additionally, the same plasmids were transformed into the  $\Delta sumO$  strain

AGB339 and the copy numbers of the integrated plasmids were likewise confirmed by Southern hybridization yielding strains AGB340 (1x⟨SynWT), AGB341 (2x⟨SynWT), AGB342 (3x⟨SynWT), AGB343 (1x⟨SynA53T), AGB344 (2x⟨SynA53T), AGB345 (3x⟨SynA53T), AGB346 (1x⟨SynA30P), AGB347 (2x⟨SynA30P), AGB348 (3x⟨SynA30P), AGB351 (1xGFP-⟨SynWT), AGB352 (2xGFP-⟨SynWT), AGB353 (3xGFP-⟨SynWT), AGB354 (1xGFP-⟨SynA53T), AGB355 (2xGFP-⟨SynA53T), AGB356 (3xGFP-⟨SynA53T), AGB357 (1xGFP-⟨SynA30P), AGB358 (2xGFP-⟨SynA30P), AGB359 (3xGFP-⟨SynA30P). As control strains for growth tests, AGB349 and AGB379 were generated by transformation of pME3321 into AGB339 and AGB152, respectively. Accordingly, the *palcA::gfp2-5* expression plasmid, pME3322 was transformed into AGB339 yielding AGB387, which served as control strain for growth tests and fluorescence analysis as well as AGB190 (Busch *et al.*, 2007). Ectopical integration of pME3321 and pME3322, respectively, was confirmed by Southern hybridization analysis using an *alcA* promoter probe as described above. Reconstitution of *sumO* in AGB348, AGB353, and AGB356, was performed by transformation of pME3319 yielding strains AGB397, AGB398, and AGB399, respectively. Ectopical integration of the plasmid was confirmed by Southern hybridization using a 5' UTR *sumO* probe amplified from genomic DNA (OLKM35, OLKM42). For Northern hybridization, an  $\alpha$ *Syn* probe was employed amplified with the primers OLKM20 and OLKM21 using pME3313 as a template.

#### **2.2.4.3 Plasmid and strain construction for bimolecular fluorescence complementation experiments with ⟨SynWT and SUMO**

For interaction studies of ⟨SynWT and SUMO, the encoding genes were fused to the N-terminal and C-terminal halves of eYFP, respectively, by fusion PCR. *ceyfp::sumO* was cloned into the blunt *SwaI* site of plasmid pME3160 (Bayram *et al.*, 2008b) containing the bidirectional *niiA/niaD* promoter yielding pME3489. Subsequently, *neyfp::⟨SynWT* was ligated into pME3489 via *PmeI* resulting in pME3490. For PCR, template plasmids pME3012 and pME3013 (Blumenstein *et al.*, 2005), pME3313 and the cDNA library pCNS4 (Krappmann *et al.*, 2006) as well as the following primers were used encoding a RSIAT linker for the *neyfp::⟨SynWT* fusion and a RPACKIPNDLKQKVMNH linker between (C)EYFP and SUMO (OLKM91, OLKM92, OLKM93, and OLKM94; OLKM86,

OLKM87, OLKM88, and OLKM89). The resulting plasmids pME3489 and pME3490, respectively, were transformed into AGB339 to test for complementation of the  $\Delta sumO$  phenotype (AGB400, AGB401). Single ectopical integration was confirmed by Southern hybridization analysis using a nitrate promoter probe amplified from genomic DNA (OLKM67, OLKM68).

#### 2.2.4.4 Plasmid and strain constructions for NUDC localization experiments

NUDC-GFP was localized in an *A. nidulans nudC3* strain after transformation of pME2823 harbouring a *nudC::sgfp* fusion into A779 (AGB241). pME2823 was created by cloning a *KpnI* fragment of *nudC* amplified with the primers OLKH115 and OLKH116 into pMCB32 (Fernández-Ábalos *et al.*, 1998).

For colocalization of NUDF and NUDC, the encoding genes were fused to the N-terminal and C-terminal halves of eYFP, respectively, by fusion PCR and cloned into the blunt *PmeI* and *SwaI* sites, respectively, of plasmid pME3160 (Bayram *et al.*, 2008b). For PCR, template plasmids pME3012 and pME3013 (Blumenstein *et al.*, 2005) and pME2822/pME2823 and the following primers were used which encoded a RSIAT linker for the *nudF::neyfp* fusion and a RPACKIPNDLKQKVMNH linker between NUDC and (C)EYFP (OLKH262, OLKH263, OLKH264, and OLKH265; OLKH258, OLKH259, OLKH260, and OLKH261). The resulting plasmid pME3238 was transformed into A779 and XX20 to test for complementation of their temperature-sensitive phenotypes at 42°C yielding strains AGB302 and AGB334. AGB334 was also transformed with pME3173 expressing the nuclear marker *<sup>p</sup>gpdA::mrfp::h2A* (Bayram *et al.*, 2008b) resulting in strain AGB303. For colocalization with  $\gamma$ -tubulin (MIPA), AGB334 was transformed with a PCR product comprising a *mipA::mrfp::<sup>p</sup>gpdA::nat<sup>R</sup>* cassette (AGB335). For this fusion PCR, a template plasmid was generated: a (GA)<sub>5</sub> linker, the *mrfp* gene and the *nat<sup>R</sup>* expression module were amplified with primers OLKH301, OLKH302 and OLKH303, OLKH304 and cloned into pBluescript via *EcoRI/BamHI* yielding plasmid pME2984. This module (OLKH306, OLKH307) was fused to a 500 bp homology region including a part of *mipA* (OLKH308, OLKH310) and a 500 bp region comprising the 3' UTR of *mipA* (OLKH311, OLKH313), which were amplified using genomic DNA, by a final fusion PCR with OLKH309 and OLKH312.

To rule out overexpression effects when localizing the *nudC-gfp* fusion, strain AGB336 was transformed with pME2985, which was generated by cloning a *KpnI* fragment with *nudC* into a pMCB17apx derivative (pME3322). In some transformants, this plasmid did not integrate ectopically, but solely at the *nudC* locus resulting in a *gfp2-5*-labeled *nudC* copy driven by the authentic promoter and an unlabeled copy driven by the *alcA* promoter from the plasmid. Therefore, this strain (AGB338) was grown in glucose medium for microscopic analysis so that no unlabeled NUDC was present in the cells. Furthermore, strain AGB338 harboured the *mipA::mrfp::<sup>p</sup>gpdA::nat<sup>R</sup>* cassette, which was introduced into A1149 before to yield AGB336.

## **2.3 Genetic manipulations**

### **2.3.1 Transformation procedures**

*E. coli* cells were transformed as described (Inoue *et al.*, 1990). *A. nidulans* was transformed by polyethylene glycol-mediated fusion of protoplasts as described (Punt and van den Hondel, 1992). *S. cerevisiae* was transformed by the modified method of Elble, 1992.

### **2.3.2 Sequence analysis**

DNA was sequenced on an ABI Prism 310 capillary sequencer (APPLERA DEUTSCHLAND GMBH, Darmstadt, Germany) at the Göttingen Genomics Laboratory. Sequences were analysed using the Lasergene software (DNASTAR INC., Madison, WI, USA).

### **2.3.3 Recombinant DNA methods**

In general, recombinant DNA technologies were performed according to the standard methods (Sambrook *et al.*, 1989). PCR experiments were carried out using *Taq* (FERMENTAS GMBH, St. Leon-Rot, D), KOD Hifi, (NOVAGEN, Nottingham, UK) *Pfu* (FERMENTAS GMBH, St. Leon-Rot, D) or Phusion High-Fidelity (FINNZYMES/NEW ENGLAND BIOLABS GMBH, Frankfurt am Main, Germany) DNA polymerases. Restriction

enzymes, Klenow fragment, and T4 DNA ligase were obtained from FERMENTAS GMBH (St. Leon-Rot, D). All reactions were carried out according to manufacturer's manuals.

#### **2.3.4 DNA isolation and hybridization**

Isolation of plasmid DNA from *E. coli* was performed using the Qiagen Plasmid Midi or Mini Kit (QIAGEN, Hilden, D) according to the manual. To obtain DNA fragments out of agarose gels, the QIAquick Gel Extraction Kit (QIAGEN, Hilden, D) was used. For extraction of genomic DNA of *A. nidulans*, mycelia were harvested by filtration through sterile Miracloth (MERCK CHEMICALS, Nottingham, UK) and ground in liquid nitrogen using mortar and pestle. Fungal genomic DNA was prepared as described (Kolar *et al.*, 1988). Southern analyses of all strains were carried out according to Southern, 1975. Non-radioactive labelling of probes and detection was performed using the Gene Images<sup>TM</sup> Random-Prime DNA labelling kit and the Gene Images<sup>TM</sup> CDP-Star<sup>TM</sup> Detection Kit (GE HEALTHCARE LIFE SCIENCES, München, D). The chemiluminescent signals were detected using Amersham Hyperfilm<sup>TM</sup> ECL (GE HEALTHCARE LTD., Little Chalfont, UK). Quantification of detected bands was performed using the KODAK MI 4.05 software (EASTMAN KODAK COMPANY, Rochester, NY, USA).

#### **2.4 RNA isolation and hybridization**

For the isolation of RNA from *A. nidulans*, strains were grown in MM containing 2% glucose for 20 h at 37°C followed by a shift to MM containing 2% glycerol/2% ethanol for 6 h. RNA was isolated with TRIzol<sup>®</sup> Reagent (INVITROGEN, Karlsruhe, D) from frozen mycelia. Northern hybridizations were performed as described previously (Brown and Mackey, 1997). For the radioactive labelling of probes, the Prime-It II Random Primer Labelling Kit (STRATAGENE, La Jolla, CA, USA) was used according to the manual. Hybridized nylon membranes ("Hybond<sup>TM</sup>-N Membrane", AMERSHAM BIOSCIENCES, Buckingham, UK) were washed and subsequently exposed to KODAK BioMax MS Films (KODAK, Rochester, NY, USA). Quantification of detected bands was performed using the KODAK MI 4.05 software (EASTMAN KODAK COMPANY, Rochester, NY, USA).

## 2.5 Protein methods

### 2.5.1 Protein isolation and analysis

For the extraction of proteins from *S. cerevisiae*, the respective strains were grown overnight in SC medium containing either 2% glucose or 2% galactose / 1% raffinose at 30°C. The next day the main culture was inoculated with the overnight grown culture and grown until an OD<sub>595</sub> of 1 was reached. The cells were harvested by centrifugation at 3.000 rpm for 4 min and resuspended in 2.5 ml breaking buffer (100 mM Tris-HCl pH 7.2, 200 mM NaCl, 20% glycerol, 5 mM EDTA pH 8; 1 µl/ml β-mercaptoethanol and 5 µl/ml 200x PIM (100 mM p-aminobenzamidin-HCL, 100 mM Na-p-tosyl-L-lysinchloromethylketon, 100 mM Na-p-tosyl-L-phenylalanin-chloromethylketone, 100 mM o-phenanthrolin and 100 mM phenylmethylsulfonyl-fluoride in DMSO) were added freshly). The cell suspension was vortexed for 5 min at 4°C and centrifuged for 15 min with 13.000 rpm at 4°C. The protein containing supernatant was stored at -20°C or used immediately for further analyses.

For protein isolation from *A. nidulans*, the breaking buffer described for protein isolation from *S. cerevisiae* was used. The respective strains were grown in MM containing 2% glucose for 20 h at 37°C followed by a shift to MM containing 2% glycerol/ 2% ethanol for 6 h. Mycelia were harvested by filtration through Miracloth (MERCK CHEMICALS, Nottingham, UK) and ground in liquid nitrogen using mortar and pestle. 200-500 µl breaking buffer were added to 200-400 µl frozen mycelia and vortexed for 10 sec followed by a centrifugation step at 4°C for 10 min. The supernatant was stored at -20°C or used directly for further analyses. Protein concentrations were determined as described (Bradford, 1976).

For Western hybridization experiments, proteins were separated by SDS-PAGE and transferred onto a nitrocellulose membrane (SCHLEICHER & SCHUELL BIOSCIENCE GMBH, Dassel, D) by electroblotting. As first antibodies mouse anti-actin IgG (MP BIOMEDICALS LLC, OH, USA), mouse anti-α-tubulin IgG (SIGMA, Saint Louis, MO, USA), mouse anti-GFP IgG (CLONTECH-TAKARA BIOEUROPE, Saint-Germainen-Laye, F), mouse anti-HA (SIGMA-ALDRICH CHEMIE GMBH, Munich, Germany), goat anti-LexA (SANTA CRUZ BIOTECHNOLOGY, INC., Heidelberg, Germany) and rabbit anti-Syn (ANASPEC INC., San Jose, CA USA) antibodies were used. As secondary antibodies, peroxidase-coupled

donkey anti-goat IgG-HRP (SANTA CRUZ BIOTECHNOLOGY, Heidelberg, D), goat anti-rabbit IgG-HRP (SANTA CRUZ BIOTECHNOLOGY, Heidelberg, D) or goat anti-mouse IgG antibodies (INVITROGEN GMBH, Karlsruhe, D) were employed. The PageRuler™ Prestained Protein Ladder (FERMENTAS GMBH, St. Leon-Rot, D) was used as a marker. After incubation, detection was performed using the ECL (enhanced chemiluminescence) method (Tesfaigzi *et al.*, 1994). Quantification of detected bands was performed using the KODAK MI 4.05 software (EASTMAN KODAK COMPANY, Rochester, NY, USA).

### 2.5.2 Yeast two-hybrid analysis

Protein-protein interactions were tested applying the interaction trap of Golemis *et al.*, 1999a. In this system, plasmids pEG202 and pJG4-5 were used for expression of open reading frames encoding bait and prey proteins and for activation of *lacZ* and *leu2* reporter constructs to discriminate on the basis of colour in the presence of X-Gal or to select for viability on medium lacking leucine.

For interaction tests, overnight SC cultures were diluted to an OD<sub>546</sub> of 0.2 with SC medium, and 10 µl of the dilution was dropped onto SC-4 plates containing either 2% galactose / 1% raffinose or 2% glucose (negative control) for growth tests. Dilutions with an OD<sub>546</sub> of 0.1 were spotted onto SC-3 plates containing 2% galactose / 1% raffinose and 1.7 mM leucine for subsequent β-galactosidase filter assays. Plates were incubated at 30°C for two days. For the filter assay, a whatman filter was placed onto the yeast plate, shock frozen in liquid nitrogen and dried. The filter was then put onto another whatman filter soaked with 3 ml of Z-buffer (60 mM Na<sub>2</sub>HPO<sub>4</sub>, 40 mM NaH<sub>2</sub>PO<sub>4</sub>, 10 mM KCl, 1 mM MgSO<sub>4</sub>, 0.1% X-Gal) and incubated at 30°C for four hours or until the positive control turned blue.

### 2.6 Microscopic analysis

Colonies, hyphae, and developmental structures of *A. nidulans* were examined with an Olympus SZX12 binocular (OLYMPUS, Hamburg, D) or a ZEISS Axiolab light microscope (ZEISS AG, Oberkochen, D). Images were taken using a KAPPA PS30 digital camera and the KAPPA ImageBase software (KAPPA OPTO-ELECTRONICS GMBH, Gleichen, D).

For the purpose of fluorescence microscopy, 500 µl of the appropriate medium were put onto cover slips, which were placed in Petri dishes, and inoculated with  $4 \times 10^4$  spores. The growth at 37°C and 42°C was conducted by placing cover slips into 6-well plates with 5 ml of medium inoculated with  $2 \times 10^5$  spores or into Petri dishes with 20 ml of medium inoculated with  $1 \times 10^6$  spores. After incubation at the respective temperature, cover slips were mounted on glass slides with nail polish. For staining of nuclei, 1 µl 4', 6'-diamidino-2-phenylindole (DAPI) was spotted onto the glass slide before placing the cover slip onto it. Alternatively, the cover slip was submerged in liquid nitrogen for a few seconds and 10 µl DAPI was placed onto the frozen cover slip before mounting it onto the glass slide.

For observation of conidiophores, 5 ml of MM containing 2% agar and the appropriate supplements were put onto glass slides placed in Petri dishes, and inoculation was performed with  $2 \times 10^4$  spores. Strains were grown at 30°C and 37°C for 20 h and 35 h, respectively. Cells were examined with a Zeiss 100 Axiovert microscope (CARL ZEISS MICROIMAGING GMBH, Jena, D) and photographs were taken using a Xillix Microimager digital camera (XILIX TECHNOLOGIES CORP., Richmond, CAN) and the Openlab 5.01 software (IMPROVISION, Coventry, UK).

For electron microscopy, embedding in Lowicryl K4M resin was performed as described (Hoppert and Holzenburg, 1998; Roth *et al.*, 1981). Resin sections of about 80 nm in thickness were cut with glass knives. The sections were stained for 3 min with 3% [w/v] phosphotungstic acid solution, pH 7.0. Specimen were analysed with a Philips EM 301 instrument (PHILIPS, Hamburg, D) at calibrated magnifications and using IMAGO electron sensitive films (ATOMIC FORCE F&E GMBH, Mannheim, D). Immunogold labelling was performed as described previously (Hoppert and Holzenburg, 1998).

## 3 Results

### 3.1 Deletion of *sumO* affects asexual and sexual spore production in *A. nidulans*

#### 3.1.1 Deletion and reconstitution of the *sumO* gene in *A. nidulans*

Sumoylation has been implicated in many cellular processes and has become increasingly important with regard to neurodegenerative diseases. Numerous proteins involved in these pathologies are target substrates for sumoylation like  $\alpha$ -synuclein ( $\alpha$ Syn) which has been attributed to Parkinson's Disease (PD) (Hughes *et al.*, 2002; Krüger *et al.*, 1998; Pountney *et al.*, 2005). Due to the fact that SUMO1 homologs in model organisms used to analyze  $\alpha$ Syn are often essential, e.g., *SMT3* in *S. cerevisiae*, advantage can be taken of *A. nidulans*. In this filamentous fungus, the single *sumO* gene AN1191.3 was identified to encode a SUMO1-like protein and it was shown that inactivation of *sumO* is not lethal (Wong *et al.*, 2008).

To investigate the role of sumoylation for  $\alpha$ Syn in *A. nidulans*, *sumO* was deleted using the *A. oryzae* pyrithiamine (*ptrA*) resistance gene flanked by parts of the 5' and 3' untranslated region (UTR) of *sumO*. The entire deletion cassette with a size of 7.6 kb (Fig. 15A) was transformed into the strain A1149 harbouring an *nkuA* deletion, which increases the frequency of gene replacement in *A. nidulans* (Nayak *et al.*, 2006). The homologous recombination event at the *sumO* locus was confirmed by Southern hybridization experiments using a *sumO* 5' UTR probe (Fig. 15A). The genomic DNA of the transformants was digested with the restriction enzymes *HindIII* and *NheI*. The parental strain A1149 served as wild type control (Fig. 15B). In case the deletion cassette was integrated at the *sumO* locus, a signal of 4.5 kb (*NheI*) and 6.4 kb (*HindIII*), respectively, was obtained, whereas the signals from the *sumO* wild type locus displayed sizes of 2.9 kb and 4.8 kb, respectively. A positive transformant could be identified and was designated AGB380. This strain was crossed with the strain UI224, to restore the *nkuA* locus.

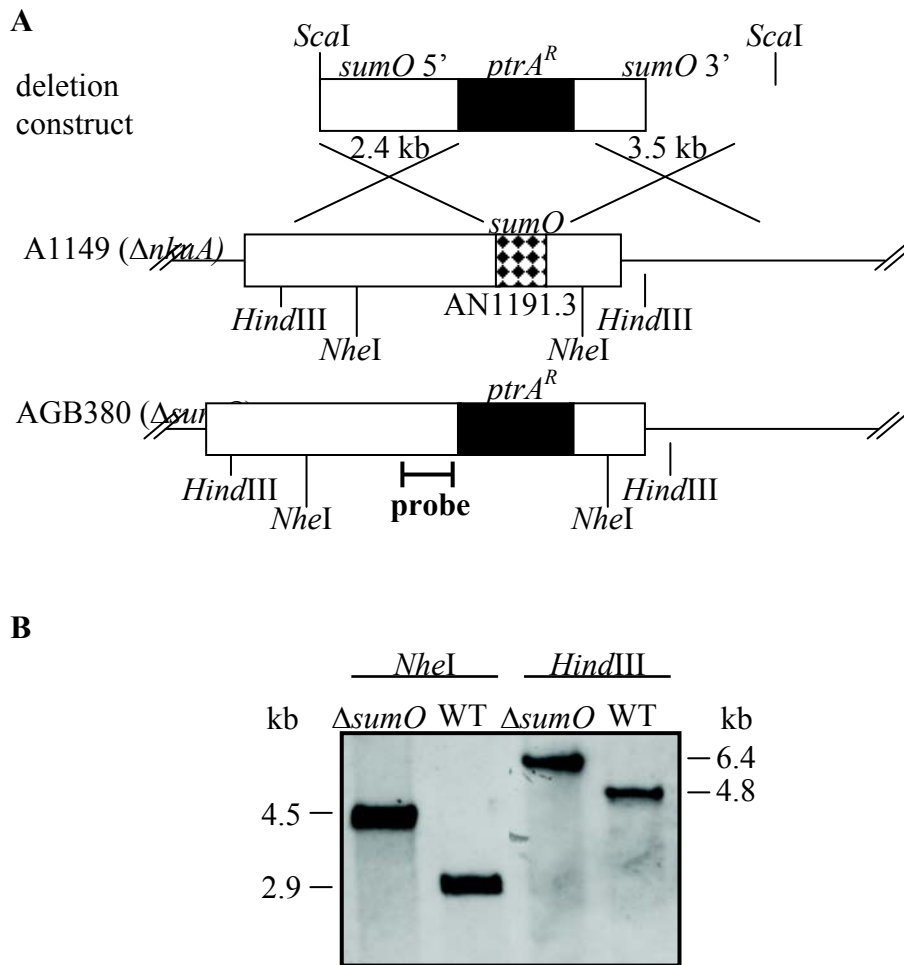


**Fig. 15: Gene replacement of *sumO* in *A. nidulans* by a *ptrA*<sup>R</sup> cassette.**

(A) Replacement of the *sumO* gene (AN1191.3) using a deletion cassette containing 2.4 kb of the 5' and 3.5 kb of the 3' UTR of *sumO* ligated with the dominant selectable marker *ptrA*. Deletion of *sumO* was achieved by homologous recombination in A1149 resulting in AGB380. (B) Homologous recombination was confirmed by Southern experiments using a 5' UTR *sumO* probe (A). The genomic DNA of AGB380 ( $\Delta sumO$ ) and of the wild type strain A1149 (WT) was digested with the restriction enzymes *NheI* and *HindIII*. In case of correct insertion of the deletion cassette at the *sumO* locus, the detected bands should have a size of 4.5 kb (*NheI*) and 6.4 kb (*HindIII*), while signals with a size of 2.9 kb and 4.8 kb, respectively, were expected from the *sumO* wild type strain.

Due to a *yA2* mutation harboured by strain UI224, the resulting  $\Delta sumO$  strain AGB339 produced yellow conidiospores. For reconstitution of the *sumO* deletion, a PCR fragment containing parts of the 5' and 3' UTR of *sumO* as well as the respective ORF was cloned into a plasmid carrying a nourseothricin (*nat*) resistance cassette. The resulting plasmid pME3319 was confirmed by sequencing followed by transformation into the  $\Delta sumO$  strain AGB339 giving AGB350. Single ectopical integration was confirmed by PCR and by Southern hybridization (data not shown).

The deletion strain AGB339 was analyzed in respect of phenotypical and developmental changes and was employed for further expression studies of  $\alpha$ Syn.

### **3.1.2 Deletion of *sumO* results in reduced conidiospore production and altered conidiophore morphology in *A. nidulans***

The *sumO* deletion strain (AGB339) was analyzed in respect of vegetative growth, the generation of asexual structures and conidia, which are induced under aerobic conditions in the light.

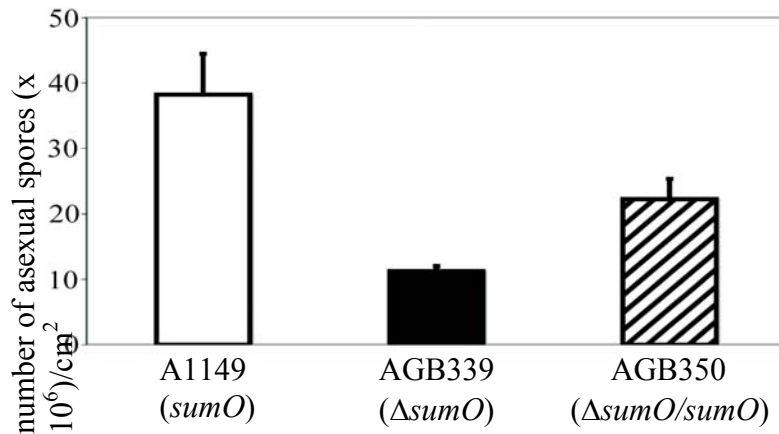
The vegetative growth behaviour was analyzed by measurement of the colony size of the wild type strain UI224 and the *sumO* deletion strain. However, in contrast to the growth cessation after three days noted by Wong *et al.*, 2008, no differences in colony size could be observed (data not shown).

The quantity of asexual spores was compared between the *sumO* wild type strain A1149, the  $\Delta$ *sumO* strain AGB339, and the complementation strain AGB350. In comparison to A1149, AGB339 produced only 30% conidiospores (Fig. 16A). The decline in the number of conidia was also shown by Wong *et al.*, 2008.

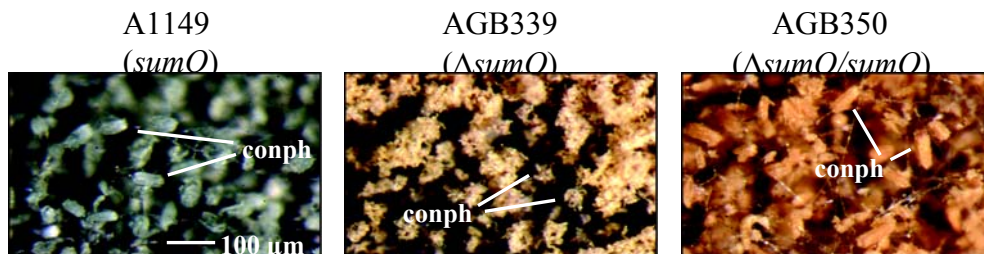
This reduction could be partly complemented in the *sumO* reconstitution strain AGB350 achieving 60% of the wild type spore production. The observation that the deletion phenotype could not be fully restored in AGB350 might be due to the ectopical integration of the complementation plasmid.

Furthermore, the conidiophore (conph) morphology of the deletion strain AGB339 is altered compared to the wild type strain A1149 (Fig. 16B). The asexual fruiting bodies of the  $\Delta$ *sumO* mutant displayed a ragged structure and differed from normally formed conidiophores with chains of asexual spores, which can be seen in the wild type strain A1149 as well as in the *sumO* complementation strain AGB350. Light microscopy revealed that about 50% of the developed conidiophores displayed irregular formed metulae (m), phialides (p), and conidia in AGB339 (Fig. 16C), which was completely complemented in AGB350. Additionally, the generation of all conidiophores is delayed in AGB339 compared to the *sumO* wild type strain A1149 and the respective complementation strain AGB350 for about 15 hours (data not shown).

A



B



C

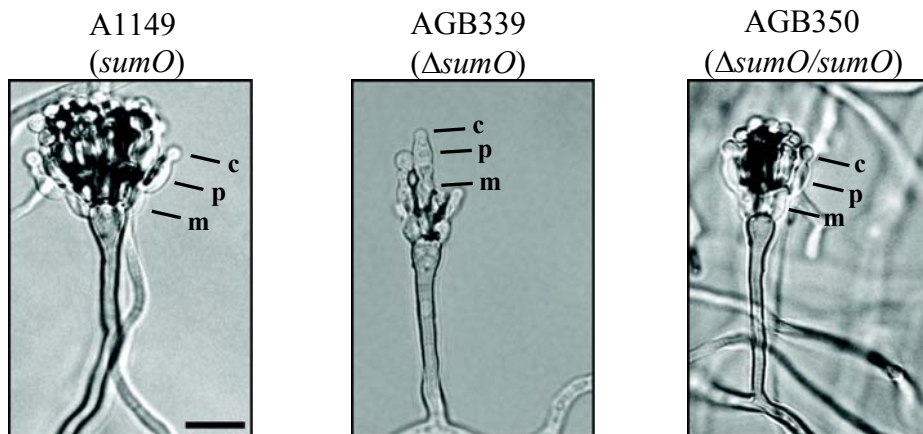


**Fig. 16: Absence of SUMO decreases asexual spore production and alters conidiophore morphology in *A. nidulans*.**

(A) The number of asexual spores is reduced to 30% in the  $\Delta$ *sumO* strain AGB339 in comparison to the *sumO* wild type strain A1149. Reconstitution of *sumO* (AGB350) leads to elevated conidiospore production of 60%. (B) Altered conidiophore (conph) morphology in the  $\Delta$ *sumO* mutant AGB339. (C) Abnormal formation of metulae (m), phialides (p), and conidia (c) in the  $\Delta$ *sumO* mutant AGB339 compared to normally structured conidiophores generated by A1149 and AGB350. Strains were grown on solid MM containing the appropriate supplements at 30°C for 20 h (A1149, AGB350) or at 37°C for 35 h (AGB350). Scale bar, 10 μm.

These results demonstrate that sumoylation is partly required for proper conidiophore formation in *A. nidulans*, which differs from findings made by Wong *et al.*, who described normally shaped asexual fruiting bodies for their  $\Delta sumO$  mutant.

### 3.1.3 The $\Delta sumO$ mutant exhibits higher sensitivity to DNA-damaging agents and oxidative stress

The deletion of the non-essential *SUMO* gene *pmt3* in *S. pombe* led to a higher sensitivity to DNA-damaging agents and DNA synthesis inhibitors (Tanaka *et al.*, 1999). Wong *et al.* showed in this year's publication that the  $\Delta sumO$  mutant displayed higher sensibility to the DNA-damaging agent methyl methanesulfonate and to the DNA synthesis inhibitor hydroxyurea. The *sumO* deletion strain constructed in this thesis was also exposed to DNA-damaging agents to examine whether AGB339 behaves like the  $\Delta sumO$  mutant described by Wong *et al.*

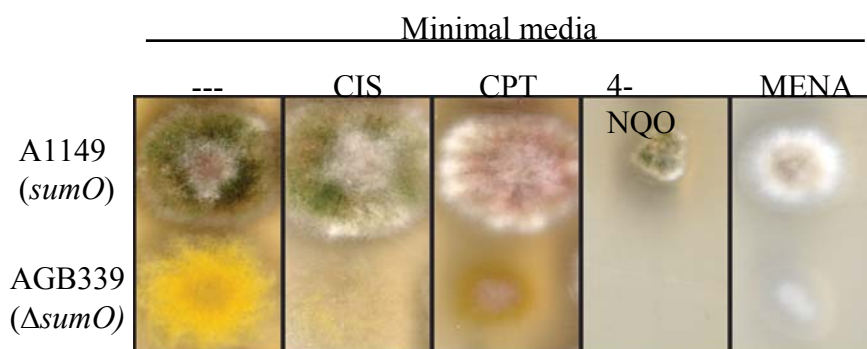


**Fig. 17: Deletion of *sumO* increases sensitivity towards stress agents in *A. nidulans*.**

Growth of wild type (A1149) and  $\Delta sumO$  (AGB339) strains on MM containing 25  $\mu$ M cisplatin (CIS), 50  $\mu$ M camptothecin (CPT), 1.3  $\mu$ M 4-nitroquinoline 1-oxide (4-NQO) or 50  $\mu$ M menadione (MENA) for three days at 37°C. AGB339 displays higher sensitivity to DNA-damaging agents like CIS, CPT or 4-NQO as well as to oxidative stress caused by MENA in comparison to the wild type strain A1149.

Moreover, the exposure to oxidative stress was analyzed. In comparison to the wild type strain A1149, the *sumO* deletion strain AGB339 displayed increased sensitivity towards the DNA-repair inhibiting agent cisplatin (CIS) as well as to camptothecin (CPT), which inhibits the DNA enzyme topoisomerase I, and 4-nitroquinoline 1-oxide (4-NQO), which

leads to an inhibition of the DNA-dependent RNA polymerase. Furthermore, the occurrence of oxidative stress caused by menadione (MENA), resulted in a decrease of growth of the  $\Delta sumO$  mutant AGB339 (Fig. 17).

Thus, deletion of *sumO* leads to higher vulnerability towards DNA-damaging agents in *A. nidulans* confirming observation made by Wong *et al.*, 2008. In addition, these results show that the sensitivity to oxidative stress is elevated in a  $\Delta sumO$  mutant.

### **3.1.4 Sumoylation is essential for ascospore production and normally sized cleistothecia in *A. nidulans***

Besides the developmental program of asexual reproduction, *A. nidulans* undergoes the sexual cycle, which generates meiotic products (ascospores). The spores are contained within fruiting bodies (cleistothecia), which are surrounded by auxiliary Hülle cells. The  $\Delta sumO$  mutant was analyzed with regard to the accomplishment of the sexual life cycle (Fig. 18). Within five days, the *sumO* wild type strain A1149 produced normally sized cleistothecia (Cl) (Fig. 18, upper row). In contrast, inspection of fruiting bodies formed by the  $\Delta sumO$  mutant AGB339 at 37°C after 14 days, revealed a severe reduction in size and were referred to as microcleistothecia (Mcl).

Analysis of the cleistothecial contents revealed that no ascospores were generated by the  $\Delta sumO$  strain AGB339 in contrast to A1149, by which red-coloured ascospores (asp) were produced (Fig. 18, lower row). The *sumO* reconstitution strain AGB350 formed regularly sized cleistothecia (Cl) with fully developed ascospores (asp) after five to eight days at 37°C (Fig. 18, lower row).

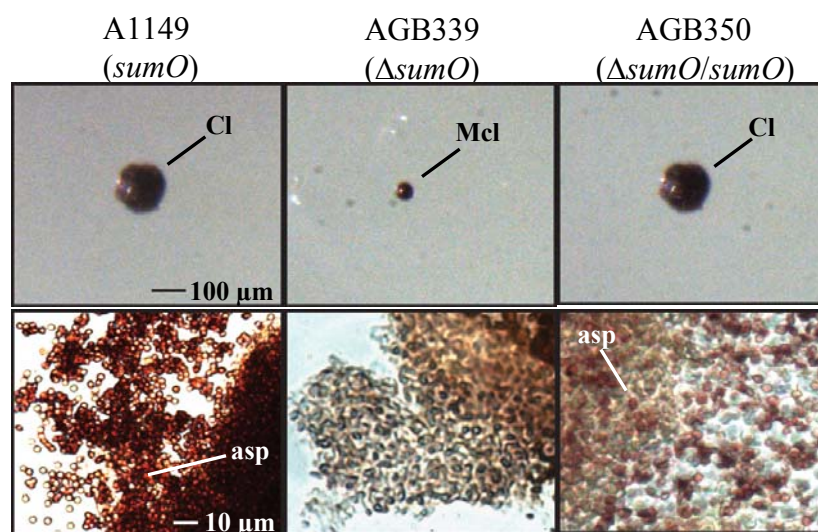


**Fig. 18: Loss of SUMO impedes proper ascosporeogenesis in *A. nidulans*.**

Analysis of fruiting bodies (Cl) generated by the  $\Delta sumO$  mutant strain (AGB339) at 37°C after 14 days shows a significant decrease in cleistothecia size designated microcleistothecia (Mcl), while regularly sized cleistothecia (Cl) are formed by the *sumO* wild type strain A1149 and the respective complementation strain AGB350 after five to eight days (upper row). When cleistothecial contents are released by squeezing mature fruiting bodies, no ascospores but an amorphous mass is extricated from  $\Delta sumO$  derived cleistothecia in comparison to A1149 and AGB350, which generate red-coloured ascospores (asp) (bottom row).

The results suggest that the process of sumoylation is involved in the formation of normally sized cleistothecia and is inevitable for ascosporeogenesis confirming data from Wong *et al.*, 2008.

### 3.1.5 The light-dependent repression of sexual development is impaired in the $\Delta sumO$ strain

When *A. nidulans* is exposed to constant white light, the fungus undergoes the asexual developmental program while the sexual reproduction is restricted to the dark.

The incubation of the  $\Delta sumO$  mutant AGB339 in constant white light led to the development of sexual structures like Hülle cells besides conidiation (Fig. 19) starting after four to five days, which was not described by Wong *et. al.* Microcleistothecia were formed after 19 days of incubation in the light (data not shown). The same observations could be made with the parental  $\Delta sumO$  strain AGB380 (data not shown). By contrast, the *sumO* wild type strain A1149 as well as the *sumO* reconstitution strain AGB350 formed no sexual structures when grown in the light for the same period of time (Fig. 19).

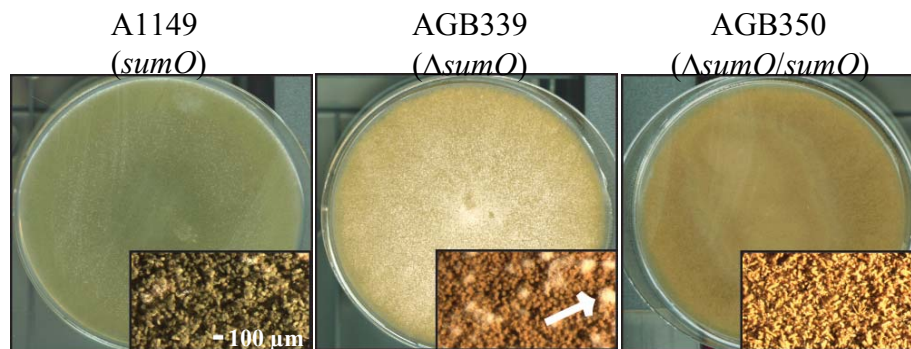


**Fig. 19: Absence of SUMO leads to abnormal production of sexual structures in the light.**

Growth of the wild type strain A1149, the  $\Delta sumO$  mutant AGB339, and the respective *sumO* complementation strain AGB350 on MM after 15 days of incubation at 37°C. In contrast to the wild type strain A1149 and the *sumO* reconstitution strain AGB350, the  $\Delta sumO$  mutant AGB339 generates sexual structures like Hülle cells (white arrow) in the light.

These new findings lead to the presumption that sumoylation is important for the perception of light, which is crucial for the repression of the sexual developmental program in *A. nidulans*.

## 3.2 Expression of human $\alpha$ Syn in *A. nidulans* with and without an intact *sumO* gene

### 3.2.1 $\alpha$ Syn<sup>WT</sup> is sumoylated *in vivo* in *A. nidulans*

Sumoylation plays an important role in many cellular processes. In the past years, sumoylation was shown to be implicated in neurodegeneration, and many proteins involved in these pathologies were found to be SUMO targets (reviewed by Dorval and Fraser, 2007). The finding that *A. nidulans* harbours a single non-essential SUMO1-like gene can be taken advantage of to investigate the role of sumoylation for fungal as well as heterologously expressed proteins. The human protein  $\alpha$ Syn, which is implicated in the pathogenesis of the neurodegenerative disorder Parkinson's disease, was shown to be monosumoylated mainly by SUMO1. This was demonstrated by overexpression of His-tagged SUMO1 and  $\alpha$ Syn in human cell cultures (Dorval and Fraser, 2006). Since, these experiments were conducted *in vitro*, the question arose whether this post-translational modification of  $\alpha$ Syn can also be shown *in vivo* using the model organism *A. nidulans*. Furthermore, the impact of sumoylation on  $\alpha$ Syn remained unclear. In this regard, a model organism like *A. nidulans* bearing a non-essential SUMO1-homologous gene could be a useful tool to decipher the role of sumoylation for  $\alpha$ Syn.

To analyze sumoylation of  $\alpha$ Syn *in vivo*, the method of bimolecular fluorescence complementation (BiFC) was employed, which is used to visualize and localize the interaction of two proteins in living cells (Hu and Kerppola, 2003). The N- and C-terminal halves of eYFP (enhanced yellow fluorescent protein) are fused to proteins of interest and eYFP emission can only be detected in case the fusion proteins interact (Fig. 20A).

(*n*)*eyfp::* $\alpha$ Syn and (*c*)*eyfp::sumO* fusion constructs were created driven by the bidirectional *niiA/niaD* promoter (Fig. 20B) to ensure similar expression levels of the fusion genes in *A. nidulans*. In the respective BiFC strain AGB400, the *sumO* deletion phenotype was partially complemented by expression of the (*c*)*eyfp::sumO* fusion. The wild type number of conidiospores and almost regularly sized cleistothecia were produced, but the block in ascospore production could not be complemented, which indicated partial functionality of the (C)eYFP-SUMO fusion (data not shown).

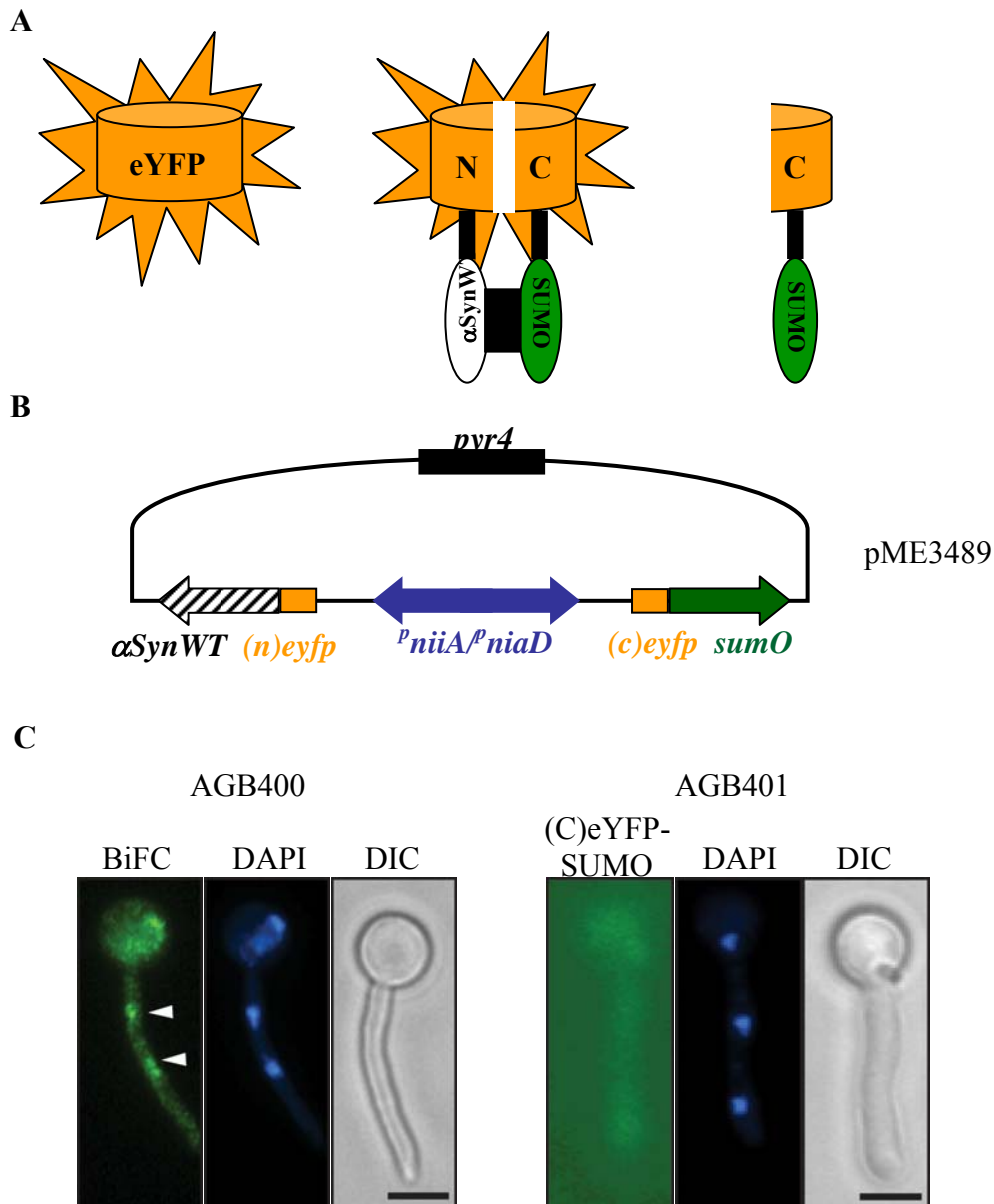


**Fig. 20: Interaction between SUMO and  $\alpha$ SynWT in *A. nidulans*.**

(A) Scheme of the bimolecular fluorescence complementation (BiFC). The N- and C-terminal parts of the enhanced yellow fluorescent protein (eYFP, left) are fused to two proteins of interest, e.g.,  $\alpha$ SynWT and SUMO. In case the proteins interact, the eYFP halves are close enough to each other that yellow fluorescence is emitted (middle). No emission is seen when only one protein is fused to a half of eYFP (right). (B) *(n)eyfp::αSynWT* and *(c)eyfp::sumO* fusions were constructed and cloned into pME3160 for expression from the bidirectional *niiA/niaD* promoter resulting in pME3489 (only the relevant genes are shown). (C) BiFC strain AGB400, expressing the *(n)eyfp::αSynWT* and *(c)eyfp::sumO* fusions, was cultivated in MM at 37°C for 14 h. Interaction of  $\alpha$ SynWT and SUMO can be observed by YFP emission predominantly in the nuclei indicated by white arrowheads (left). Colocalization with the nuclei is shown by DAPI staining. In the control strain AGB401 expressing only *(c)eyfp::sumO*, no YFP signal can be seen (right). Scale bars, 10  $\mu$ m. DAPI, 4',6'-Diamino-2'-phenylindol. DIC, differential interference contrast.

In AGB400, fluorescence was detected indicating that  $\zeta$ Syn<sup>WT</sup> and SUMO interact (Fig. 20C, left). Counterstaining with 4'-6'-Diamino-2'-phenylindol (DAPI) revealed that this interaction took predominantly place in the nuclei. In contrast, the strain AGB401 expressing only *(c)eyfp::sumO* showed no YFP emission (Fig. 20C, right).

These data clearly demonstrate that  $\alpha$ Syn<sup>WT</sup> is sumoylated *in vivo* by the fungal SUMO1-like protein SUMO of *A. nidulans*.

### 3.2.2 Expression of $\zeta$ Syn in a wild type strain and the $\Delta$ sumO mutant of *A. nidulans*

Since sumoylation of  $\alpha$ Syn<sup>WT</sup> was shown *in vivo* in *A. nidulans*, the importance of this modification for  $\alpha$ Syn was to be elucidated. For this purpose, heterologous expression effects of  $\zeta$ Syn were analyzed with regard to sumoylation in *A. nidulans*.

In earlier studies, it was reported that point mutations in the  $\zeta$ Syn gene as well as multiplications of the  $\zeta$ Syn<sup>WT</sup> allele cause Parkinson's disease (Ahn *et al.*, 2008; Cookson, 2005; Krüger *et al.*, 1998; Singleton *et al.*, 2003). Furthermore, it was shown that more than one copy of some  $\zeta$ Syn alleles is necessary to show a growth defect in *S. cerevisiae* (Outeiro and Lindquist, 2003).

Therefore, various  $\zeta$ Syn alleles were integrated up to threefold in the genome of the wild type strain AGB152 and of the  $\Delta$ sumO strain AGB339 of *A. nidulans*. The  $\zeta$ Syn alleles *WT*, *A53T*, and *A30P* were cloned into pME3321 harbouring the inducible *alcA* promoter (Fig. 21A) for regulable expression in *A. nidulans*. Transformants were analyzed by Southern hybridization using an *alcA* promoter probe (Fig. 21B). DNA restriction with *MseI* resulted in a 1.5 kb fragment containing the *alcA* promoter of the integrated plasmid and a 500 bp fragment with the authentic *alcA* promoter (Fig. 21B). The expression of the integrated  $\zeta$ Syn alleles was confirmed by Western hybridization experiments using an anti- $\zeta$ Syn antibody. As an example, the Southern and Western hybridization analyses of the *sumO* wild type strains AGB361, AGB362, and AGB363 are shown harbouring one, two, and three copies of the  $\zeta$ Syn<sup>WT</sup> allele, respectively (Fig. 21C).

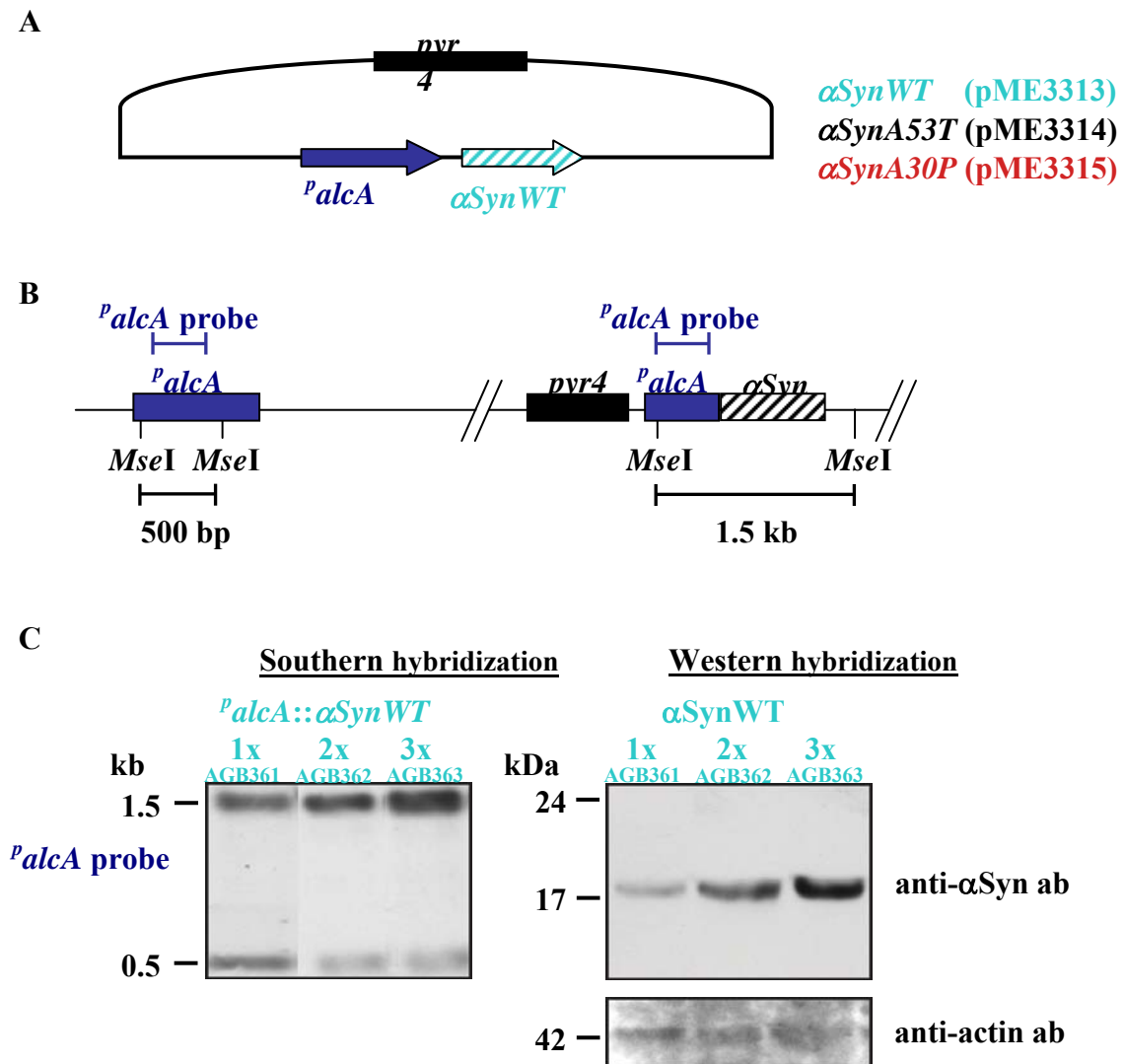


**Fig. 21: Expression of  $\zeta$ Syn alleles in *A. nidulans*.**

(A) Schematic view of pME3321. *αSyn*WT, A53T, and A30P were cloned into the plasmid pME3321 for expression from the inducible *alcA* promoter resulting in pME3313, pME3314, and pME3315. (B) Southern hybridization strategy. Application of an *alcA* promoter probe to determine the number of ectopic integrations of the  $\zeta$ Syn plasmids after transformation into *A. nidulans*. Digestion with the restriction enzyme *MseI* leads to the detection of two signals, one with a size of 0.5 kb, which results from binding to the authentic *alcA* promoter and a second signal of 1.5 kb as a consequence of detecting the *alcA* promoter sequence of the integrated plasmids. (C) Example of Southern and Western hybridization analyses of the *sumO* wild type strains AGB361, AGB362, and AGB363 expressing one, two, and three copies of  $\zeta$ SynWT, respectively. By comparing the signal intensities of the bands detected from the authentic *alcA* promoter and from the promoter sequence of the plasmids in Southern hybridization experiments, the number of the integrations can be determined (left). For Western hybridization experiments, strains were grown in MM containing 2% glucose at 37°C for 20 h followed by a shift to MM containing 2% glycerol / 2% ethanol for 6 h.  $\zeta$ SynWT can be detected at a size of 17 kDa in Western hybridization experiments with 60  $\mu$ g crude extract and anti- $\zeta$ Syn antibody. The protein amount increases from left to right due to increasing numbers of

$\zeta$ Syn<sup>WT</sup> copies (right). Utilization of an anti-actin antibody demonstrates equal protein amount (right, bottom row).

Appropriate control strains were received by transformation of the empty expression plasmid pME3321 into AGB152 and AGB339 designated AGB379 and AGB349, respectively.

Thus, viable *A. nidulans* strains were obtained expressing various  $\alpha$ Syn alleles in wild type and  $\Delta$ sumO background.

### 3.2.3 Expression of three copies of $\zeta$ SynA30P in the $\Delta$ sumO mutant leads to a one-third growth reduction in *A. nidulans*

In the single cell organism *S. cerevisiae*, the expression of more than one copy of human  $\alpha$ Syn<sup>WT</sup> or A53T led to growth inhibition (Outeiro and Lindquist, 2003). The expression of  $\alpha$ Syn has not been tested in a eukaryotic multicellular fungus like *A. nidulans* yet. In addition, since *S. cerevisiae* harbours an essential SUMO1-like gene, SMT3, the expression of different  $\alpha$ Syn alleles in *A. nidulans* provides the advantage to analyze the impact of sumoylation on different  $\alpha$ Syn proteins in a viable  $\Delta$ sumO background.

Therefore, vegetative growth tests were conducted with wild type and  $\Delta$ sumO strains of *A. nidulans*. Due to the findings in *S. cerevisiae*, these strains harboured different numbers of each  $\alpha$ Syn allele.

A definite number of spores was inoculated on solid media containing glycerol and ethanol for the induction of the *alcA* promoter to observe growth changes due to the expression of the  $\zeta$ Syn alleles. Accordingly, glucose-containing solid media was used repressing the *alcA* promoter to ensure that growth effects did not depend on the site of integration. The colony size of the strains was measured over a period of seven days.

Under repressing conditions, the strains harbouring three copies of  $\zeta$ Syn<sup>WT</sup>, A53T, and A30P both in the wild type background (AGB363, AGB366, AGB369) and the  $\Delta$ sumO background (AGB342, AGB345, AGB348) grew comparable to the corresponding control strains AGB379 and AGB349 (no  $\zeta$ Syn) (Fig. 22A, B left). Hence, the threefold integration of the  $\zeta$ Syn alleles carrying plasmids did not impair the growth behaviour of the respective strains. Silimar observations were made with strains harbouring either one or two copies of the respective  $\zeta$ Syn plasmids (data not shown). Under inducing conditions, the strains

expressing three copies of  $\zeta$ Syn $WT$  or  $A53T$  both in the  $sumO$  wild type and  $\Delta sumO$  background did not show any apparent growth alterations in comparison to the control strains (no  $\langle$ Syn) (Fig. 22A, B right). Same was observed for strains harbouring either one or two copies of the corresponding  $\zeta$ Syn alleles (data not shown).

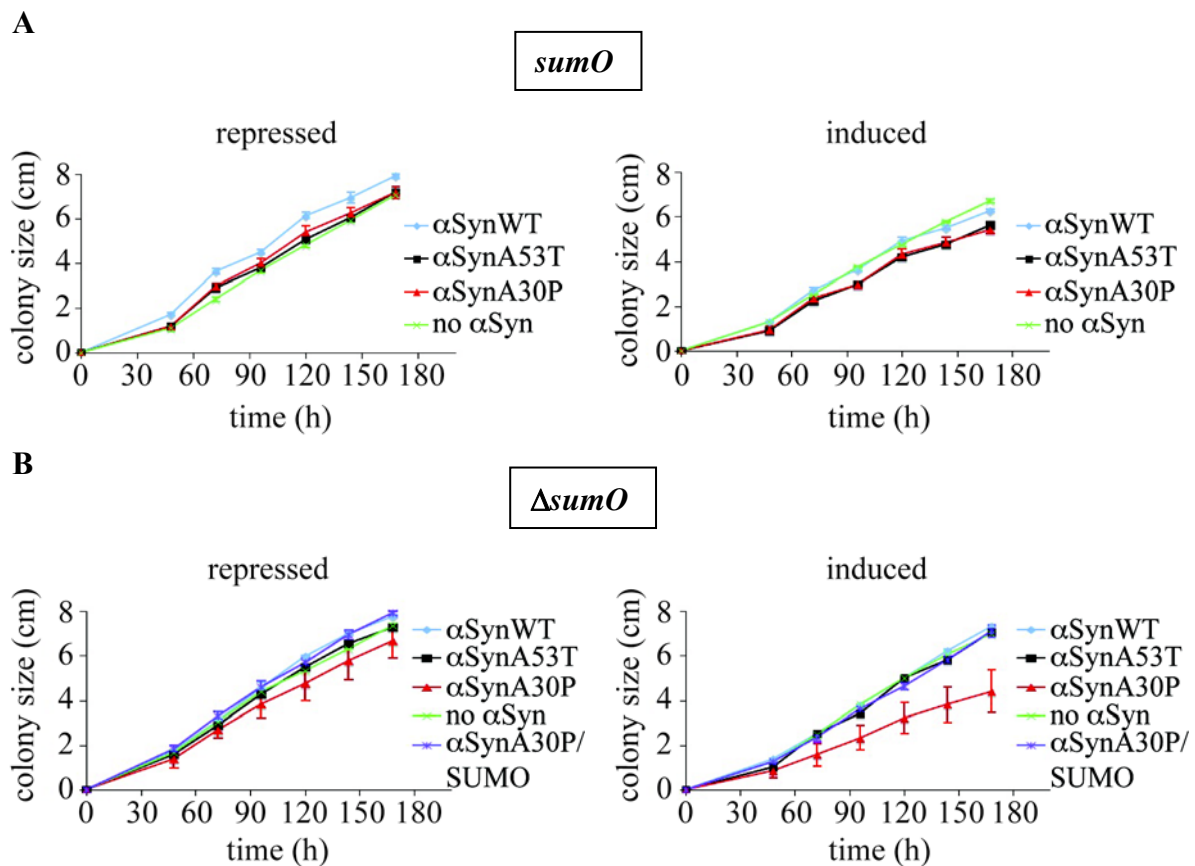


**Fig. 22: High expression of  $\zeta$ Syn $A30P$  reduces the vegetative growth rate in a  $\Delta sumO$  mutant strain of *A. nidulans* by approximately one-third.**

Strains were grown on solid MM containing 2% glucose for repression and 2% glycerol / 2% ethanol for induction of the *alcA* promoter, respectively. 2  $\mu$ l of the respective spore suspension containing 500 spores were spotted onto MM plates in triplicate and the colony size was measured every day over 168 h. (A) Expression of three copies of the  $\zeta$ Syn alleles  $WT$  (AGB363),  $A53T$  (AGB366), and  $A30P$  (AGB369), respectively, in the  $sumO$  wild type background ( $sumO$ ), shows no difference in vegetative growth over 168 h compared to a control strain (AGB379) without  $\langle$ Syn) (no  $\langle$ Syn). (B) The corresponding  $\Delta sumO$  strains expressing the  $\zeta$ Syn alleles display normal growth under repressive conditions (left). While the vegetative growth of the  $\Delta sumO$  mutant strains harbouring three copies of  $\zeta$ Syn $WT$  (AGB342) and  $A53T$  (AGB345), respectively, was similar to the control strain (AGB349) (no  $\langle$ Syn) under inducing conditions, the  $\Delta sumO$  mutant expressing three copies of  $\zeta$ Syn $A30P$  (AGB348) displays impaired vegetative growth (right). Reconstitution of  $sumO$  in AGB348 resulting in AGB397 ( $\zeta$ Syn $A30P$ /SUMO) fully restores the growth impairment of AGB348 under inducing conditions.

In contrast to this, the  $\Delta sumO$  mutant bearing three copies of  $\zeta SynA30P$  (AGB348) showed an obvious growth defect (Fig. 22B, right), while the analogous strain in the *sumO* wild type background (AGB369) displayed normal growth (Fig. 22A, right). This reduction in growth could not be seen for strains expressing either one or two copies of  $\zeta SynA30P$  (data not shown).

The growth rates of AGB348 and of the corresponding control strain AGB349 were determined revealing that AGB348 (0,0295 cm/h) accomplished only 63% of the growth rate of AGB349 (0,0472 cm/h). To ensure that this growth reduction was due to absent sumoylation, a respective complementation strain was constructed by transforming the reconstitution plasmid pME3319 into AGB348 giving AGB397 ( $\zeta SynA30P/SUMO$ ). Like the other strains, AGB397 was analyzed in respect of vegetative growth and a normal growth rate of 0,0493 cm/h (105%) compared to AGB349 was observed under inducing conditions (Fig. 22B, right). Thus, it was shown that expression of three copies of  $\alpha SynA30P$  in a  $\Delta sumO$  mutant strain of *A. nidulans* led to impairment of vegetative growth. These data show that the fungus tolerates the expression of even higher levels of  $\zeta SynWT$  and  $A53T$  independently of sumoylation, while unsumoylated  $\zeta SynA30P$  causes growth reduction in a concentration-dependent manner in *A. nidulans*.

#### **3.2.4 Expression of three copies of $egfp::\zeta SynA30P$ in the $\Delta sumO$ mutant confirms growth reduction in *A. nidulans***

The  $\zeta Syn$  protein has an increased propensity to form aggregates and this property was analyzed in *A. nidulans* wild type and  $\Delta sumO$  strains to elucidate the role of sumoylation in this context.

For this purpose,  $egfp::\zeta SynWT$ ,  $A53T$ , and  $A30P$  fusion constructs driven by the inducible *alcA* promoter were transformed into the wild type strain AGB152 as well as into the  $\Delta sumO$  strain AGB339. Similar to the analysis of the primarily constructed  $\zeta Syn$  strains, the ectopical integration of the  $egfp::\zeta Syn$  fusion plasmids was confirmed by Southern hybridization experiments to obtain strains with one to three copies of each  $egfp$  fusion construct (data not shown). In the *sumO* wild type background, the strains harbouring three

copies of *egfp:: $\zeta$ Syn<sup>WT</sup>*, *egfp:: $\zeta$ Syn<sup>A53T</sup>*, and *egfp:: $\zeta$ Syn<sup>A30P</sup>* were designated AGB372, AGB375, and AGB378, respectively, and in the  $\Delta$ *sumO* background AGB353, AGB356, and AGB359, respectively. As appropriate control strains served the *sumO* wild type strain AGB190 (Busch *et al.*, 2007) expressing one copy of *sgfp* and the  $\Delta$ *sumO* strain AGB387 harbouring three copies of *gfp2-5*. The *gfp* expression in the control strains was also driven by the *alcA* promoter.

All strains were tested with regard to vegetative growth to compare expression effects of the *egfp:: $\zeta$ Syn* fusion constructs with the  $\zeta$ *Syn* harbouring strains. Under repressing conditions, the strains expressing three copies of  $\zeta$ *Syn<sup>WT</sup>*, *A53T*, and *A30P* both in the wild type and in the  $\Delta$ *sumO* background, grew comparable to the corresponding control strains (no  $\zeta$ *Syn*) (Fig. 23A, B left). Similar observations were made with strains harbouring either one or two copies of the respective  $\zeta$ *Syn* plasmids (data not shown). Under inducing conditions, the strains expressing either three copies of *egfp:: $\zeta$ Syn<sup>WT</sup>* or *egfp:: $\zeta$ Syn<sup>A53T</sup>* displayed regular growth compared to the corresponding control strains in the wild type and  $\Delta$ *sumO* background (Fig. 23A, B right).

The same was observed for the strains harbouring either one or two copies of the respective *egfp:: $\zeta$ Syn* allele (data not shown). While threefold expression of *egfp:: $\zeta$ Syn<sup>A30P</sup>* in the wild type strain AGB378 exhibited normal growth (Fig. 22A, right), the accordant  $\Delta$ *sumO* mutant AGB359 revealed growth reduction under inducing conditions (Fig. 23B, right), which could not be observed for the  $\Delta$ *sumO* strains with one or two copies of *egfp:: $\zeta$ Syn<sup>A30P</sup>* (data not shown). Growth rates were determined, displaying that AGB359 (0,033 cm/h) achieved only 66% of the growth rate of the corresponding control strain AGB387 (0,05 cm/h).

These observations demonstrate that expression of *gfp:: $\alpha$ Syn* fusion constructs resemble the phenotype shown by  $\alpha$ *Syn* harbouring strains namely that higher levels of unsumoylated  $\alpha$ *Syn<sup>A30P</sup>* lead to growth reduction in *A. nidulans*. Therefore, the  $\alpha$ *Syn* fusion proteins appear to be functional and represent a useful tool for the following studies.

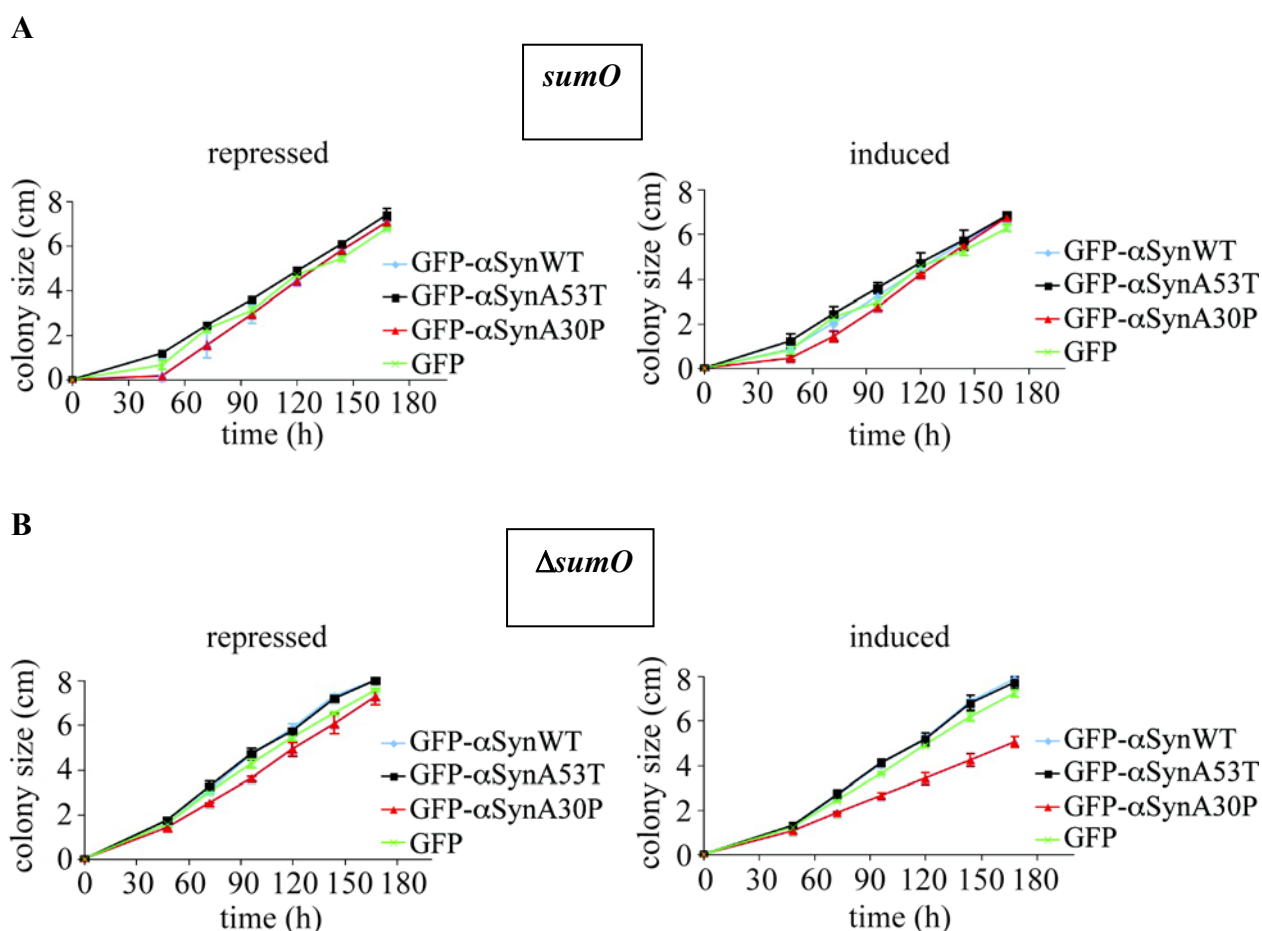


**Fig. 23: Expression of three copies of *egfp::SynA30P* leads to growth inhibition in the  $\Delta$ *sumO* mutant of *A. nidulans*.**

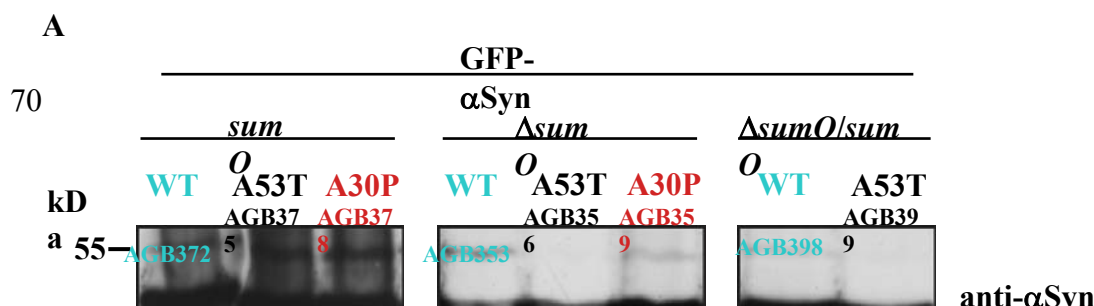
Strains were grown on solid MM containing 2% glucose for repression and 2% glycerol / 2% ethanol for induction of the *alcA* promoter, respectively. 2  $\mu$ l of the respective spore suspension containing 500 spores were spotted onto MM plates in triplicate and the colony size was measured every day over 168 h. (A) Expression of three copies of the *egfp::Syn* alleles *WT* (AGB372), *A53T* (AGB375), and *A30P* (AGB378), respectively, in the *sumO* wild type background (*sumO*) shows no difference in vegetative growth over 168 h compared to a control strain with *sgfp* expression (AGB190) (GFP). (B) Under repressing conditions, the corresponding  $\Delta$ *sumO* strains expressing the *egfp::Syn* alleles show normal growth (left). In contrast, the  $\Delta$ *sumO* strain harbouring three copies of *egfp::SynA30P* (AGB359) displays growth impairment under inducing conditions in opposition to strains expressing three copies of *egfp::SynWT* (AGB353) or *egfp::SynA53T* (AGB356), which display normal vegetative growth like the control strain with *gfp2-5* expression (GFP, AGB387) (right).

### 3.2.5 Sumoylation stabilizes GFP- $\zeta$ SynWT and GFP- $\zeta$ SynA53T in *A. nidulans*

The  $\zeta$ Syn harbouring strains and the respective *gfp::\zeta*Syn expressing strains showed similar phenotypes with regard to vegetative growth. Therefore, the subsequent  $\zeta$ Syn experiments were conducted with the latter strains in terms of correlating developmental observations with protein localization. Because one and two copies of the  $\zeta$ Syn variants did not have an effect on *A. nidulans*, the strains expressing three copies of each *gfp::\zeta*Syn fusion allele were used for further experiments.

It was shown that *A. nidulans* tolerates the expression of higher levels of *aSyn*WT and *A53T* regardless of sumoylation. Same could be observed for *aSynA30P* until a certain threshold is reached in the  $\Delta$ *sumO* strain. To investigate, whether differences in the steady state levels of the fusion proteins are implicated in these findings, Western hybridization experiments of the respective wild type and  $\Delta$ *sumO* strains were conducted. For Western hybridization, an anti- $\zeta$ Syn antibody (Fig. 24A) as well as an anti-GFP antibody (data not shown) were used. In the wild type background (*sumO*), GFP- $\zeta$ SynWT, A53T, and A30P fusion proteins with a size of 46 kDa appeared to be evenly produced in high amounts (Fig 24A, left). Quantification of the detected bands revealed that the GFP- $\zeta$ SynA30P amount in the  $\Delta$ *sumO* strain was only slightly reduced by 19% (AGB339) compared to the protein level in the wild type background (AGB378) (Fig. 24A, B). By contrast, the amount of the GFP- $\zeta$ SynWT and GFP- $\zeta$ SynA53T proteins was strongly diminished in the *sumO* deletion strains AGB353 and AGB356, respectively, ( $\Delta$ *sumO*) (Fig. 24A, middle). The protein amount of GFP- $\zeta$ SynWT in AGB353 equalled only 45% of the respective fusion protein in AGB372 (Fig. 24B). In case of GFP- $\zeta$ SynA53T (AGB356), 49% of the fusion protein was detected in comparison to the corresponding *sumO* wild type strain AGB375 (Fig. 24B). Both strains were complemented with *sumO* by transforming AGB353 and AGB356 with the reconstitution plasmid pME3319 resulting into AGB398 and AGB399. In the *sumO* reconstitution strains ( $\Delta$ *sumO/sumO*), the protein amount of GFP- $\zeta$ SynWT and GFP-A53T was elevated to 80% and 63%, respectively, of the protein amount in the corresponding wild type strains AGB372 and AGB375 (Fig. 24A, B right).

These data suggest that sumoylation stabilizes GFP- $\zeta$ SynWT and GFP- $\zeta$ SynA53T on the protein level.



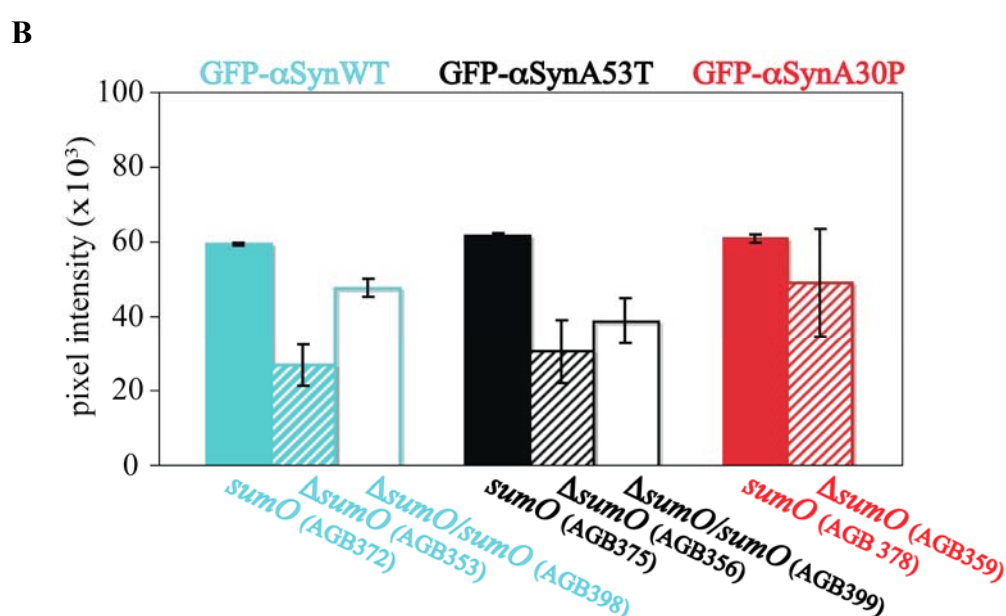
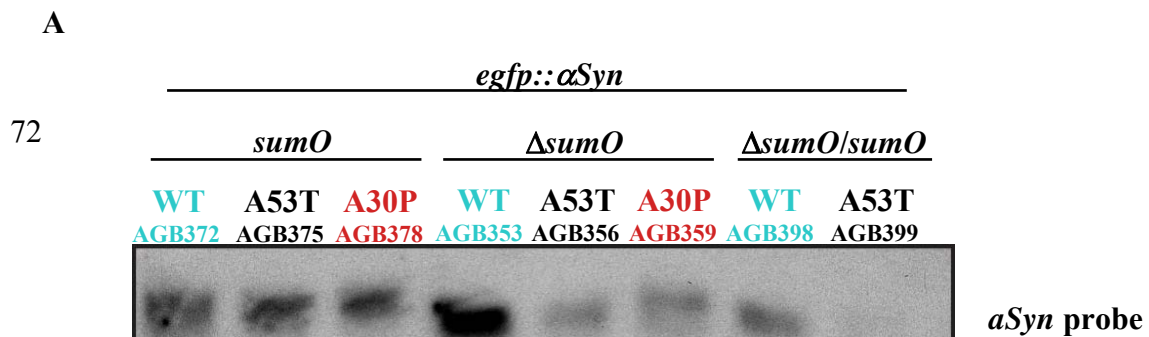


**Fig. 24: Western hybridization analysis of strains expressing *gfp::Syn* variants in *A. nidulans*.**

Strains were grown in MM containing 2% glucose at 37°C for 20 h followed by a shift to MM containing 2% glycerol / 2% ethanol for 6 h. (A) Western hybridization using an anti- $\zeta$ Syn antibody and 100  $\mu$ g of crude extract show comparable expression of three copies of *egfp::Syn*WT, *A53T*, and *A30P* in the *sumO* wild type strains AGB372, AGB375, and AGB378, respectively (left). In the corresponding  $\Delta$ *sumO* strains (AGB353 and AGB356), the amounts of GFP- $\zeta$ SynWT and GFP- $\zeta$ SynA53T are significantly reduced, whereas only a slight decrease of GFP- $\zeta$ SynA30P can be observed in AGB359 (middle). The *sumO* reconstitution in the  $\Delta$ *sumO* strains expressing *egfp::Syn*WT and *egfp::SynA53T* (AGB398 and AGB399) leads to an increase of the protein amounts. Utilization of an anti- $\alpha$ -tubulin antibody demonstrated equal loading of protein (bottom row). (B) Quantification analysis of the detected bands in the Western hybridization experiments.

To distinguish between a posttranscriptional or transcriptional effect causing reduced protein amounts of GFP- $\zeta$ SynWT and GFP- $\zeta$ SynA53T, Northern hybridization experiments

were performed using a  $\zeta$ Syn probe (Fig.25A). In contrast to the protein level of GFP- $\zeta$ SynWT, the appropriate mRNA amount is increased in the  $\Delta$ sumO mutant AGB353 (Fig. 25A). Quantification of the detected bands revealed an elevation of 87% of *egfp:: $\zeta$ SynWT* mRNA compared to the respective wild type background strain AGB372 and the intensity of the signal is more than threefold higher as the signal of the complementation strain AGB398 (Fig. 25B). In case of the GFP- $\zeta$ SynA53T variant, the mRNA alterations resembled the differences of the protein levels observed in Western hybridization experiments (Fig. 24) except for the corresponding *sumO* complementation strain AGB399 (Fig. 25A). Quantification of the mRNA amount of *egfp:: $\zeta$ SynA53T* in AGB356 displayed a decrease of 65% compared to the wild type strain AGB375, while the mRNA level of *egfp:: $\zeta$ SynA53T* in the *sumO* reconstitution strain AGB399 is decreased to 6% in comparison to AGB356 (Fig. 25B). In respect of the mRNA level of *egfp:: $\zeta$ SynA30P*, a decline of 39% was observed in the  $\Delta$ sumO mutant AGB359 compared to the corresponding wild type background strain AGB378 (Fig. 25A, B), which is higher than the decrease noted in the Western hybridization analysis (Fig. 24).



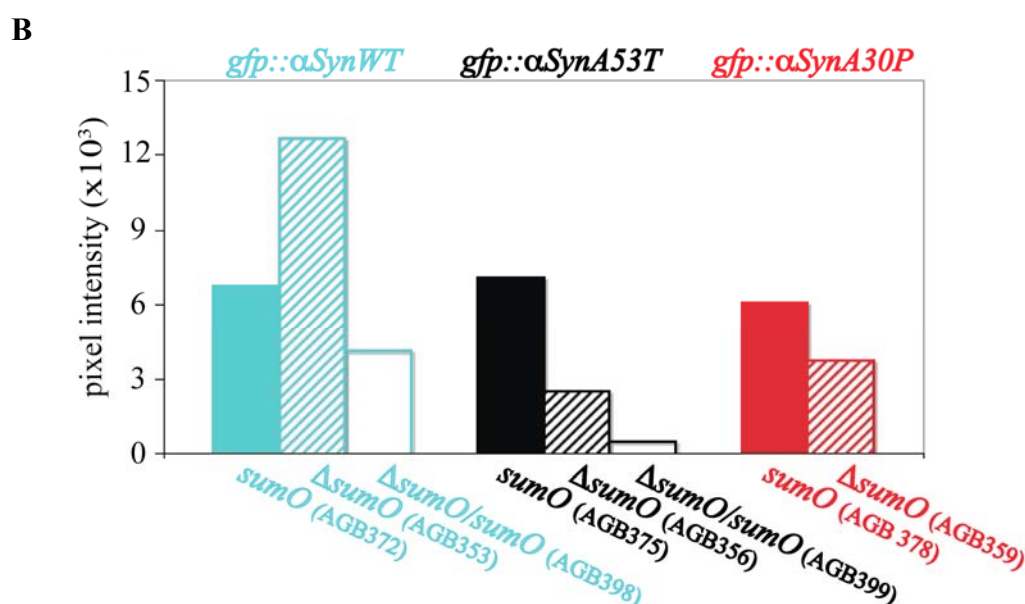


**Fig. 25: Northern hybridization analysis of *A. nidulans* strains expressing *gfp::Syn* variants.**

Strains were grown in MM containing 2% glucose at 37°C for 20 h followed by a shift to MM containing 2% glycerol / 2% ethanol for 6 h. (A) Northern hybridization using a *Syn* probe and 25 μg of RNA shows comparable transcription of three copies of *gfp::Syn*WT, *A53T*, and *A30P* in *sumO* wild type strains AGB372, AGB375, and AGB378, respectively. In the appropriate *ΔsumO* strains, the amount of *gfp::Syn*WT mRNA is significantly elevated in AGB353, whereas the mRNA level in the corresponding reconstitution strain AGB398 is decreased compared to the wild type strain AGB372. Examination of the mRNA amount of *gfp::Syn*A53T shows a strong decrease in the *ΔsumO* strain AGB356 and almost no respective mRNA could be detected in the complementation strain AGB399 compared to the wild type strain AGB375. Detection of the mRNA of *gfp::Syn*A30P shows a slight decrease in the *ΔsumO* AGB359 strain compared to the corresponding wild type strain AGB378. EtBr-stained rRNA evaluated equal loading of total RNA (lower panel). (B) Quantification analysis of the detected bands in the Northern hybridization experiments.

The Northern hybridization results appear to be contradictory with regard to observations made for vegetative growth tests and Western experiments. Especially the detected mRNA

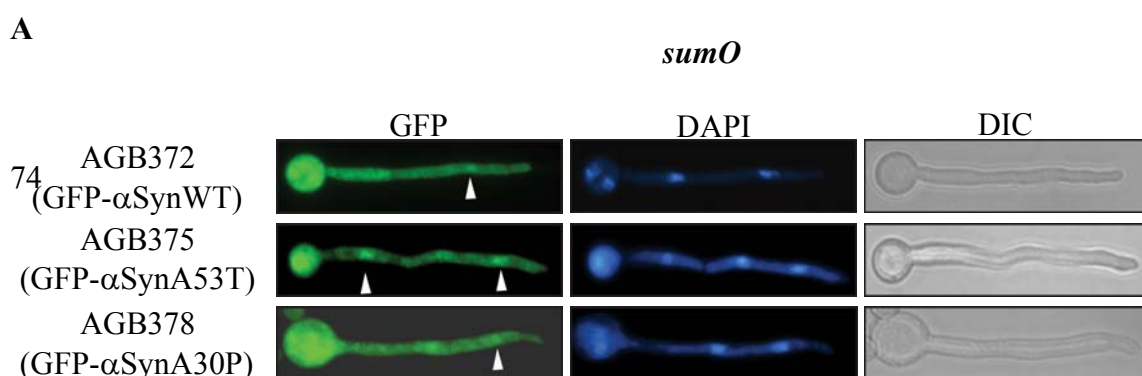
amounts of *gfp:: $\zeta$ Syn<sup>WT</sup>* and *A53T* in the complementation strains in comparison to the corresponding  $\Delta$ *sumO* strains appear to be elusive. However, the mRNA levels observed for the three  $\zeta$ *Syn* alleles in the *sumO* wild type strains suggest equal transcription of *gfp:: $\zeta$ Syn<sup>WT</sup>*, *A30P* and *A53T* confirming Western experiment data.

In summary, Western results propose that GFP- $\zeta$ Syn<sup>WT</sup> and GFP- $\zeta$ Syn<sup>A53T</sup> are stabilized by sumoylation on the protein level, which could be due to an interference with the degradation pathway of  $\alpha$ Syn in *A. nidulans*, e.g., by antagonizing the conjugation of ubiquitin to these proteins. With respect to the similarities observed for growth effects displayed by untagged and *gfp*-tagged  $\alpha$ Syn expressing strains, it can be proposed that the respective untagged  $\zeta$ Syn proteins behave in a similar way.

### 3.2.6 Aggregation of GFP- $\zeta$ Syn<sup>A53T</sup> in the $\Delta$ *sumO* mutant of *A. nidulans*

In *S. cerevisiae*, cytoplasmic aggregation of  $\alpha$ Syn<sup>WT</sup> and A53T was described (Outeiro and Lindquist, 2003). To analyze this circumstance in *A. nidulans* with respect to the sumoylation of  $\alpha$ Syn, the intracellular localization of the GFP- $\zeta$ Syn fusion proteins was observed by fluorescence microscopy. In addition, DAPI staining was performed to visualize the position of the nuclei (Fig. 26). Fluorescence signalling of GFP- $\zeta$ Syn<sup>WT</sup>, A53T and A30P was observed in the cytoplasm of the entire hyphae in AGB372, AGB375, and AGB378, respectively (*sumO*) (Fig. 26A). Furthermore, a slightly higher GFP emission was seen in the nuclei illustrated by white arrowheads and affirmed by respective DAPI staining.

In the  $\Delta$ *sumO* background, fluorescence signalling of GFP- $\zeta$ Syn<sup>WT</sup> (AGB353) and GFP- $\zeta$ Syn<sup>A30P</sup> (AGB359) was observed in the cytoplasm of the entire hyphae without nuclear enrichment (Fig. 26B), but in case of  $\zeta$ Syn<sup>WT</sup>, the emission was strongly reduced compared to the corresponding wild type strain AGB372. The *sumO* complementation strain AGB398 showed an enhancement of the cytoplasmic GFP- $\zeta$ Syn<sup>WT</sup> signal (Fig. 26B).



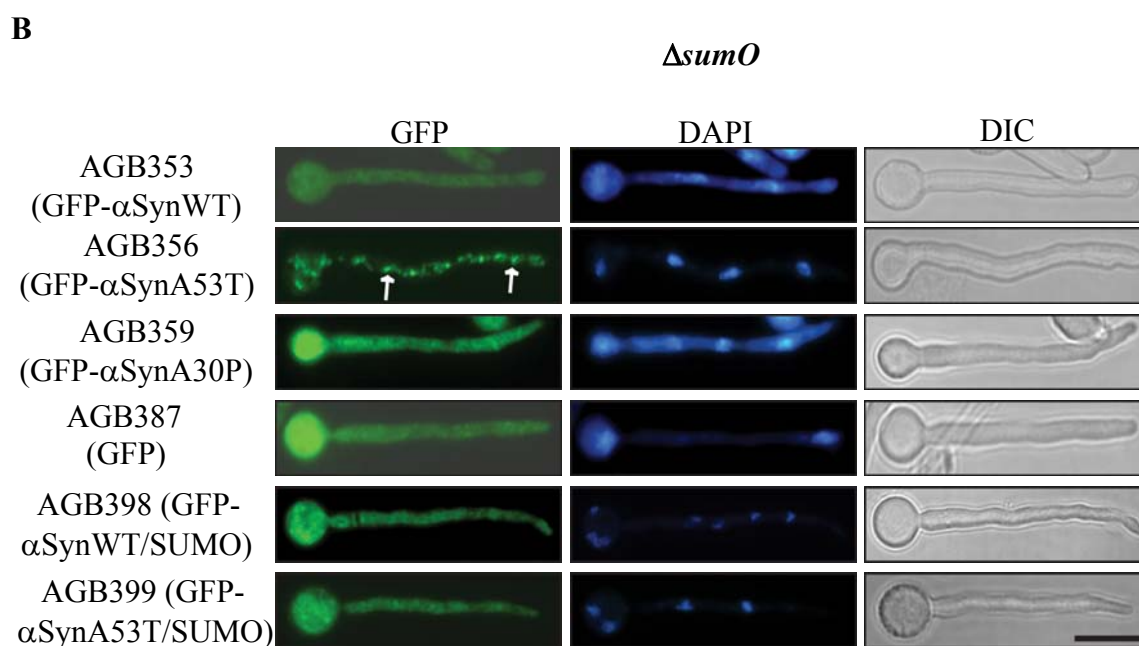


**Fig. 26: Localization of GFP- $\langle$ Syn variants in *A. nidulans*.**

(A) Wild type strains (*sumO*), expressing three copies of *gfp::\langle*SynWT (AGB372), *gfp::\langle*SynA30P (AGB378) and *gfp::\langle*SynA53T (AGB375), respectively, show evenly distributed GFP- $\langle$ Syn signalling over the entire hypha with slight enrichment in the nuclei (white arrowheads). The cytoplasmic localization pattern resembles GFP signalling in the control strain AGB190 (GFP). (B) The cytoplasmic emission of GFP- $\langle$ SynWT in the  $\Delta sumO$  mutant AGB353 is decreased without nuclear enrichment in comparison to the corresponding wild type strain AGB372 in (A). Complementation of *sumO* in AGB353 increases fluorescence in AGB398 ( $\langle$ SynWT/SUMO). Aggregation formation by GFP- $\langle$ SynA53T in AGB356 (white arrows) is prevented by reconstitution of *sumO* in AGB399 ( $\langle$ SynA53T/SUMO). The cytoplasmic localization of GFP- $\langle$ SynA30P is unaltered in AGB359 and resembles the analogous wild type strain AGB378 without nuclear enrichment. DAPI staining of all strains displays nuclear positions. All strains were grown in MM containing 2% glycerol / 2% ethanol at 37°C for 14 h. Scale bars, 10  $\mu$ M. DAPI, 4'-6'-Diamino-2'-phenylindol. DIC, differential interference contrast.

Regarding the detection of GFP- $\langle$ SynA53T in the  $\Delta sumO$  strain AGB356, an alteration in the localization pattern was observed compared to the corresponding wild type strain

AGB375. Aggregates of GFP- $\langle$ SynA53T were found in the cytoplasm of AGB356 (Fig. 26B, white arrows). This circumstance could be prevented, by complementing AGB356 with *sumO* resulting in AGB399, which displayed cytoplasmic GFP signalling again (Fig. 26B).

The observation of the weaker GFP- $\langle$ SynWT signalling in the  $\Delta$ *sumO* strain AGB353 compared to the wild type strain AGB372 and the *sumO* complementation strain AGB398, confirm the Western hybridization results substantiating a stabilization role for SUMO. Additionally, the amount of cytoplasmic GFP- $\langle$ SynA30P remained unchanged in AGB359 compared the wild type strain AGB378 except for the nuclear enrichment confirming only slight protein reduction in Western hybridization data.

It has to be noted that the complementation strains for GFP- $\langle$ SynWT and A53T (AGB398, AGB399) could not restore the nuclear enrichment seen for the corresponding wild type strains AGB372 and AGB375, respectively. The observation that only partial complementation is achieved, was also noted for Western experiments, which might be due to ectopical integration of the *sumO* reconstitution plasmid. However, the nuclear enrichment seen for all three  $\langle$ Syn forms in the wild type but not in the corresponding  $\Delta$ *sumO* strains strongly suggests that this observation is SUMO-dependent and might be a result of sumoylation of the different  $\langle$ Syn variants in the nucleus.

With respect to the aggregation of GFP- $\langle$ SynA53T in the  $\Delta$ *sumO* strain AGB356, these data suggest that sumoylation impedes the aggregation of GFP- $\langle$ SynA53T and presumably also of untagged  $\langle$ SynA53T in *A. nidulans*.

### 3.3 Localization studies on NUDC in *A. nidulans*

#### 3.3.1 NUDC is localized to immobile dots at the cell cortex

Besides the examination of  $\alpha$ Syn in *A. nidulans*, the nuclear distribution protein NUDC was analyzed in this work. Like  $\alpha$ Syn, mammalian NUDC is associated with a neuronal disease namely lissencephaly type 1. In *A. nidulans* it was shown that fungal NUDC stabilizes the nuclear distribution protein NUDF posttranslationally, the human homolog which is LIS1 (Xiang *et al.*, 1995a). Mutations in the *Lis1* gene lead to impaired neuronal migration causing autosomal-dominant lissencephaly type 1 (Dobyns *et al.*, 1993; Hirotsumi *et al.*, 1998). Similarly, nuclear migration defects are the consequence of mutations in the *nudF* gene of *A. nidulans* (Xiang *et al.*, 1995a). Due to the fact that the biochemical function of NUDC is still unknown, the precise mechanism of NUDF regulation remains unclear. Therefore, NUDC was characterized in more detail to gain some insights in the regulation of NUDF as well as in the implication of NUDC in the nuclear migration process. As a first step towards deciphering its molecular function, NUDC was localized in *A. nidulans*.

An *P<sub>alcA</sub>::nudC::sgfp* fusion was expressed in the *nudC3* strain (AGB241) and the functionality of the fusion protein was confirmed by complementation of the temperature-sensitive *nudC3* phenotype by growing AGB241 at 42°C (data not shown). Fluorescence microscopy was performed and NUDC-GFP was observed as immobile dots along hyphae, obviously near the cytoplasmic membrane (data not shown). Furthermore, immunoelectron microscopy was conducted for a more detailed view of the NUDC-GFP position. In fact, NUDC-GFP was detected at the hyphal cortex with isolated spots in the cytoplasm (Fig. 27). In the enlarged tip section, NUDC decorated the cortex also around the hyphal tip. Thus, the majority of NUDC obviously localized differently from NUDF which was detected at spindle poles and microtubule plus-ends.

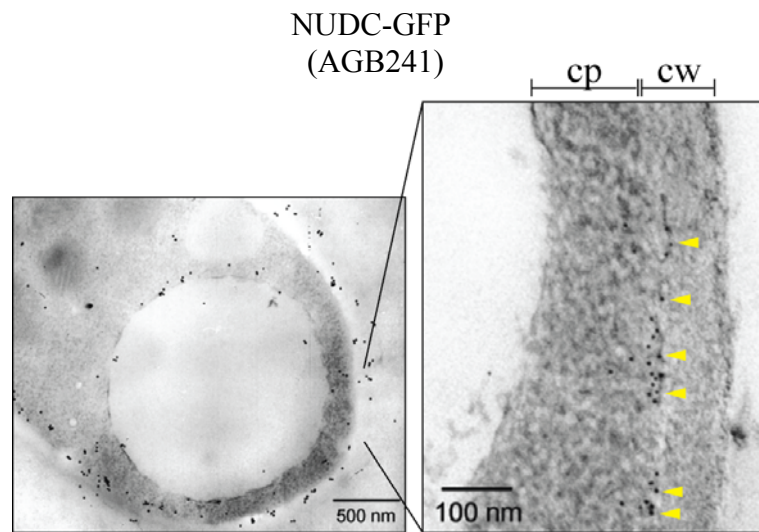


**Fig. 27: NUDC is localized to immobile dots at the *A. nidulans* hyphal cortex.**

Immunoelectron microscopy of strain AGB241 shows that NUDC-GFP dots are positioned along the hyphal cortex and the tip (examples are indicated by arrowheads). The strain was grown in MM containing 2% ethanol at 42°C for 15 h. The abbreviations mean cytoplasm (cp) and cell wall (cw).

### 3.3.2 NUDF associates with NUDC at spindle pole bodies and at the cortex

In earlier studies, it was described that mammalian NUDC and the NUDF homolog LIS1 interact and colocalize (Hirotsume *et al.*, 1998). Although at first sight NUDF and NUDC localized at different sites in *A. nidulans*, the colocalization of their homologs in mammalian cells led to the investigation of the putative interaction between the *Aspergillus* proteins. An analysis of their association in a yeast two-hybrid assay was performed based on LexA and B42 fusions, respectively. It was intended to fuse NUDC to the B42 activation domain, but the fusion protein was not correctly expressed so that it could not be detected by Western hybridization (data not shown). Therefore, NUDC was fused to the LexA binding domain and this fusion was successfully detected by Western hybridization (data not shown). Association of LexA-NUDC with the B42-NUDF fusion was observed as indicated by expression of the *LEU2* and *lacZ* reporter genes (Fig. 28B). Furthermore, the domains should be specified by which the attachment between NUDF and NUDC is accomplished. Based on computer programs and the similarity to p23 (Garcia-Ranea *et al.*, 2002), NUDC was predicted to consist of an N-terminal coiled-coil helix which replaces a large coiled-coil domain of mammalian NUDC, a p23-like central domain (a  $\beta$ -sandwich), and an unknown C-terminal domain of 83 amino acids (Fig. 28A).

NUDF contains an N-terminal LisH dimerization motif followed by a coiled-coil helix and a large WD40 domain (a  $\beta$ -sheet propeller, Fig. 28A) (Kim *et al.*, 2004; Tarricone *et al.*, 2004). The parts of the open reading frames encoding these domains were fused to the respective two-hybrid domains and expressed in yeast in comparison to the full-length ORFs. The growth assay as well as the  $\beta$ -galactosidase filter assay revealed an interaction between the full-length NUDC and the WD40 domain of NUDF (Fig. 28B). In the growth assay, also a presumably false-positive interaction was detected between the coiled-coil domains of NUDF and NUDC through the expression of the more sensitive *LEU2* reporter construct. No interactions were observed involving the separate p23 and C-terminal domain of NUDC, respectively, although all fusion proteins were detected by Western hybridization (data not shown). Thus, using two-hybrid analysis, the interacting domain of NUDC could not be identified.

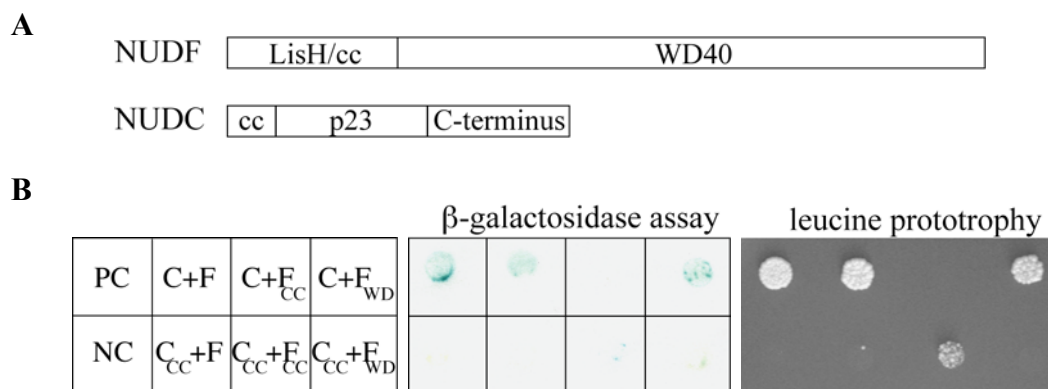


**Fig. 28 NUDF binds to NUDC via its WD40 domain.**

(A) NUDF consists of a LisH dimerization motif followed by a coiled-coil helix (cc) and a WD40 domain. NUDC was predicted to form an N-terminal coiled-coil helix, a p23 domain and a C-terminal domain of unknown structure. (B) In this yeast two-hybrid analysis, LexA-NUDC interacts with B42-NUDF and B42-NUDF<sub>WD40</sub> and induces *LEU2* and *lacZ* reporter gene expression (EGY48 pRB1840 pME3246 pME3237 and EGY48 pRB1840 pME3246 pME3243). NUDF binding to the coiled-coil of NUDE (EGY48 pRB1840 pME2938 pME2939) was used as positive control (PC). NUDF and the empty prey vector (EGY48 pRB1840 pME2938 pJG4-5) were used as the negative control (NC). cc: coiled-coil. WD: WD40 domain.

To confirm the NUDF-NUDC interaction *in vivo*, the method of BiFC was used. For that purpose, the N-terminal and C-terminal halves of eYFP were fused to NUDF and NUDC, respectively, to observe bimolecular fluorescence complementation in case both fusion proteins were in close contact with each other. The fusions were expressed from the

bidirectional *niiA/niaD* promoter and partially complemented the temperature-sensitive phenotypes when expressed in the *nudC3* and *nudF6* strain, respectively (AGB302, AGB303). These strains grew faster and produced more conidia than the temperature-sensitive parental strains at 42°C, but did not grow as fast as at 30°C which indicated partial functionality of the NUDF-nEYFP and NUDC-cEYFP fusions (data not shown). Although the eYFP emission was low, numerous dots were detected along hyphae, but also at nuclei, which were labelled by constitutive expression of an *mrfp::h2A* fusion (Fig 29A). Fluorescence was also detected at both poles of mitotic nuclei (Fig. 29A, lower row) showing that NUDF-NUDC interaction takes place at spindle pole bodies (SPBs) also during mitosis.

To clearly identify the colocalization of NUDC and NUDF at the spindle pole bodies, strain AGB335 was constructed harbouring the respective BiFC fusion construct and  $\gamma$ -tubulin (MIPA) fused to mRFP (Fig. 29B). In this strain again among several fainter fluorescent spots in the cytoplasm, a few prominent spots were observed, which could clearly be allocated to the mRFP-labelled spindle pole bodies. The SPBs often jerked in the cells, but were also found immobilized near the cortex in which case accurate superimposition with BiFC spots could be achieved best.

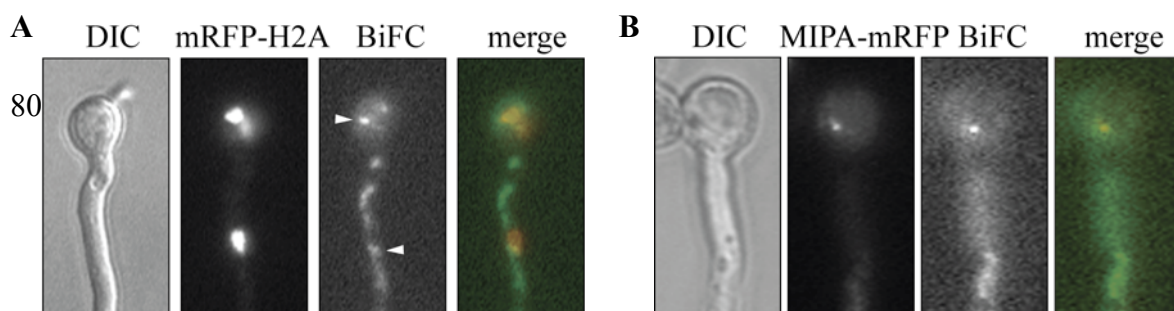


**Fig. 29: NUDF binds to NUDC at spindle pole bodies.**

(A) Bimolecular fluorescence complementation. Strain AGB303 expressing the *nudF::neyfp* and *nudC::ceyfp* fusions and the nuclear marker *mrfp::h2A* was cultivated in MM at 42°C for 8 h. Colocalization of NUDF and NUDC is shown through the fluorescence emission which can only be generated by the colocalization of the N- and C-terminal halves of eYFP (examples are indicated by arrowheads). Scale bars: 5 µm. (B) Bimolecular fluorescence complementation. Strain AGB335 expressing the BiFC constructs and the spindle pole body marker *mipA::mrfp* was grown in MM at 42°C for 8h. Scale bar: 5 µm.

To investigate whether the colocalization with SPBs could be confirmed for NUDC-GFP alone, a *nudC::gfp* fusion was introduced into a strain harbouring the *mipA::mrfp* fusion (AGB338, Fig. 30). In addition, *nudC* was not overexpressed, but expressed from the authentic promoter and was fused to the more stable *gfp2-5* version. In fact, NUDC-GFP spots could be colocalized with MIPA-mRFP signals, even in mitotic nuclei (Fig. 30, lower row).

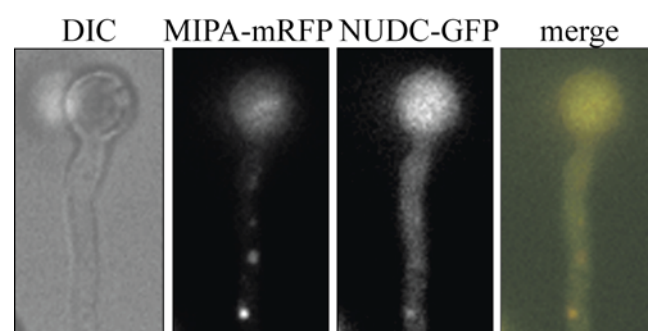


**Fig. 30: NUDC is localized at spindle pole bodies in *A. nidulans*.**

In strain AGB338, NUDC-GFP colocalizes with  $\gamma$ -tubulin (MIPA) at spindle pole bodies. The strain was grown in glucose-containing MM at room temperature for 8 h. Scale bar: 5  $\mu$ m.

These data demonstrate that NUDC and NUDF interact in *A. nidulans*. It was shown that the proteins colocalize at spindle pole bodies and at the cell cortex and that the association is mediated by the WD40 domain of NUDF. These findings correlate with observation in murine cells, where NUDC and LIS1 were colocalized at the microtubule organization center proposing fungal NUDC might be involved in spindle formation like hNUDC.

## 4 Discussion

In this study, a  $\Delta sumO$  mutant was phenotypically characterized, displaying various effects on the accomplishment of asexual and sexual development in *A. nidulans*.

Heterologous expression of  $\langle SynWT$  revealed that the human protein is sumoylated *in vivo* in *A. nidulans*, which had only been shown *in vitro* before. Expression of three copies of the  $\langle SynA30P$  variant significantly reduced growth of the  $\Delta sumO$  mutant. Without sumoylation, GFP- $\langle SynWT$  fusion proteins are less stable and GFP- $\langle SynA53T$  forms aggregates.

Localization studies on the nuclear distribution protein NUDC demonstrated that the protein is present at the cell cortex, in the cytoplasm and at spindle pole bodies of *A. nidulans*. The interaction of NUDC and NUDF was shown in the cytoplasm near the cortex and at spindle pole bodies.

### 4.1 Deletion of the *sumO* gene in *A. nidulans* shows pleiotropic effects

Posttranslational modifications control the function of proteins through numerous mechanisms. The small ubiquitin-related modifier, SUMO, has been studied intensively in the last years and was shown to be involved in various cellular processes. Sumoylation is a conserved modification from fungi to mammals (Bossis and Melchior, 2006b), which provides the opportunity to analyse the role of sumoylation in different organisms.

The filamentous fungus *A. nidulans* was shown to possess a single, non-essential SUMO1-like gene, named *sumO*, the deletion of which shows various effects in the accomplishment of the asexual and sexual life cycles (Wong *et al.*, 2008). In this work, a  $\Delta sumO$  strain was constructed, and further phenotypically analyzed to subsequently serve for heterologous  $\alpha Syn$  expression and analysis. The SUMO protein was shown to play a role during asexual and sexual development in *A. nidulans*. Deletion of *sumO* led to pleiotropic effects including enhanced sensitivity to DNA-damaging agents and oxidative stress, abnormally shaped conidiophores, decreased conidia generation, decelerated formation of microcleistothecia, block in ascosporeogenesis, as well as light-independent sexual development.

#### 4.1.1 SUMO protects cells from DNA-damaging agents and oxidative stress

The application of stress agents can be helpful to decipher the function of a certain protein by comparing the behaviour of the respective deletion strain with a wild type strain. The susceptibility to oxidative stress was tested for the *sumO* deletion strain, employing the redox-cycling agent menadione. The  $\Delta$ *sumO* strain exhibited an increased sensitivity to oxidative stress suggesting that SUMO plays a role in the oxidative stress response of *A. nidulans*. It has been shown for *S. pombe* that the *pmt3* deletion mutant exhibited a higher sensitivity to DNA-damaging agents and DNA synthesis inhibitors (Tanaka *et al.*, 1999). To elucidate whether the sumoylation process in *A. nidulans* affects similar pathways as in *S. pombe*, the  $\Delta$ *sumO* strain was exposed to the DNA-repair repressor cisplatin, the topoisomerase I inhibiting agent camptothecin, and the DNA-dependent RNA polymerase-impairing drug 4-nitroquinoline 1-oxide. An increased sensitivity towards these agents was observed in comparison with the wild type strain. This was also reported by Wong *et al.*, using the DNA-damaging agent methyl methanesulfonate and the DNA synthesis inhibitor hydroxyurea (Wong *et al.*, 2008).

In earlier reports it was described that sumoylation is implicated in DNA replication as well as in DNA repair and cell cycle events (Bossis and Melchior, 2006b). In agreement with this, the SUMO-1 homolog, Smt3p in *S. cerevisiae* is necessary for mitotic cell cycle progression and chromosome segregation. Thus, the increased sensitivity towards DNA-damaging agents described in this thesis and by Wong *et al.* proposes a similar requirement of SUMO for the cell cycle progression in *A. nidulans*.

#### 4.1.2 Involvement of SUMO in conidiation

The deletion of *sumO* in *A. nidulans* led to a decrease in conidiospore production in comparison to a wild type strain. This could be observed with the naked eye, because the deletion strain appeared less colourful on plates possibly due to the decline of conidia.

In the publication of Wong *et al.* this conidiospore reduction phenotype has been described in a more severe way in addition to a vegetative growth cessation after three days. However, within this study no vegetative growth impairment was noted.

The delayed formation of abnormally shaped conidiophores was recognized for the *sumO* deletion strain within this thesis. This observation might be a result of aberrant cytokinesis.

In earlier reports it was described that sumoylation is implicated in DNA replication as well as in DNA repair and cell cycle events (reviewed by Bossis and Melchior, 2006b). In agreement with this, the SUMO-1 homolog, Smt3p in *S. cerevisiae* is necessary for mitotic cell cycle progression and chromosome segregation. Deletion of *SMT3* resulted in aberrant cell division and divergent chromosome segregation (Biggins *et al.*, 2001; Dieckhoff *et al.*, 2004; Meluh and Koshland, 1995; Motegi *et al.*, 2006). Furthermore, deletion of *pmt3* in *S. pombe* was shown to cause aberrant cell division (Tanaka *et al.*, 1999). Taking into account, that the budding process as well as nuclear division and migration are essential for the appropriate development of conidiophores, the *sumO* deletion in *A. nidulans* seems to affect similar cellular processes as in the yeasts. Biggins *et al.* described that 50% of the cells of a temperature-sensitive *smt3* mutant strain displayed a large-budding phenotype and 30% of the cells failed to bud (Biggins *et al.*, 2001). The conidiophore phenotype of the  $\Delta$ *sumO* strain in *A. nidulans*, which affected approximately 50% of the asexual fruiting bodies, comprises elongated metulea and phialides as well as delayed conidia production. This could be due to the same aberrances in the budding process, which have been observed for the *smt3* mutant of *S. cerevisiae*.

Therefore, the decline in conidiospore production appears to be a combination of partial aberrances in the formation of primary and secondary sterigmata and a reduction in the generation of conidia.

The production of asexual structures is under control of several transcription factors. SUMO could be involved in this regulation by mediating, e.g., the intracellular translocation or facilitating other posttranslational modifications of these regulators, thereby affecting downstream targets involved in conidiophore development. Since only 50% of the conidiophores are affected, the possible SUMO conjugation to target proteins involved in the asexual fruiting body development rather represents a supporting role than an essential requirement.

The  $\Delta$ *sumO* conidiophore morphology resembles in some cases the *nudF6* mutant phenotype displaying asymmetric developed metulae. The NUDF protein is involved in the nuclear migration in hyphae and conidiophores, and therefore the deletion mutant shows a block in nuclear translocation into the metulae, of which in rare cases a single chain of conidiospores is derived (Xiang *et al.*, 1995a). However, the analysis of nuclear migration in vegetative mycelia in the  $\Delta$ *sumO* strain displayed no difference to a wild type strain

(data not shown). This indicates that SUMO is at least not implicated in the nuclear distribution pathway in vegetative hyphae.

In conclusion, SUMO is involved in the development of conidiophores and in the production of conidia (Fig. 31A) possibly by participating in the budding process required for the generation of metulae, phialides and spores.

#### **4.1.3 The $\Delta sumO$ mutant displays self-sterility**

In addition to the asexual cycle, the  $\Delta sumO$  strain was analyzed with respect to the accomplishment of the sexual developmental program, revealing severe disturbances during this process. The generation of cleistothecia, which is normally performed within five days from inoculation in a wild type strain, is delayed up to 14 days in the deletion strain. Furthermore, in comparison to normally sized fruiting bodies derived from a wild type strain, the cleistothecia of the deletion strain are significantly decreased in size. In addition, the  $\Delta sumO$  strain displays self-sterility as ascospore production is completely impaired. The deficiencies in cleistothecia size and in ascospore formation were also reported by Wong *et al.*, 2008 but not the delay observed for the generation of microcleistothecia.

Several mutants retarded in sexual development have been described in *A. nidulans* like deletion of *csnD* or *csnE*, which are components of the COP9 signalosome (Busch *et al.*, 2003), disruption of *grrA* (Krappmann *et al.*, 2006), which encodes an F-box protein, or deletion of one of the  $\alpha$ -tubulin encoding genes, *tubB* (Kirk and Morris, 1991). Whereas deletion of either *csnD* or *csnE* led to a block in early development of cleistothecial primordia (Busch *et al.*, 2003), *grrA* and *tubB* deletion strains formed normal cleistothecia, but failed to accomplish ascosporeogenesis (Kirk and Morris, 1991; Krappmann *et al.*, 2006).

Cytological studies on the cleistothecial contents of these mutants revealed a block at a stage prior to the first meiotic division in the *tubB* mutant, whereas meiosis itself seemed to be inhibited at an early stage in the *grrA* deletion strain. Interestingly, both deletion strains initiated sexual development with Hülle cells and produced normal amounts of regularly sized pigmented, asci containing cleistothecia (Kirk and Morris, 1991; Krappmann *et al.*, 2006).

The *sumO* deletion strain appears to be blocked at an earlier stage. The attempt to investigate at which time point the ascosporeogenesis is inhibited failed because of the severely reduced cleistothecia size and tightly packed Hülle cells around them. However, the content derived from lightly brownish-pigmented microcleistothecia appeared as an amorphous mass without any distinct sexual structures like dikaryotic hyphae or ascus mother cells (data not shown) as seen in the  $\Delta grrA$  and  $\Delta tubB$  strains. It can be assumed, that SUMO is dispensable for the initiation of sexual development as Hülle cells are produced. Furthermore, SUMO is not required for the formation of pigmented cleistothecia since dark-coloured microcleistothecia have been derived from the  $\Delta sumO$  strain. The lack of asci formation in the *sumO* deletion strain in combination with the reduced dimensions of cleistothecia, links the size of the latter to ascosporeogenesis. When ascospore development is completely blocked as a result of the *sumO* deletion, there seems to be no necessity to expand the cleistothecium itself, which leads to small, ascospore-lacking microcleistothecia. Thus, SUMO might be required for early ascosporeogenesis in *A. nidulans* (Fig. 31B).

In this context, a connection can be established between asexual and sexual developmental deficiencies with regard to nuclear division and migration, as both processes are required for the production of conidiophores as well as the formation of croiziers and zygote generation.

#### **4.1.4 Light-dependent development is disturbed in the *sumO* deletion strain**

In general, light sensing is an important factor for organisms in all kingdoms. In *A. nidulans*, light induces asexual and represses sexual development (Mooney and Yager, 1990). This study revealed that the  $\Delta sumO$  strain predominantly undergoes the sexual cycle independent of illumination.

One component of the light-regulatory pathway is the *veA* gene product, which was shown to be involved in the maintenance of the light-dependent balance between asexual and sexual cycle. The overexpression of *veA* leads to an excessive increase in sexual fruiting body generation, whereas gene deletion results in an acleistothecial phenotype (Kim *et al.*, 2002; Mooney and Yager, 1990). VeA itself displays no characteristic features of a transcriptional regulator or light receptor, but was shown to be located both in the

cytoplasm and in the nucleus, where an accumulation was noted in the dark (Calvo, 2008; Kim *et al.*, 2002; Stinnett *et al.*, 2007). It was reported that the phytochrome FphA and the two blue-light receptors systems, LreA and LreB might act as upstream regulators of VeA (Blumenstein *et al.*, 2005; Purschwitz *et al.*, 2008).

In general, red light stimulates asexual development and represses sexual sporulation (Mooney and Yager, 1990). The phytochrome FphA (fungal phytochrome) was shown to be a sensor of red light in *A. nidulans* (Blumenstein *et al.*, 2005). The protein's localization was predominantly restricted to the cytoplasm, but interaction with VeA was shown in the nucleus. FphA was found to be autophosphorylated, which proposes a signal transduction of the light response through phosphorylation (Blumenstein *et al.*, 2005). It remains unclear, whether autophosphorylation is conducted in the cytoplasm or in the nucleus.

It was reported that only the combination of red and blue light achieved conidiation levels observed for white light (Purschwitz *et al.*, 2008). The two blue-light receptors referred to as White Collars, LreA and LreB (light response), were suggested to activate the sexual cycle in the dark, which is repressed by FphA in the light. LreA and LreB are both localized to the nucleus, but LreB in addition to the cytoplasm. The interaction between LreB and LreA as well as FphA was observed in the nucleus although the association of the latter with LreA could only be shown indirectly.

VeA was shown to coimmunoprecipitate with LreA and FphA substantiating a large light-sensing protein complex (Fig. 31) (Purschwitz *et al.*, 2008).

Although VeA is probably not able to sense light, it was proposed that a certain threshold of the protein is needed in the nucleus to initiate sexual development (Bayram *et al.*, 2008b). Therefore, asexual development might require degradation of VeA in the nucleus supported by fast protein turnover sequences in the VeA protein (Fischer, 2008). Accordingly, deletion of *csnD* which belongs to the COP9 signalosome involved in protein degradation, led to induction of the sexual cycle independent of light (Busch *et al.*, 2003), which was also observed for the  $\Delta$ *sumO* mutant in this study.

Although proteins localized in the cytoplasm can be sufficiently sumoylated, in most cases nuclear targeting is required for SUMO conjugation (Hay, 2005). Consistent with this hypothesis, Wong *et al.* reported that GFP-SUMO accumulates in the nucleus in interphase cells in *A. nidulans*, whereas the fluorescence signal was undetectable from entry to

mitosis until telophase (Wong *et al.*, 2008). Therefore, it seems likely that sumoylation in *A. nidulans* is restricted to the nucleus.

Given the fact, that sumoylation can represent a necessity for degradation (Huang *et al.*, 2003), it is tempting to assume that nuclear VeA might be a target for sumoylation (Fig. 31D). Thus, it could be possible that sumoylation is conducted in the light promoting degradation of VeA in order to reduce the protein level in the nucleus to induce asexual development (Fig. 31D).

In higher eukaryotes it was shown that sumoylation is implicated amongst others in transcription regulation (Gill, 2004; Johnson, 2004; Verger *et al.*, 2003). The *veA* expression was demonstrated to be negatively regulated by the phytochrome/photolyase-like protein CryA. Thus, an alternative approach could be that CryA, which is restricted to the nucleus in *A. nidulans* (Bayram *et al.*, 2008a), requires sumoylation to conduct its regulatory function in order to repress *veA* expression (Fig. 31C).

Although it remains elusive where light sensing occurs, a primary light-perception signal from the cytoplasm to the nucleus was suggested (Blumenstein *et al.*, 2005). A signal cascade including autophosphorylation of FphA (FphA<sup>P</sup>) was proposed to be implicated in the light response in *A. nidulans* (Purschwitz *et al.*, 2008). Even though it was not shown where autophosphorylation of FphA occurs, it can be assumed that this modification is conducted in the cytoplasm where the protein is highly concentrated (Purschwitz *et al.*, 2008). Light reception might lead to autophosphorylation, which in turn mediates translocation of FphA<sup>P</sup> to the nucleus. FphA was proposed to act as negative regulator on sexual development by repressing activity of the blue light receptors LreA and LreB in the light (Purschwitz *et al.*, 2008). LreA and LreB interact in the nucleus, and the colocalization of FphA and LreB was also shown in this cell department (Purschwitz *et al.*, 2008). Since LreA and FphA were only shown to interact indirectly, LreB could act as a bridge between the two proteins.



sumoylation (Bossis and Melchior, 2006b), autophosphorylation of FphA could stimulate the sumoylation of FphA in the nucleus. Since it was assumed that sumoylation could facilitate the association of the target substrate with other proteins by serving as binding interface (Meulmeester and Melchior, 2008) sumoylation of FphA<sup>P</sup> might in turn mediate the binding of FphA<sup>P</sup> to the VeA/LreA/LreB complex in order to repress its activity and induce asexual development (Fig. 31E). Since White Collar proteins are transcription factors in *Neurospora crassa* (He *et al.*, 2002) it could be proposed that binding of sumoylated FphA<sup>P</sup> to the VeA/LreA/LreB complex might lead to negative regulation of *veA* expression through, e.g., LreA which bears a DNA binding domain at its C-terminus (Purschwitz *et al.*, 2008). Thereby, the abundance of nuclear VeA would be reduced, which might be a prerequisite for asexual development in *A. nidulans*.

In this context, direct sumoylation of VeA discussed above could mediate the release of VeA from the LreA/LreB complex in order to mediate degradation of VeA (Fig. 31D).

However, many factors remain unclear as the light dependence of the described protein complexes is elusive as well as the modulations of the protein activities by interaction with FphA.

In general, deletion of *sumO* might lead to increased levels of nuclear VeA, which results in sexual development despite of illumination.

The light-independent sexual development displayed by the  $\Delta$ *sumO* strain leaves room for several speculations, which might lead to a better understanding of the connection between light and development.

## 4.2 Sumoylation stabilizes $\alpha$ Syn and prevents aggregation in *A. nidulans*

Sumoylation has been implicated in neurodegenerative diseases (Dorval and Fraser, 2007). Similar to ubiquitin, SUMO proteins are components of inclusions in several neurodegenerative diseases like multiple system atrophy or Huntington's disease (Dorval and Fraser, 2007). Numerous proteins involved in neurodegenerative disorders have been shown to be SUMO substrates (Dorval and Fraser, 2006).

In many model organisms like mice, *Drosophila* or *S. cerevisiae* used for the analysis of human proteins such as  $\alpha$ Syn or Tau implicated in PD and AD, respectively the sumoylation pathway is essential.

The viable  $\Delta$ *sumO* strain of *A. nidulans* was employed to analyse the impact of sumoylation on the stability and aggregation property of human  $\alpha$ Syn.

### 4.2.1 Human $\alpha$ Syn is a substrate for sumoylation in *A. nidulans*

In 2006, Dorval and Fraser demonstrated the sumoylation of  $\alpha$ Syn *in vitro*. In this study, the sumoylation of heterologously expressed  $\alpha$ Syn<sup>WT</sup> could be shown for the first time *in vivo*.

In addition to this finding, the mutant forms of  $\alpha$ Syn, A30P and A53T were recently analyzed with regard to sumoylation employing BiFC. Detection of YFP emission revealed that both mutant forms of  $\alpha$ Syn are sumoylated in *A. nidulans*. Furthermore, higher fluorescence signalling was observed in the nuclei resembling BiFC results obtained for  $\alpha$ Syn<sup>WT</sup> (R. Harting, personal communication) confirming nuclear enrichment seen for the GFP- $\alpha$ Syn variants in the *sumO* wild type strains.

Since recently, Wong, *et al.* reported that GFP-SUMO is located in the nucleus (Wong *et al.*, 2008), these results indicate that sumoylation in *A. nidulans* is restricted to this cell compartment.

The finding that human  $\alpha$ Syn can in fact be sumoylated *in vivo* even by the fungal SUMO machinery of *A. nidulans* confirms the high conservation of this modification mechanism among eukaryotic organisms.

#### 4.2.2 Growth impairment provoked by higher levels of unsumoylated $\alpha$ SynA30P in *A. nidulans*

The fact that human  $\alpha$ Syn is sumoylated in *A. nidulans*, led to heterologous expression studies of  $\alpha$ Syn<sup>WT</sup> as well as of the patient-derived alleles  $\alpha$ Syn<sup>A30P</sup> and  $\alpha$ Syn<sup>A53T</sup> in wild type and  $\Delta$ sumO strains. Surprisingly, the expression of the different alleles did not affect fungal growth except for  $\langle$ Syn<sup>A30P</sup>. Three copies of the  $\langle$ Syn<sup>A30P</sup> variant significantly reduced growth of the  $\Delta$ sumO mutant what was neither observed for  $\alpha$ Syn<sup>WT</sup> nor for  $\alpha$ Syn<sup>A53T</sup>.

The results of this thesis indicate, that (i) this growth defect is a result of the missing sumoylation of  $\alpha$ Syn<sup>A30P</sup>, (ii) that some kind of threshold with regard to the amount of  $\alpha$ Syn<sup>A30P</sup> must be achieved before *A. nidulans* shows sensitivity towards the expression of this  $\alpha$ Syn variant, and (iii) that this growth impairment property is restricted to  $\alpha$ Syn<sup>A30P</sup> since the expression of the other two forms did not affect the growth rates of the respective strains. Thus, the concentration-dependent toxicity displayed by duplication and triplication of wild type  $\alpha$ Syn observed in PD patients (Chartier-Harlin *et al.*, 2004; Singleton *et al.*, 2003) can be mimicked in model organisms like yeast or *A. nidulans*.

In addition to the strains harbouring  $\alpha$ Syn, strains expressing the respective GFP- $\alpha$ Syn fusions were constructed. Growth tests confirmed toxicity of GFP- $\alpha$ Syn<sup>A30P</sup>, which revealed the functionality of the GFP- $\langle$ Syn fusions and allows that the findings obtained for the GFP fusion constructs can be applied to the untagged  $\alpha$ Syn proteins.

The outcome of GFP fusion growth tests strengthen the hypothesis that somehow *A. nidulans* is able to cope with higher amounts of either  $\langle$ Syn<sup>WT</sup> or  $\langle$ Syn<sup>A53T</sup> independently of sumoylation, whereas sumoylation of elevated levels of  $\langle$ Syn<sup>A30P</sup> is required for the integrity of the cells.

Apart from sumoylation, these results differ completely from findings in *S. cerevisiae*, where higher levels of  $\langle$ Syn<sup>WT</sup> and  $\langle$ Syn<sup>A53T</sup> led to growth inhibition, whereas  $\langle$ Syn<sup>A30P</sup> did not show any affect (Outeiro and Lindquist, 2003).

It can be speculated that the situation in *A. nidulans* is more similar to that seen in *S. pombe*, where  $\langle$ Syn proteins were reported to be nontoxic (Brandis *et al.*, 2006). In fission yeast it was proposed that toxicity of  $\langle$ Syn is linked to the membrane binding

capacity, which was observed for  $\langle$ SynWT and  $\langle$ SynA53T in *S. cerevisiae* but neither in *S. pombe* nor in *A. nidulans*.

The sensibility to  $\langle$ SynA30P expression displayed by the  $\Delta$ *sumO* strain resembles studies in *Drosophila*, where  $\langle$ SynA30P was reported to be more harmful than  $\langle$ SynA53T (Feany and Bender, 2000). This similar finding proposes a special feature displayed only by this mutant form of  $\langle$ Syn, which leads to higher toxicity in a  $\Delta$ *sumO* mutant of *A. nidulans* and *Drosophila*.

#### **4.2.3 SUMO conjugation antagonizes degradation of $\langle$ Syn and mediates solubility of the human protein in *A. nidulans***

Earlier studies revealed that SUMO conjugation to a target protein can block lysine dependent modification such as ubiquitination. Thus, ubiquitin-dependent degradation of the substrate is prevented. This was shown for the inhibitor protein I $\kappa$ B. This protein maintains the NF- $\kappa$ B transcription factor in an inactive state until polyubiquitination of I $\kappa$ B leads to degradation and in turn to activation of NF- $\kappa$ B. SUMO1 conjugation to the same lysine residue of I $\kappa$ B, blocks ubiquitination and prevents degradation. Therefore, sumoylation leads to repression of NF- $\kappa$ B in an indirect manner (Desterro *et al.*, 1998).

To analyse, if sumoylation might also affect the stability of the different  $\langle$ Syn variants in *A. nidulans*, Western hybridization experiments were conducted with wild type and  $\Delta$ *sumO* strains expressing three copies of  $\langle$ SynWT, A30P and A53T, respectively.

Without sumoylation, the GFP- $\langle$ SynWT and GFP- $\langle$ SynA53T fusion protein were shown to be less stable, which was not observed for GFP- $\langle$ SynA30P. The reduction of the protein amounts of GFP- $\langle$ SynWT and GFP- $\langle$ SynA53T was only partially complemented by reconstitution of *sumO*. In general, these observations might be a result of ectopical integration of the respective complementation plasmid. Although this plasmid carried part of the 5' UTR of the *sumO* gene, the region required for full transcriptional efficiency might be longer. Given the fact, that under normal conditions, free SUMO1 is limited (Saitoh and Hinchey, 2000), it could be possible that a reduced number of SUMO molecules due to decreased transcription, is only sufficient enough to partially complement the phenotypes caused by the *sumO* deletion but not completely. This hypothesis can be

also applied to the findings that condition was not fully restored in the reconstitution strain AGB350 as well as the nuclear enrichment seen for the GFP- $\zeta$ Syn variants in *sumO* wild type strains could not be observed in the respective reconstitution strains.

Northern hybridization experiments were conducted to distinguish between a posttranscriptional or transcriptional effect causing decreased amounts of GFP- $\zeta$ SynWT and GFP- $\zeta$ SynA53T. The results were very ambiguous as in some cases mRNA levels of the *gfp:: $\alpha$ Syn* fusions appeared strikingly divergent to protein amounts noted in Western experiments.

However, localization of the GFP-fusion constructs confirmed Western hybridization results for GFP- $\zeta$ SynWT and for GFP-A30P. Furthermore, the formation of GFP- $\zeta$ SynA53T aggregation in the  $\Delta$ *sumO* mutant of *A. nidulans* was noted, which was prevented by ectopical reconstitution of the *sumO* gene. The decreased amount of  $\alpha$ SynA53T in Western hybridization experiments could be due to the fact that the insoluble aggregates were not detected in Western experiments conducted within this work and therefore only the signal of the residual soluble, unfolded form of  $\alpha$ SynA53T was received. Since deletion of *sumO* leads to less stable  $\alpha$ SynWT, involvement of SUMO in degradation can be suggested.

A competition of the SUMO and ubiquitination pathways was proposed for the human protein Tau, which is involved in Alzheimer's disease. Tau was shown to be covalently modified by SUMO1 and to a lesser extent by SUMO2 and SUMO3 *in vitro* (Dorval and Fraser, 2006). Treatment with the proteasome inhibitor agent MG132 led to an increase of ubiquitin-conjugated Tau and a marked decrease of sumoylated Tau levels (Dorval and Fraser, 2006). These observations led to the proposal of an antagonistic relationship between SUMO and ubiquitin. Same experiments were conducted for cell lines coexpressing SUMO1 and  $\zeta$ Syn, which remained unaffected by MG132 treatment (Dorval and Fraser, 2006).

However, *in vivo* studies in *A. nidulans* might differ from these findings and therefore, an antagonistic role for SUMO with regard to ubiquitin could be proposed for  $\zeta$ SynWT. It was reported that the RING-type E3 ubiquitin-protein ligase Siah-1 facilitates mono- and di-ubiquitination of  $\zeta$ SynWT and A53T *in vivo*. Ubiquitination of  $\zeta$ SynA30P could not be shown for this E3 ligase, probably due to the fact that the respective lysine residues

required for the attachment of ubiquitin are close to position 30. The point mutation might lead to conformational changes thereby impairing the conjugation of ubiquitin (Lee *et al.*, 2007). Although the ubiquitin conjugation mediated by Siah-1 was shown to promote aggregation instead of degradation, a similar process with regard to degradation could be possible in *A. nidulans* (Fig. 32 B). Decreased amounts of  $\alpha$ SynWT in the  $\Delta$ *sumO* strain of *A. nidulans* raise the possibility that the conjugation of SUMO might impair the association to ubiquitin, mediated by an E3 ligase similar to Siah-1 (Fig. 32A). In case of *sumO* deletion, ubiquitin can be conjugated to  $\alpha$ SynWT (Fig. 32B), but not to A30P (Fig. 32C), and degradation can be conducted. The inhibition of ubiquitin attachment by sumoylation is not necessarily connected to the modification of the same lysine residue because sumoylation can also affect the folding or conformational change of a protein (Meulmeester and Melchior, 2008) thereby impeding the conjugation of ubiquitin. Since the mutant form  $\alpha$ SynA30P is not degraded, as ubiquitin cannot be attached to this variant in the proposed model, the formation of protofibrils favoured by  $\alpha$ SynA30P is conducted (Fig. 32C). These oligomeric fibrils have been assumed to be the most toxic aggregation species (Lashuel *et al.*, 2002; Tofaris and Spillantini, 2007) and thus could cause vegetative growth reduction observed in the respective  $\Delta$ *sumO* strain. Since protofibrils are not visible by normal fluorescence microscopy, the GFP- $\alpha$ SynA30P fusion signal was observed equally distributed over the entire hypha. Therefore, sumoylation would prevent the formation of soluble oligofibrils of  $\alpha$ SynA30P, thereby protecting *A. nidulans* from this toxic matter (Fig. 32A).

Although *sumO* deletion led also to decreased protein amounts for  $\alpha$ SynA53T and the degradation model proposed for  $\alpha$ SynWT could also be applied to this variant (Fig. 32B), the generation of aggregates observed for  $\alpha$ SynA53T suggests a different pathway independent of degradation. In earlier studies,  $\alpha$ SynA53T was shown to degrade more slowly than the wild type form (Bennett *et al.*, 1999). Furthermore, it was demonstrated that  $\alpha$ SynA53T showed a higher propensity to aggregate in comparison to  $\alpha$ SynWT (Bennett *et al.*, 1999). This was also reported for expression studies in *S. pombe*, where  $\alpha$ SynA53T was shown to form intracytoplasmic inclusions faster and at a lower  $\alpha$ Syn concentration in comparison to  $\alpha$ SynWT (Brandis *et al.*, 2006).

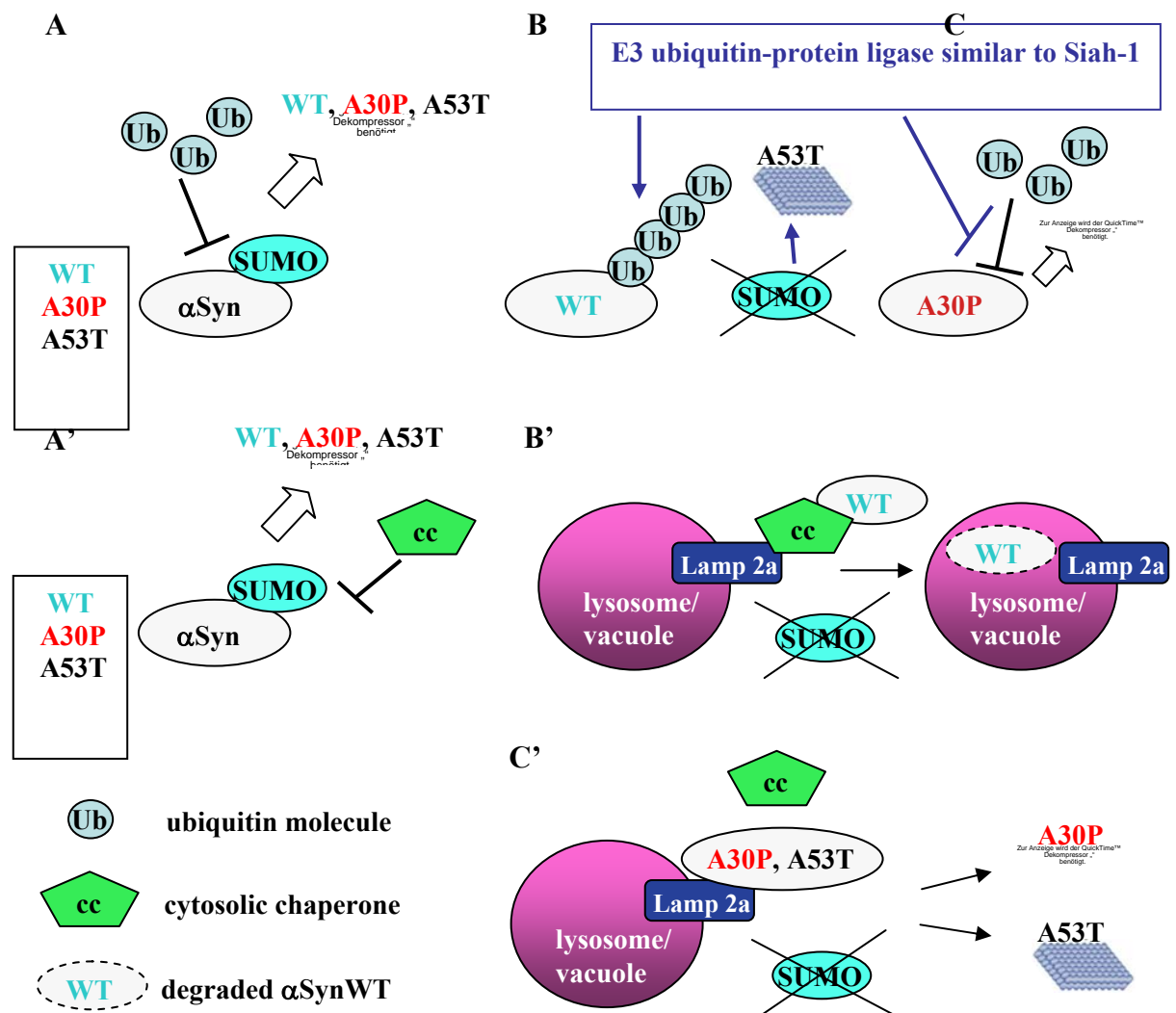


**Fig. 32: Sumoylation, degradation and aggregation of  $\alpha$ Syn in *A. nidulans*.**

(A) All  $\alpha$ Syn variants are sumoylated, which impairs the attachment of ubiquitin molecules. Furthermore,  $\alpha$ SynWT, A30P and A53T remain as unfolded monomers due the attachment of SUMO. (B) In the *sumO* deletion strain, ubiquitin can be attached to  $\alpha$ SynWT by an E3 ligase similar to Siah-1. In the absence of SUMO,  $\alpha$ SynA53T generates insoluble nontoxic cytoplasmic aggregates, whereas  $\alpha$ SynWT can be degraded in a faster way so that no mature aggregates are formed. (C)  $\alpha$ SynA30P cannot be ubiquitinated in the  $\Delta$ *sumO* strain and higher concentrations of the mutated protein lead to the formation of toxic oligomers, which impair vegetative growth. (A') Sumoylation of all  $\alpha$ Syn forms prevents degradation by chaperone-mediated autophagy (CMA) conducted in the lysosome or vacuole.  $\alpha$ SynWT, A30P and A53T remain as unfolded monomers due the attachment of SUMO. (B')  $\alpha$ SynWT is recognized by a cytosolic chaperone. This complex binds to the lysosomal-associated membrane protein type 2A (Lamp 2a), a CMA receptor at the lysosomal membrane. After crossing the membrane,  $\alpha$ SynWT is rapidly degraded inside the lysosome. (C') The two mutant forms  $\alpha$ SynA30P and A53T bind to the CMA lysosomal receptor with a high affinity, thus blocking chaperone-mediated autophagy. Hence,  $\alpha$ SynA30P forms soluble toxic protofibrils, while  $\alpha$ SynA53T generates nontoxic insoluble aggregates (parts of the model have been adopted from Cookson, 2005).

If these findings were applied to the results in *A. nidulans*, it could be possible that  $\alpha$ SynA53T initiates aggregation in the  $\Delta$ sumO strain earlier than  $\alpha$ SynWT and insoluble, presumably nontoxic aggregates are formed in the cytoplasm (Fig. 32B), which cannot be degraded. Therefore, it can be assumed that  $\alpha$ SynWT is degraded in much faster way compared to  $\alpha$ SynA53T until a level is reached that is not prone to aggregation anymore, since this process is concentration-dependent (Wood *et al.*, 1999). In support of this hypothesis,  $\alpha$ SynWT aggregates were shown to be formed in a concentration-dependent manner in *S. pombe* (Brandis *et al.*, 2006).

Taking into account that no aggregates were generated by any of the  $\alpha$ Syn variants in the wild type strain, these findings raise the hypothesis that SUMO conjugation mediates solubility of the different  $\alpha$ Syn proteins in *A. nidulans* (Fig. 32A). In this regard, Dorval and Fraser analyzed the SUMO1 conjugation to Tau. This protein is prone to bind to microtubules thereby regulating the stability of MTs. Treatment with the microtubule-destabilizing drug colchicine was found to stimulate sumoylation of Tau suggesting that sumoylation is preferentially conducted to the soluble protein fraction (Dorval and Fraser, 2006). Accordingly, SUMO could be prone to be conjugated to soluble monomers of the different  $\alpha$ Syn variants, thereby preventing self-aggregation of the proteins (Fig. 32 A).

In terms of degradation, a different pathway could also be possible for  $\alpha$ Syn in *A. nidulans*. Earlier reports have shown that monomers and dimers but not oligomers of  $\alpha$ Syn are removed by the lysosome via chaperone-mediated autophagy (CMA) (Cuervo *et al.*, 2004). Autophagy is a process, which is omnipresent in eukaryotes as proteins or sequestered material are degraded and recycled in the lysosome (reviewed by Klionsky and Kumar, 2006). Furthermore, whereas  $\alpha$ SynWT can be degraded by the CMA, the mutant forms  $\alpha$ SynA30P and A53T were shown to be rather poorly degraded by the lysosome. In addition, both mutated proteins bind to the lysosomal receptor with high affinity, which leads to a block of the degradation machinery and may increase the propensity to form aggregates (Cuervo *et al.*, 2004).

In principle, the model for ubiquitin-dependent degradation could be adopted for the vacuole-dependent degradation in *A. nidulans*. All three forms of  $\alpha$ Syn are not degraded by the lysosome/vacuole when SUMO has been attached due to conformational changes, which prevent their recognition by the cytosolic chaperone (Fig. 32A'). Furthermore, the

proteins stay in solution due to SUMO attachment. In the *sumO* deletion strain,  $\alpha$ SynWT can be degraded by the vacuole (Fig. 32B'), but the mutant forms  $\alpha$ SynA30P and A53T rather not, which leads to aggregation of both forms (Fig. 32C').

In addition, this alternative degradation pathway would explain why treatment with the proteasome inhibitor agent MG132 did not affect the amount of detected sumoylated  $\alpha$ Syn shown by Dorval and Fraser, 2006.

This study clearly demonstrated that sumoylation affects the stability and localization of proteins involved in neurodegenerative diseases, which might help to elucidate the molecular mechanisms through which these proteins become toxic for human cells.

### **4.3 NUDC localizes to the cell cortex and to spindle pole bodies in *A. nidulans***

The nuclear distribution process in hyphal cells and developmental structures of *A. nidulans* is similar to the neuronal migration during human embryogenesis (reviewed by Wynshaw-Boris and Gambello, 2001). Therefore, nuclear migration was analyzed in more detail in this filamentous fungus. Numerous genes were identified, which participate in nuclear migration and were found to encode for components of the dynein or dynactin multisubunit complex like *nudA* (Xiang *et al.*, 1994; Xiang *et al.*, 1995b) or *nudM* (Xiang *et al.*, 1999). In addition, other genes were identified, which do not belong to these complexes, but have also been shown to be highly conserved like *nudF* (Xiang *et al.*, 1995a), *nudC* (Osmani *et al.*, 1990) or *nudE* (Efimov and Morris, 2000).

The third part of this work intended to localize fungal NUDC to gain some insights into the function of this protein.

#### **4.3.1 Cortical localization of NUDC**

In order to characterize the fungal protein NUDC in more detail, localization studies were performed in *A. nidulans*. NUDC-GFP signalling was observed in form of immotile dots along hyphae near the cytoplasmic membrane. A more precise analysis using immunoelectron microscopy revealed that NUDC-GFP is localized at the hyphal cortex as well as at the tip cortex, with isolated spots in the cytoplasm.

The noted immobile dots in the cytoplasm resembled the specks observed for GFP-NUDE or GFP-NUDA fusion proteins in *A. nidulans*. These signals were also described as immobile dots and have been proposed to represent artefacts of protein overexpression (Efimov, 2003). Therefore, it can be assumed that the cytoplasmic localization of NUDC is artificial and does not display a significant position of the fungal protein. However, the NUDC-GFP fusion protein was also found at the cortex, which is similar to the finding in amphibian oocytes, where NudC was highly enriched at the cell cortex (Swan *et al.*, 1999). The cortical localization of the fungal protein would support the requirement of NUDC for polar growth and cell wall integrity, which has been proposed by Chiu *et al* in 1997. These authors showed that absence of NUDC in *A. nidulans* led to abnormal thick cell wall formation due to the overproduction of chitin and glucan. In addition, a loss of polarity was noted since cell wall synthesis, which is normally concentrated at the growing tip was distributed over the entire range of the cell membrane. These factors led finally to globular cell swelling and lysis (Chiu *et al.*, 1997). The localization of NUDC at the hyphal cortex could therefore be required for the stabilization and regulation of cell wall production, whereas the cortical positioning at the tips might assure the main recruitment of cell membrane material to the growing end of hyphal cells.

#### **4.3.2 Colocalization of NUDF and NUDC in *A. nidulans***

Fungal NUDC was reported to stabilize NUDF posttranslationally (Xiang *et al.*, 1995a) and the mammalian NUDC homolog was shown to bind and colocalize with LIS1 in the developing mouse brain (Aumais *et al.*, 2001; Morris *et al.*, 1998b). Therefore, the association between NUDC and NUDF was analyzed in this study using the yeast two-hybrid method. The interaction between the two proteins could be shown and the WD40 domain of NUDF was identified as mediator of this association. The interaction of NUDC and NUDF was also confirmed *in vivo* employing the BiFC method. It was shown that fungal NUDC binds NUDF in the cytoplasm near the cortex and at spindle pole bodies (SPBs), which were clearly identified by colocalization with  $\gamma$ -tubulin, at different stages of the cell cycle. Additionally, the NUDC localization at SPBs was confirmed by a NUDC-GFP fusion under control of the authentic promoter in combination with  $\gamma$ -tubulin.

The NUDC-NUDF interaction in the cytoplasm resembled again immobile specks suggesting that this localization is an artefact due to the overexpression of both genes as described above for NUDC-GFP. However, it cannot be ruled out that these spots represent functional associations. At the cortex, NUDC might be involved in the binding and activation of dynein, which is assumed to be performed by the association of NUDF and the cortical landmark protein APSA (Veith *et al.*, 2005).

In earlier studies, the colocalization of NUDC, LIS1, and dynein at the microtubule organization center (MTOC) was described in murine cells (Aumais *et al.*, 2001). Since hNUDC is essential for bipolar spindle formation, which proposed a function in MT organization at spindle poles (Zhang *et al.*, 2002b), the findings of this thesis suggest that fungal NUDC might also be part of the SPBs and involved in MT organization for nuclear migration and spindle formation. Human NUDC was shown to play a broad role during mitosis as the protein was also found to be localized to kinetochores and to regulate MT attachment to chromosomes (Nishino *et al.*, 2006). Thus, the localization of NUDC at SPBs might indicate a mitotic role for NUDC in *A. nidulans* in addition to the involvement in cell wall processes. During mitosis, NUDC might function in combination with NUDF and dynein, since LIS1 and dynein were shown to regulate spindle orientation, chromosome attachment, and the cortical tethering of astral MTs (Faulkner *et al.*, 2000; Tanaka *et al.*, 2004).

However, it remains unclear, how NUDC is attached to SPBs or the cortex. Given that NUDF is required for the SPB localization of dynein, it seems likely that NUDF is additionally responsible for NUDC positioning, but also the opposite could be true. On the other hand, it is also possible that NUDC binds to integral SPB components, other dynein subunits or additional regulatory proteins.

It is an interesting goal for the future research to elucidate how dynein and its regulatory proteins are recruited to SPBs.

## 4.4 Outlook

In this study, the model organism *A. nidulans* was shown to be a useful tool to analyze basic cellular and developmental processes and to investigate the functions of proteins for which no homologous counterpart exist.

The phenotypical analysis of the *sumO* deletion revealed pleiotrophic effects on the accomplishment of asexual and sexual development in *A. nidulans*. Deletion of *sumO* resulted in fungi which exhibit reduced production of asexual spores (conidia) and altered conidiophore morphology. Budding process as well as nuclear division and migration are essential for the appropriate development of conidiophores. SUMO was shown to be implicated in DNA replication as well as in DNA repair and cell cycle events in other model organism. Thus, the analysis of nuclear distribution and division in metulae and phialides in the  $\Delta sumO$  strain could help deciphering the role of sumoylation in asexual sporogenesis.

In addition, the  $\Delta sumO$  mutant revealed that sumoylation is essential for sexual ascospore production and normally sized fruit bodies in *A. nidulans*. The self-sterility displayed by the  $\Delta sumO$  strain is similar to phenotypes observed for the *tubB* or *grrA* deletion mutants, which show a block at the stage of meiosis. Therefore, further experiments like electron microscopy of sexual structures are needed to resolve at which stage the ascospore formation is impaired and to decipher the regulatory role of SUMO in ascospore formation. Interestingly, deletion of *sumO* also resulted in sexual differentiation independent of illumination. A connection between sumoylation and the VeA protein, which is involved in light perception has been proposed. To investigate, whether SUMO is implicated in the regulation and/or abundance of VeA, a double deletion mutant should be constructed. The phenotype of such a  $\Delta sumO/\Delta veA$  double mutant could reveal whether VeA and SUMO might belong to the same pathway. Since deletion of *veA* displays an acleistothecial phenotype, it would be interesting to analyze if the  $\Delta sumO$  phenotype could be overcome in a double mutant. In addition, the abundance of VeA could be analyzed in dependence of SUMO availability and illumination. Higher levels of VeA in the  $\Delta sumO$  mutant would suggest that sumoylation is somehow involved in the regulation of VeA availability.

In general, it could be interesting to perform an interaction screen or an immunoprecipitation assay to identify potential sumoylation targets in *A. nidulans*. Such an approach could clarify, if components of the presumed light sensing complex are

modified by sumoylation. Furthermore, the identification of potential SUMO interaction partners might lead to a better understanding of pathways involved in development in *A. nidulans* and might facilitate the analysis of such homologous proteins in higher eukaryotes.

Since the analysis of proteins involved in neuronal diseases has revealed that posttranslational modifications are of high importance, the  $\Delta sumO$  strain constructed in this thesis was employed to address the question whether SUMO1 affects  $\alpha$ Syn stability and/or aggregation. In fact, heterologous expression of different  $\langle Syn$  alleles revealed that availability of SUMO in *A. nidulans* mediates stability of  $\langle Syn$ WT and prevents aggregation  $\langle Syn$ A53T and presumably of  $\langle Syn$ A30P. A sumoylation pathway antagonizing ubiquitination or chaperone-mediated autophagy of  $\langle Syn$ WT was proposed to explain reduced protein levels observed for this protein. To analyze whether  $\alpha$ Syn is ubiquitinated in *A. nidulans*, coimmunoprecipitation of the  $\alpha$ Syn variants could be conducted in the wild type and  $\Delta sumO$  background. Western hybridization with an anti-ubiquitin antibody would reveal if ubiquitination of  $\alpha$ Syn takes place, and if there is a difference with regard to sumoylation. Furthermore, such an approach would elucidate whether all  $\alpha$ Syn variants are ubiquitinated or differences can be observed as proposed in the degradation model. Besides, in order to decipher whether  $\alpha$ Syn might be degraded by the 26S proteasome, respective proteasome inhibitors could be used to see whether the protein level of the  $\alpha$ Syn variants is increased due to impaired degradation by the proteasome. Such experiments might reveal whether  $\alpha$ SynA30P is not affected by this ubiquitin-dependent degradation pathway in *A. nidulans* confirming unaltered protein levels regardless of sumoylation. For the purpose of analyzing the lysosome-dependent degradation pathway, the fluorescence analysis could be repeated with the main focus on the localization of the GFP- $\alpha$ Syn proteins in vacuoles. However, this approach could be complicated due to the fact that cleaved off GFP can be used to visualize autophagy (reviewed by Klionsky and Kumar, 2006) and hence GFP signalling and not GFP- $\alpha$ Syn could be observed in vacuoles. Therefore, rather immunofluorescence microscopy should be conducted to track such pathways in the cell.

In order to exclude that a transcriptional regulation in the  $\Delta sumO$  strain leads to lower amounts of the GFP- $\alpha$ Syn proteins observed in Western hybridization assays the transcript

levels of the different  $\alpha$ Syn alleles should be analyzed again in the  $\alpha$ Syn expressing strains. Since the appliance of Northern experiments was not very successful in this matter alternative methods like real-time PCR could be performed to distinguish between transcriptional and posttranscriptional regulation.

It will be a fascinating challenge for future research to elucidate the impact of SUMO on the degradation and/or aggregation of  $\alpha$ Syn, which might help to elucidate the molecular mechanisms through which these proteins become toxic for human cells.

The finding that *A. nidulans* is somehow able to cope with even higher amounts of different  $\alpha$ Syn variants might provide molecular insight into this protection against toxicity in future genetic analyses.

The model organism *A. nidulans* was also shown to be a useful tool to study nuclear migration to gain insights in the neuronal migration during human embryogenesis.

The nuclear distribution protein NUDC was analyzed in this study to address the question where the protein is localized in the cell to decipher the function of NUDC. It could be shown that NUDC is present at the cell cortex, in the cytoplasm and at spindle pole bodies of *A. nidulans*. Furthermore, the interaction of NUDC and NUDF was demonstrated in the cytoplasm near the cortex and at spindle pole bodies and is mediated by the WD40 domain of NUDF. However, it still remains elusive how NUDC is recruited to the SPBs. The colocalization of NUDC and NUDF at SPBs, but not at MT plus ends, where NUDF was found in high amounts, suggests the existence of different subsets of NUDC and NUDF. At spindle pole bodies, important regulatory mechanisms take place. Mitotic kinases and phosphatases like NIMA, PLKA or BIMG are located there in *A. nidulans* controlling mitotic events through phosphorylation/dephosphorylation cascades (Bachewich *et al.*, 2005; De Souza *et al.*, 2000; Fox *et al.*, 2002). LIS1 is a phosphoprotein (Sapir *et al.*, 1999), and also NUDF was shown to be modified (K. Helmstaedt, personal communication). This raises the possibility that NUDF is phosphorylated at spindle pole bodies and therefore, due to conformational changes is able to associate with specific proteins like NUDC at this site, but not at others. The described phosphorylation of hNUDC by PLK1 (Zhou *et al.*, 2003) suggests that also fungal NUDC is phosphorylated when located at or in the nucleus. hNUDC was shown to bind PLK1 and upon its phosphorylation by PLK1, associates with kinetochores (Nishino *et al.*, 2006).

That the phosphorylation of proteins can affect their localization was also shown for

NDEL1, which can be phosphorylated by Cdk5 (Wynshaw-Boris and Gambello, 2001). Therefore, it is also possible that the different localizations of NUDC and NUDF depend on phosphorylation, which in turn affects the ability to interact with other proteins due to the change in localization.

The localization results in this study, however, imply that NUDF and NUDC must be able to form a complex in their different assumed phosphorylation states. While a NUDC/NUDF complex has to be assumed at the cortex during interphase, a NUDC/NUDF<sup>p</sup> complex might be present at SPBs during interphase while during mitosis, a NUDC<sup>p</sup>/NUDF<sup>p</sup> complex could be postulated at SPBs and probably kinetochores.

Therefore a future goal could be to analyze the phosphorylation of NUDC in *A. nidulans*. Furthermore NUDC localization as well as that of NUDF or other potential interaction partners like NUDA at spindle pole bodies should be analyzed to elucidate if these proteins rely on the phosphorylation status of NUDC to conduct their function.

In summary, it is very likely that regulation of these nuclear migration proteins by phosphorylation is a means to control associations with specific factors which in turn account for the different functions of dynein in the cell.

Finally, in this study protein modifications like sumoylation or phosphorylation have been shown or proposed to contribute to several control mechanisms like cell-cycle progression, degradation or aggregation. In addition, modulation of intracellular localization or participation in protein complexes has been suggested.

Therefore, in future research not only the analysis of knock-out phenotypes and the localization of proteins should be performed, but also the types and sites of modifications have to be investigated to elucidate the true meaning of a protein in the cell.

## 5 References

- Adames, N.R., and Cooper, J.A. (2000) Microtubule interactions with the cell cortex causing nuclear movements in *Saccharomyces cerevisiae*. *J Cell Biol* **149**: 863-874.
- Ahn, C., and Morris, N.R. (2001) NUDF, a fungal homolog of the human LIS1 protein, functions as a dimer *in vivo*. *J Biol Chem* **276**: 9903-9909.
- Ahn, T.B., Kim, S.Y., Kim, J.Y., Park, S.S., Lee, D.S., Min, H.J., Kim, Y.K., Kim, S.E., Kim, J.M., Kim, H.J., Cho, J., and Jeon, B.S. (2008)  $\alpha$ -Synuclein gene duplication is present in sporadic Parkinson disease. *Neurology* **70**: 43-49.
- Anckarsäter, H. (2006) Central nervous changes in social dysfunction: autism, aggression, and psychopathy. *Brain Res Bull* **69**: 259-265.
- Anthony, T.E., Klein, C., Fishell, G., and Heintz, N. (2004) Radial glia serve as neuronal progenitors in all regions of the central nervous system. *Neuron* **41**: 881-890.
- Arai, K., Kato, N., Kashiwado, K., and Hattori, T. (2000) Pure autonomic failure in association with human  $\alpha$ -synucleinopathy. *Neurosci Lett* **296**: 171-173.
- Arawaka, S., Saito, Y., Murayama, S., and Mori, H. (1998) Lewy body in neurodegeneration with brain iron accumulation type 1 is immunoreactive for  $\alpha$ -synuclein. *Neurology* **51**: 887-889.
- Aumais, J.P., Tunstead, J.R., McNeil, R.S., Schaar, B.T., McConnell, S.K., Lin, S.H., Clark, G.D., and Yu-Lee, L.Y. (2001) NudC associates with Lis1 and the dynein motor at the leading pole of neurons. *J Neurosci* **21**: RC187.
- Aumais, J.P., Williams, S.N., Luo, W., Nishino, M., Caldwell, K.A., Caldwell, G.A., Lin, S.H., and Yu-Lee, L.Y. (2003) Role for NudC, a dynein-associated nuclear movement protein, in mitosis and cytokinesis. *J Cell Sci* **116**: 1991-2003.
- Axelrod, D.E., Gealt, M., and Pastushok, M. (1973) Gene control of developmental competence in *Aspergillus nidulans*. *Dev Biol* **34**: 9-15.
- Bachewich, C., Masker, K., and Osmani, S. (2005) The polo-like kinase PLKA is required for initiation and progression through mitosis in the filamentous fungus *Aspergillus nidulans*. *Mol Microbiol* **55**: 572-587.
- Bayram, Ö., Biesemann, C., Krappmann, S., Galland, P., and Braus, G.H. (2008a) More Than a Repair Enzyme: *Aspergillus nidulans* Photolyase-like CryA Is a Regulator of Sexual Development. *Mol Biol Cell* **19**: 3254-3262.
- Bayram, Ö., Krappmann, S., Ni, M., Bok, J.W., Helmstaedt, K., Valerius, O., Braus-Stromeyer, S., Kwon, N.J., Keller, N.P., Yu, J.H., and Braus, G.H. (2008b) VelB/VeA/LaeA complex coordinates light signal with fungal development and secondary metabolism. *Science* **320**: 1504-1506.
- Beckwith, S.M., Roghi, C.H., Liu, B., and Ronald Morris, N. (1998) The "8-kD" cytoplasmic dynein light chain is required for nuclear migration and for dynein heavy chain localization in *Aspergillus nidulans*. *J Cell Biol* **143**: 1239-1247.
- Bence, N.F., Sampat, R.M., and Kopito, R.R. (2001) Impairment of the ubiquitin-proteasome system by protein aggregation. *Science* **292**: 1552-1555.
- Bennett, M.C., Bishop, J.F., Leng, Y., Chock, P.B., Chase, T.N., and Mouradian, M.M. (1999) Degradation of  $\alpha$ -synuclein by proteasome. *J Biol Chem* **274**: 33855-33858.
- Bergen, L.G., and Morris, N.R. (1983) Kinetics of the nuclear division cycle of *Aspergillus nidulans*. *J Bacteriol* **156**: 155-160.
- Bertani, G. (1951) Studies on lysogenesis. I. The mode of phage liberation by lysogenic *Escherichia coli*. *J Bacteriol* **62**: 293-300.

- Betarbet, R., Sherer, T.B., MacKenzie, G., Garcia-Osuna, M., Panov, A.V., and Greenamyre, J.T. (2000) Chronic systemic pesticide exposure reproduces features of Parkinson's disease. *Nat Neurosci* **3**: 1301-1306.
- Biggins, S., Bhalla, N., Chang, A., Smith, D.L., and Murray, A.W. (2001) Genes involved in sister chromatid separation and segregation in the budding yeast *Saccharomyces cerevisiae*. *Genetics* **159**: 453-470.
- Blumenstein, A., Vienken, K., Tasler, R., Purschwitz, J., Veith, D., Frankenberg-Dinkel, N., and Fischer, R. (2005) The *Aspergillus nidulans* phytochrome FphA represses sexual development in red light. *Curr Biol* **15**: 1833-1838.
- Bodles, A.M., Guthrie, D.J., Greer, B., and Irvine, G.B. (2001) Identification of the region of non-A $\beta$  component (NAC) of Alzheimer's disease amyloid responsible for its aggregation and toxicity. *J Neurochem* **78**: 384-395.
- Bohren, K.M., Nadkarni, V., Song, J.H., Gabbay, K.H., and Owerbach, D. (2004) A M55V polymorphism in a novel SUMO gene (SUMO-4) differentially activates heat shock transcription factors and is associated with susceptibility to type I diabetes mellitus. *J Biol Chem* **279**: 27233-27238.
- Bossis, G., and Melchior, F. (2006a) Regulation of SUMOylation by reversible oxidation of SUMO conjugating enzymes. *Mol Cell* **21**: 349-357.
- Bossis, G., and Melchior, F. (2006b) SUMO: regulating the regulator. *Cell Div* **1**: 13.
- Bowman, A.B., Patel-King, R.S., Benashski, S.E., McCaffery, J.M., Goldstein, L.S., and King, S.M. (1999) *Drosophila roadblock* and *Chlamydomonas* LC7: a conserved family of dynein-associated proteins involved in axonal transport, flagellar motility, and mitosis. *J Cell Biol* **146**: 165-180.
- Braak, H., Del Tredici, K., Rub, U., de Vos, R.A., Jansen Steur, E.N., and Braak, E. (2003) Staging of brain pathology related to sporadic Parkinson's disease. *Neurobiol Aging* **24**: 197-211.
- Bradford, M.M. (1976) A rapid and sensitive method for the quantitation of microgram quantities of protein utilizing the principle of protein-dye binding. *Anal Biochem* **72**: 248-254.
- Brandis, K.A., Holmes, I.F., England, S.J., Sharma, N., Kukreja, L., and DebBurman, S.K. (2006)  $\alpha$ -Synuclein fission yeast model: concentration-dependent aggregation without plasma membrane localization or toxicity. *J Mol Neurosci* **28**: 179-191.
- Braus, G.H., Krappmann, S., and Eckert, S.E. (2002) Sexual development in ascomycetes: fruit body formation of *Aspergillus nidulans*. In Molecular biology of fungal development. Osiewacz, H.D. (ed). New York, Basel: Marcel Dekker, Inc., pp. 215-244.
- Brown, T., and Mackey, K. (1997) Analysis of RNA by Northern and slot blot hybridization. In *Current protocols in molecular biology* (New York, NY: John Wiley and Sons Inc.), pp. 4.9.1-4.9.16.
- Busch, S., Eckert, S.E., Krappmann, S., and Braus, G.H. (2003) The COP9 signalosome is an essential regulator of development in the filamentous fungus *Aspergillus nidulans*. *Mol Microbiol* **49**: 717-730.
- Busch, S., Schwier, E.U., Nahlik, K., Bayram, Ö., Helmstaedt, K., Draht, O.W., Krappmann, S., Valerius, O., Lipscomb, W.N., and Braus, G.H. (2007) An eight-subunit COP9 signalosome with an intact JAMM motif is required for fungal fruit body formation. *Proc Natl Acad Sci U S A* **104**: 8089-8094.

- Bussink, H.J., and Osmani, S.A. (1998) A cyclin-dependent kinase family member (PHOA) is required to link developmental fate to environmental conditions in *Aspergillus nidulans*. *Embo J* **17**: 3990-4003.
- Calvo, A.M. (2008) The VeA regulatory system and its role in morphological and chemical development in fungi. *Fungal Genet Biol* **45**: 1053-1061.
- Cardozo, T., and Pagano, M. (2004) The SCF ubiquitin ligase: insights into a molecular machine. *Nat Rev Mol Cell Biol* **5**: 739-751.
- Casselton, L., and Zolan, M. (2002) The art and design of genetic screens: filamentous fungi. *Nat Rev Genet* **3**: 683-697.
- Castro-Volio, I., and Cuenca-Berger, P. (2005) [Neurodevelopmental (fragile X syndrome) and neurodegenerative (tremor/ataxia syndrome) disorders associated to the 'growth' of a gene]. *Rev Neurol* **40**: 431-437.
- Champe, S.P., Kurtz, M.B., Yager, L.N., Butnick, N.J., and Axelrod, D.E. (1981) Spore formation in *Aspergillus nidulans*: In Competence and other developmental processes. In Hohl, H.R., Turian, G. (eds.), *Fungal Spores: Morphogenic Controls*, Academic Press, New York, pp. 255-276.
- Champe, S.P., Nagle, D.L., and Yager, L.N. (1994) Sexual sporulation. *Prog Ind Microbiol* **29**: 429-454.
- Chandra, S., Chen, X., Rizo, J., Jahn, R., and Südhof, T.C. (2003) A broken  $\alpha$ -helix in folded  $\alpha$ -Synuclein. *J Biol Chem* **278**: 15313-15318.
- Chartier-Harlin, M.C., Kachergus, J., Roumier, C., Mouroux, V., Douay, X., Lincoln, S., Levecque, C., Larvor, L., Andrieux, J., Hulihan, M., Waucquier, N., Defebvre, L., Amouyel, P., Farrer, M., and Destée, A. (2004)  $\alpha$ -synuclein locus duplication as a cause of familial Parkinson's disease. *Lancet* **364**: 1167-1169.
- Chen, L., and Feany, M.B. (2005)  $\alpha$ -synuclein phosphorylation controls neurotoxicity and inclusion formation in a *Drosophila* model of Parkinson disease. *Nat Neurosci* **8**: 657-663.
- Chiu, Y.H., Xiang, X., Dawe, A.L., and Morris, N.R. (1997) Deletion of *nudC*, a nuclear migration gene of *Aspergillus nidulans*, causes morphological and cell wall abnormalities and is lethal. *Mol Biol Cell* **8**: 1735-1749.
- Chung, T.L., Hsiao, H.H., Yeh, Y.Y., Shia, H.L., Chen, Y.L., Liang, P.H., Wang, A.H., Khoo, K.H., and Shoen-Lung Li, S. (2004) In vitro modification of human centromere protein CENP-C fragments by small ubiquitin-like modifier (SUMO) protein: definitive identification of the modification sites by tandem mass spectrometry analysis of the isopeptides. *J Biol Chem* **279**: 39653-39662.
- Clutterbuck, A.J. (1974) *Aspergillus nidulans*. In *Handbook of Genetics*. King, R.C. (ed). Plenum, New York, pp. 447-510.
- Conway, K.A., Lee, S.J., Rochet, J.C., Ding, T.T., Harper, J.D., Williamson, R.E., and Lansbury, P.T., Jr. (2000a) Accelerated oligomerization by Parkinson's disease linked  $\alpha$ -synuclein mutants. *Ann N Y Acad Sci* **920**: 42-45.
- Conway, K.A., Lee, S.J., Rochet, J.C., Ding, T.T., Williamson, R.E., and Lansbury, P.T., Jr. (2000b) Acceleration of oligomerization, not fibrillization, is a shared property of both  $\alpha$ -synuclein mutations linked to early-onset Parkinson's disease: implications for pathogenesis and therapy. *Proc Natl Acad Sci USA* **97**: 571-576.
- Conway, K.A., Rochet, J.C., Bieganski, R.M., and Lansbury, P.T., Jr. (2001) Kinetic stabilization of the  $\alpha$ -synuclein protofibril by a dopamine- $\alpha$ -synuclein adduct. *Science* **294**: 1346-1349.

- Cookson, M.R. (2005) The biochemistry of Parkinson's disease. *Annu Rev Biochem* **74**: 29-52.
- Crowther, R.A., Jakes, R., Spillantini, M.G., and Goedert, M. (1998) Synthetic filaments assembled from C-terminally truncated  $\alpha$ -synuclein. *FEBS Lett* **436**: 309-312.
- Cuervo, A.M., and Dice, J.F. (1996) A receptor for the selective uptake and degradation of proteins by lysosomes. *Science* **273**: 501-503.
- Cuervo, A.M., Stefanis, L., Fredenburg, R., Lansbury, P.T., and Sulzer, D. (2004) Impaired degradation of mutant  $\alpha$ -synuclein by chaperone-mediated autophagy. *Science* **305**: 1292-1295.
- Cunniff, J., Chiu, Y.H., Morris, N.R., and Warrior, R. (1997) Characterization of DnudC, the *Drosophila* homolog of an *Aspergillus* gene that functions in nuclear motility. *Mech Dev* **66**: 55-68.
- da Costa, C.A., Ancolio, K., and Checler, F. (2000) Wild-type but not Parkinson's disease-related ala-53  $\rightarrow$  Thr mutant  $\alpha$ -Synuclein protects neuronal cells from apoptotic stimuli. *J Biol Chem* **275**: 24065-24069.
- Davidson, W.S., Jonas, A., Clayton, D.F., and George, J.M. (1998) Stabilization of  $\alpha$ -synuclein secondary structure upon binding to synthetic membranes. *J Biol Chem* **273**: 9443-9449.
- Dawe, A.L., Caldwell, K.A., Harris, P.M., Morris, N.R., and Caldwell, G.A. (2001) Evolutionarily conserved nuclear migration genes required for early embryonic development in *Caenorhabditis elegans*. *Dev Genes Evol* **211**: 434-441.
- De Souza, C.P., Osmani, A.H., Wu, L.P., Spotts, J.L., and Osmani, S.A. (2000) Mitotic histone H3 phosphorylation by the NIMA kinase in *Aspergillus nidulans*. *Cell* **102**: 293-302.
- Desterro, J.M., Thomson, J., and Hay, R.T. (1997) Ubch9 conjugates SUMO but not ubiquitin. *FEBS Lett* **417**: 297-300.
- Desterro, J.M., Rodriguez, M.S., and Hay, R.T. (1998) SUMO-1 modification of I $\kappa$ B $\alpha$  inhibits NF- $\kappa$ B activation. *Mol Cell* **2**: 233-239.
- Desterro, J.M., Rodriguez, M.S., Kemp, G.D., and Hay, R.T. (1999) Identification of the enzyme required for activation of the small ubiquitin-like protein SUMO-1. *J Biol Chem* **274**: 10618-10624.
- Di Monte, D.A. (2003) The environment and Parkinson's disease: is the nigrostriatal system preferentially targeted by neurotoxins? *Lancet Neurol* **2**: 531-538.
- Dice, J.F. (2007) Chaperone-mediated autophagy. *Autophagy* **3**: 295-299.
- Dieckhoff, P., Bolte, M., Sancak, Y., Braus, G.H., and Irniger, S. (2004) Smt3/SUMO and Ubc9 are required for efficient APC/C-mediated proteolysis in budding yeast. *Mol Microbiol* **51**: 1375-1387.
- Dobyns, W.B., Stratton, R.F., and Greenberg, F. (1984) Syndromes with lissencephaly. I: Miller-Dieker and Norman-Roberts syndromes and isolated lissencephaly. *Am J Med Genet* **18**: 509-526.
- Dobyns, W.B., Curry, C.J., Hoyme, H.E., Turlington, L., and Ledbetter, D.H. (1991) Clinical and molecular diagnosis of Miller-Dieker syndrome. *Am J Hum Genet* **48**: 584-594.
- Dobyns, W.B., Reiner, O., Carrozzo, R., and Ledbetter, D.H. (1993) Lissencephaly. A human brain malformation associated with deletion of the *LIS1* gene located at chromosome 17p13. *Jama* **270**: 2838-2842.
- Dorval, V., and Fraser, P.E. (2006) Small ubiquitin-like modifier (SUMO) modification of natively unfolded proteins tau and  $\alpha$ -synuclein. *J Biol Chem* **281**: 9919-9924.

- Dorval, V., and Fraser, P.E. (2007) SUMO on the road to neurodegeneration. *Biochim Biophys Acta* **1773**: 694-706.
- Eckley, D.M., Gill, S.R., Melkonian, K.A., Bingham, J.B., Goodson, H.V., Heuser, J.E., and Schroer, T.A. (1999) Analysis of dynactin subcomplexes reveals a novel actin-related protein associated with the arp1 minifilament pointed end. *J Cell Biol* **147**: 307-320.
- Efimov, V.P., and Morris, N.R. (2000) The LIS1-related NUDF protein of *Aspergillus nidulans* interacts with the coiled-coil domain of the NUDE/RO11 protein. *J Cell Biol* **150**: 681-688.
- Efimov, V.P. (2003) Roles of NUDE and NUDF proteins of *Aspergillus nidulans*: insights from intracellular localization and overexpression effects. *Mol Biol Cell* **14**: 871-888.
- Efimov, V.P., Zhang, J., and Xiang, X. (2006) CLIP-170 homologue and NUDE play overlapping roles in NUDF localization in *Aspergillus nidulans*. *Mol Biol Cell* **17**: 2021-2034.
- Elble, R. (1992) A simple and efficient procedure for transformation of yeasts. *Biotechniques* **13**: 18-20.
- Faulkner, N.E., Dujardin, D.L., Tai, C.Y., Vaughan, K.T., O'Connell, C.B., Wang, Y., and Vallee, R.B. (2000) A role for the lissencephaly gene *LIS1* in mitosis and cytoplasmic dynein function. *Nat Cell Biol* **2**: 784-791.
- Feany, M.B., and Bender, W.W. (2000) A *Drosophila* model of Parkinson's disease. *Nature* **404**: 394-398.
- Feng, Y., Olson, E.C., Stukenberg, P.T., Flanagan, L.A., Kirschner, M.W., and Walsh, C.A. (2000) LIS1 regulates CNS lamination by interacting with mNudE, a central component of the centrosome. *Neuron* **28**: 665-679.
- Fernández-Abalos, J.M., Fox, H., Pitt, C., Wells, B., and Doonan, J.H. (1998) Plant-adapted green fluorescent protein is a versatile vital reporter for gene expression, protein localization and mitosis in the filamentous fungus, *Aspergillus nidulans*. *Mol Microbiol* **27**: 121-130.
- Fischer, R. (2002) Conidiation in *Aspergillus nidulans*. In *Molecular biology of fungal development*. Osiewacz, H.D. (ed). New York, Basel: Marcel Dekker, Inc., pp. 59-86.
- Fischer, R. (2008) Developmental biology. Sex and poison in the dark. *Science* **320**: 1430-1431.
- Forno, L.S. (1996) Neuropathology of Parkinson's disease. *J Neuropathol Exp Neurol* **55**: 259-272.
- Fox, H., Hickey, P.C., Fernandez-Abalos, J.M., Lunness, P., Read, N.D., and Doonan, J.H. (2002) Dynamic distribution of BIMG(PP1) in living hyphae of *Aspergillus* indicates a novel role in septum formation. *Mol Microbiol* **45**: 1219-1230.
- Frasier, M., Walzer, M., McCarthy, L., Magnuson, D., Lee, J.M., Haas, C., Kahle, P., and Wolozin, B. (2005) Tau phosphorylation increases in symptomatic mice overexpressing A30P  $\alpha$ -synuclein. *Exp Neurol* **192**: 274-287.
- Fujiwara, H., Hasegawa, M., Dohmae, N., Kawashima, A., Masliah, E., Goldberg, M.S., Shen, J., Takio, K., and Iwatsubo, T. (2002)  $\alpha$ -Synuclein is phosphorylated in synucleinopathy lesions. *Nat Cell Biol* **4**: 160-164.
- Fukata, M., Watanabe, T., Noritake, J., Nakagawa, M., Yamaga, M., Kuroda, S., Matsuura, Y., Iwamatsu, A., Perez, F., and Kaibuchi, K. (2002) Rac1 and Cdc42 capture microtubules through IQGAP1 and CLIP-170. *Cell* **109**: 873-885.

- Galagan, J.E., Calvo, S.E., Cuomo, C., Ma, L.J., Wortman, J.R., Batzoglou, S., Lee, S.I., Bastürkmen, M., Spevak, C.C., Clutterbuck, J., Kapitonov, V., Jurka, J., Scazzocchio, C., Farman, M., Butler, J., Purcell, S., Harris, S., Braus, G.H., Draht, O., Busch, S., D'Enfert, C., Bouchier, C., Goldman, G.H., Bell-Pedersen, D., Griffiths-Jones, S., Doonan, J.H., Yu, J., Vienken, K., Pain, A., Freitag, M., Selker, E.U., Archer, D.B., Peñalva, M.A., Oakley, B.R., Momany, M., Tanaka, T., Kumagai, T., Asai, K., Machida, M., Nierman, W.C., Denning, D.W., Caddick, M., Hynes, M., Paoletti, M., Fischer, R., Miller, B., Dyer, P., Sachs, M.S., Osmani, S.A., and Birren, B.W. (2005) Sequencing of *Aspergillus nidulans* and comparative analysis with *A. fumigatus* and *A. oryzae*. *Nature* **438**: 1105-1115.
- Garcia-Ranea, J.A., Mirey, G., Camonis, J., and Valencia, A. (2002) p23 and HSP20/ $\alpha$ -crystallin proteins define a conserved sequence domain present in other eukaryotic protein families. *FEBS Lett* **529**: 162-167.
- George, J.M., Jin, H., Woods, W.S., and Clayton, D.F. (1995) Characterization of a novel protein regulated during the critical period for song learning in the zebra finch. *Neuron* **15**: 361-372.
- Giaever, G., Chu, A.M., Ni, L., Connelly, C., Riles, L., Véronneau, S., Dow, S., Lucau-Danila, A., Anderson, K., André, B., Arkin, A.P., Astromoff, A., El-Bakkoury, M., Bangham, R., Benito, R., Brachat, S., Campanaro, S., Curtiss, M., Davis, K., Deutschbauer, A., Entian, K.D., Flaherty, P., Foury, F., Garfinkel, D.J., Gerstein, M., Gotte, D., Güldener, U., Hegemann, J.H., Hempel, S., Herman, Z., Jaramillo, D.F., Kelly, D.E., Kelly, S.L., Kötter, P., LaBonte, D., Lamb, D.C., Lan, N., Liang, H., Liao, H., Liu, L., Luo, C., Lussier, M., Mao, R., Menard, P., Ooi, S.L., Revuelta, J.L., Roberts, C.J., Rose, M., Ross-Macdonald, P., Scherens, B., Schimmack, G., Shafer, B., Shoemaker, D.D., Sookhai-Mahadeo, S., Storms, R.K., Strathern, J.N., Valle, G., Voet, M., Volckaert, G., Wang, C.Y., Ward, T.R., Wilhelmy, J., Winzeler, E.A., Yang, Y., Yen, G., Youngman, E., Yu, K., Bussey, H., Boeke, J.D., Snyder, M., Philippsen, P., Davis, R.W., and Johnston, M. (2002) Functional profiling of the *Saccharomyces cerevisiae* genome. *Nature* **418**: 387-391.
- Giasson, B.I., Uryu, K., Trojanowski, J.Q., and Lee, V.M. (1999) Mutant and wild type human  $\alpha$ -synucleins assemble into elongated filaments with distinct morphologies in vitro. *J Biol Chem* **274**: 7619-7622.
- Giasson, B.I., Duda, J.E., Murray, I.V., Chen, Q., Souza, J.M., Hurtig, H.I., Ischiropoulos, H., Trojanowski, J.Q., and Lee, V.M. (2000) Oxidative damage linked to neurodegeneration by selective  $\alpha$ -synuclein nitration in synucleinopathy lesions. *Science* **290**: 985-989.
- Giasson, B.I., Murray, I.V., Trojanowski, J.Q., and Lee, V.M. (2001) A hydrophobic stretch of 12 amino acid residues in the middle of  $\alpha$ -synuclein is essential for filament assembly. *J Biol Chem* **276**: 2380-2386.
- Gill, G. (2004) SUMO and ubiquitin in the nucleus: different functions, similar mechanisms? *Genes Dev* **18**: 2046-2059.
- Glickman, M.H., and Ciechanover, A. (2002) The ubiquitin-proteasome proteolytic pathway: destruction for the sake of construction. *Physiol Rev* **82**: 373-428.
- Goedert, M. (2001)  $\alpha$ -Synuclein and neurodegenerative diseases. *Nat Rev Neurosci* **2**: 492-501.
- Goldberg, A.L. (2005) Nobel committee tags ubiquitin for distinction. *Neuron* **45**: 339-344.

- Golemis, E., Serebriiskii, I., Finley, J.R., Kolonin, M., Gyuris, J., and Brent, R. (1999a) Interaction trap/two-hybrid system to identify interacting protein, p. 20.1.1-20.1.40. *In* F. M. Ausubel, R. Brent, R. E. Kingston, D. D. Moore, J. G. Seidmann, A. J. Smith, and K. Struhl (ed.), *Current protocols in molecular biology*. John Wiley & Sons, Inc., New York, NY.
- Golemis, E.A., Serebriiskii, I., and Law, S.F. (1999b) The yeast two-hybrid system: criteria for detecting physiologically significant protein-protein interactions. *Curr Issues Mol Biol* **1**: 31-45.
- Guthrie, C., and Fink, G. (1991) Guide to yeast genetics and molecular biology. *Methods Enzymol* **194**: 1-863.
- Hamilton, B.A. (2004)  $\alpha$ -Synuclein A53T substitution associated with Parkinson disease also marks the divergence of Old World and New World primates. *Genomics* **83**: 739-742.
- Han, G., Liu, B., Zhang, J., Zuo, W., Morris, N.R., and Xiang, X. (2001a) The *Aspergillus cytoplasmic* dynein heavy chain and NUDF localize to microtubule ends and affect microtubule dynamics. *Curr Biol* **11**: 719-724.
- Han, K.H., Han, K.Y., Yu, J.H., Chae, K.S., Jahng, K.Y., and Han, D.M. (2001b) The *nsdD* gene encodes a putative GATA-type transcription factor necessary for sexual development of *Aspergillus nidulans*. *Mol Microbiol* **41**: 299-309.
- Hanashima, C., Li, S.C., Shen, L., Lai, E., and Fishell, G. (2004) Foxg1 suppresses early cortical cell fate. *Science* **303**: 56-59.
- Harris, S.D. (1999) Morphogenesis is coordinated with nuclear division in germinating *Aspergillus nidulans* conidiospores. *Microbiology* **145** ( Pt 10): 2747-2756.
- Harris, S.D. (2001) Septum formation in *Aspergillus nidulans*. *Curr Opin Microbiol* **4**: 736-739.
- Harris, T.W., Chen, N., Cunningham, F., Tello-Ruiz, M., Antoshechkin, I., Bastiani, C., Bieri, T., Blasiar, D., Bradnam, K., Chan, J., Chen, C.K., Chen, W.J., Davis, P., Kenny, E., Kishore, R., Lawson, D., Lee, R., Muller, H.M., Nakamura, C., Ozersky, P., Petcherski, A., Rogers, A., Sabo, A., Schwarz, E.M., Van Auken, K., Wang, Q., Durbin, R., Spieth, J., Sternberg, P.W., and Stein, L.D. (2004) WormBase: a multi-species resource for nematode biology and genomics. *Nucleic Acids Res* **32**: D411-417.
- Hashimoto, M., Rockenstein, E., Mante, M., Mallory, M., and Masliah, E. (2001)  $\beta$ -Synuclein inhibits  $\alpha$ -synuclein aggregation: a possible role as an anti-parkinsonian factor. *Neuron* **32**: 213-223.
- Hatten, M.E. (2005) LIS-less neurons don't even make it to the starting gate. *J Cell Biol* **170**: 867-871.
- Hattori, N., and Mizuno, Y. (2004) Pathogenetic mechanisms of parkin in Parkinson's disease. *Lancet* **364**: 722-724.
- Hay, R.T. (2005) SUMO: a history of modification. *Mol Cell* **18**: 1-12.
- He, Q., Cheng, P., Yang, Y., Wang, L., Gardner, K.H., and Liu, Y. (2002) White collar-1, a DNA binding transcription factor and a light sensor. *Science* **297**: 840-843.
- Helmstaedt, K., Laubinger, K., Vosskuhl, K., Bayram, Ö., Busch, S., Hoppert, M., Valerius, O., Seiler, S., and Braus, G.H. (2008) The nuclear migration protein NUDF/LIS1 forms a complex with NUDC and BNFA at spindle pole bodies. *Eukaryot Cell* **7**: 1041-1052.
- Hershko, A., and Ciechanover, A. (1992) The ubiquitin system for protein degradation. *Annu Rev Biochem* **61**: 761-807.

- Hicke, L., and Dunn, R. (2003) Regulation of membrane protein transport by ubiquitin and ubiquitin-binding proteins. *Annu Rev Cell Dev Biol* **19**: 141-172.
- Hirokawa, N., Noda, Y., and Okada, Y. (1998) Kinesin and dynein superfamily proteins in organelle transport and cell division. *Curr Opin Cell Biol* **10**: 60-73.
- Hirotsune, S., Fleck, M.W., Gambello, M.J., Bix, G.J., Chen, A., Clark, G.D., Ledbetter, D.H., McBain, C.J., and Wynshaw-Boris, A. (1998) Graded reduction of Pafah1b1 (Lis1) activity results in neuronal migration defects and early embryonic lethality. *Nat Genet* **19**: 333-339.
- Hodara, R., Norris, E.H., Giasson, B.I., Mishizen-Eberz, A.J., Lynch, D.R., Lee, V.M., and Ischiropoulos, H. (2004) Functional consequences of  $\alpha$ -synuclein tyrosine nitration: diminished binding to lipid vesicles and increased fibril formation. *J Biol Chem* **279**: 47746-47753.
- Hokenson, M.J., Uversky, V.N., Goers, J., Yamin, G., Munishkina, L.A., and Fink, A.L. (2004) Role of individual methionines in the fibrillation of methionine-oxidized  $\alpha$ -synuclein. *Biochemistry* **43**: 4621-4633.
- Holleran, E.A., Tokito, M.K., Karki, S., and Holzbaur, E.L. (1996) Centractin (ARP1) associates with spectrin revealing a potential mechanism to link dynactin to intracellular organelles. *J Cell Biol* **135**: 1815-1829.
- Holleran, E.A., Karki, S., and Holzbaur, E.L. (1998) The role of the dynactin complex in intracellular motility. *Int Rev Cytol* **182**: 69-109.
- Holzbaur, E.L., and Vallee, R.B. (1994) DYNEINS: molecular structure and cellular function. *Annu Rev Cell Biol* **10**: 339-372.
- Hoppert, M., and Holzenburg, A. (1998) Electron microscopy in microbiology, p. 48. *Bios Scientific*, Oxford, United Kingdom.
- Horio, T., and Oakley, B.R. (2005) The role of microtubules in rapid hyphal tip growth of *Aspergillus nidulans*. *Mol Biol Cell* **16**: 918-926.
- Horio, T. (2007) Role of microtubules in tip growth of fungi. *J Plant Res* **120**: 53-60.
- Hsu, L.J., Mallory, M., Xia, Y., Veinbergs, I., Hashimoto, M., Yoshimoto, M., Thal, L.J., Saitoh, T., and Masliah, E. (1998) Expression pattern of synucleins (non-A $\beta$  component of Alzheimer's disease amyloid precursor protein/ $\alpha$ -synuclein) during murine brain development. *J Neurochem* **71**: 338-344.
- Hsu, L.J., Sagara, Y., Arroyo, A., Rockenstein, E., Sisk, A., Mallory, M., Wong, J., Takenouchi, T., Hashimoto, M., and Masliah, E. (2000)  $\alpha$ -Synuclein promotes mitochondrial deficit and oxidative stress. *Am J Pathol* **157**: 401-410.
- Hu, C.D., and Kerppola, T.K. (2003) Simultaneous visualization of multiple protein interactions in living cells using multicolor fluorescence complementation analysis. *Nat Biotechnol* **21**: 539-545.
- Huang, T.T., Wuerzberger-Davis, S.M., Wu, Z.H., and Miyamoto, S. (2003) Sequential modification of NEMO/IKK $\gamma$  by SUMO-1 and ubiquitin mediates NF- $\kappa$ B activation by genotoxic stress. *Cell* **115**: 565-576.
- Hughes, A.J., Daniel, S.E., Ben-Shlomo, Y., and Lees, A.J. (2002) The accuracy of diagnosis of parkinsonian syndromes in a specialist movement disorder service. *Brain* **125**: 861-870.
- Inoue, H., Nojima, H., and Okayama, H. (1990) High efficiency transformation of *Escherichia coli* with plasmids. *Gene* **96**: 23-28.

- Iwata, A., Christianson, J.C., Bucci, M., Ellerby, L.M., Nukina, N., Forno, L.S., and Kopito, R.R. (2005) Increased susceptibility of cytoplasmic over nuclear polyglutamine aggregates to autophagic degradation. *Proc Natl Acad Sci U S A* **102**: 13135-13140.
- Jellinger, K., and Rett, A. (1976) Agyria-pachygyria (lissencephaly syndrome). *Neuropadiatrie* **7**: 66-91.
- Jenco, J.M., Rawlingson, A., Daniels, B., and Morris, A.J. (1998) Regulation of phospholipase D2: selective inhibition of mammalian phospholipase D isoenzymes by  $\alpha$ - and  $\beta$ -synucleins. *Biochemistry* **37**: 4901-4909.
- Jentsch, S., and Pyrowolakis, G. (2000) Ubiquitin and its kin: how close are the family ties? *Trends Cell Biol* **10**: 335-342.
- Johnson, E.S., Schwienhorst, I., Dohmen, R.J., and Blobel, G. (1997) The ubiquitin-like protein Smt3p is activated for conjugation to other proteins by an Aos1p/Uba2p heterodimer. *Embo J* **16**: 5509-5519.
- Johnson, E.S., and Gupta, A.A. (2001) An E3-like factor that promotes SUMO conjugation to the yeast septins. *Cell* **106**: 735-744.
- Johnson, E.S. (2004) Protein modification by SUMO. *Annu Rev Biochem* **73**: 355-382.
- Jones, D., Crowe, E., Stevens, T.A., and Candido, E.P. (2002) Functional and phylogenetic analysis of the ubiquitylation system in *Caenorhabditis elegans*: ubiquitin-conjugating enzymes, ubiquitin-activating enzymes, and ubiquitin-like proteins. *Genome Biol* **3**: RESEARCH0002.
- Jones, M.G. (2007) The first filamentous fungal genome sequences: *Aspergillus* leads the way for essential everyday resources or dusty museum specimens? *Microbiology* **153**: 1-6.
- Käfer, E. (1965) Origins of translocations in *Aspergillus nidulans*. *Genetics* **52**: 217-232.
- Käfer, E. (1977) Meiotic and mitotic recombination in *Aspergillus* and its chromosomal aberrations. *Adv Genet* **19**: 33-131.
- Kagey, M.H., Melhuish, T.A., and Wotton, D. (2003) The polycomb protein Pc2 is a SUMO E3. *Cell* **113**: 127-137.
- Kahyo, T., Nishida, T., and Yasuda, H. (2001) Involvement of PIAS1 in the sumoylation of tumor suppressor p53. *Mol Cell* **8**: 713-718.
- Kamp, F., and Beyer, K. (2006) Binding of  $\alpha$ -synuclein affects the lipid packing in bilayers of small vesicles. *J Biol Chem* **281**: 9251-9259.
- Kanda, S., Bishop, J.F., Eglitis, M.A., Yang, Y., and Mouradian, M.M. (2000) Enhanced vulnerability to oxidative stress by  $\alpha$ -synuclein mutations and C-terminal truncation. *Neuroscience* **97**: 279-284.
- Kapelari, B., Bech-Otschir, D., Hegerl, R., Schade, R., Dumdey, R., and Dubiel, W. (2000) Electron microscopy and subunit-subunit interaction studies reveal a first architecture of COP9 signalosome. *J Mol Biol* **300**: 1169-1178.
- Karcher, R.L., Deacon, S.W., and Gelfand, V.I. (2002) Motor-cargo interactions: the key to transport specificity. *Trends Cell Biol* **12**: 21-27.
- Karki, S., and Holzbaur, E.L. (1995) Affinity chromatography demonstrates a direct binding between cytoplasmic dynein and the dynactin complex. *J Biol Chem* **270**: 28806-28811.
- Karki, S., and Holzbaur, E.L. (1999) Cytoplasmic dynein and dynactin in cell division and intracellular transport. *Curr Opin Cell Biol* **11**: 45-53.
- Kim, H., Han, K., Kim, K., Han, D., Jahng, K., and Chae, K. (2002) The *veA* gene activates sexual development in *Aspergillus nidulans*. *Fungal Genet Biol* **37**: 72-80.

- Kim, M.H., Cooper, D.R., Oleksy, A., Devedjiev, Y., Derewenda, U., Reiner, O., Otlewski, J., and Derewenda, Z.S. (2004) The structure of the N-terminal domain of the product of the lissencephaly gene *Lis1* and its functional implications. *Structure* **12**: 987-998.
- King, S.J., and Schroer, T.A. (2000) Dynactin increases the processivity of the cytoplasmic dynein motor. *Nat Cell Biol* **2**: 20-24.
- King, S.M., Barbarese, E., Dillman, J.F., 3rd, Benashski, S.E., Do, K.T., Patel-King, R.S., and Pfister, K.K. (1998) Cytoplasmic dynein contains a family of differentially expressed light chains. *Biochemistry* **37**: 15033-15041.
- King, S.M. (2000) AAA domains and organization of the dynein motor unit. *J Cell Sci* **113** (Pt 14): 2521-2526.
- Kirk, K.E., and Morris, N.R. (1991) The *tubB*  $\alpha$ -tubulin gene is essential for sexual development in *Aspergillus nidulans*. *Genes Dev* **5**: 2014-2023.
- Kitada, T., Asakawa, S., Hattori, N., Matsumine, H., Yamamura, Y., Minoshima, S., Yokochi, M., Mizuno, Y., and Shimizu, N. (1998) Mutations in the parkin gene cause autosomal recessive juvenile parkinsonism. *Nature* **392**: 605-608.
- Kitagawa, M., Umezu, M., Aoki, J., Koizumi, H., Arai, H., and Inoue, K. (2000) Direct association of LIS1, the lissencephaly gene product, with a mammalian homologue of a fungal nuclear distribution protein, rNUDE. *FEBS Lett* **479**: 57-62.
- Klionsky, D.J., and Kumar, A. (2006) A systems biology approach to learning autophagy. *Autophagy* **2**: 12-23.
- Kolar, M., Punt, P.J., van den Hondel, C.A., and Schwab, H. (1988) Transformation of *Penicillium chrysogenum* using dominant selection markers and expression of an *Escherichia coli lacZ* fusion gene. *Gene* **62**: 127-134.
- Komarova, Y.A., Akhmanova, A.S., Kojima, S., Galjart, N., and Borisy, G.G. (2002) Cytoplasmic linker proteins promote microtubule rescue *in vivo*. *J Cell Biol* **159**: 589-599.
- Kotzbauer, P.T., Trojanowski, J.Q., and Lee, V.M. (2001) Lewy body pathology in Alzheimer's disease. *J Mol Neurosci* **17**: 225-232.
- Krappmann, S., Jung, N., Medic, B., Busch, S., Prade, R.A., and Braus, G.H. (2006) The *Aspergillus nidulans* F-box protein GrrA links SCF activity to meiosis. *Mol Microbiol* **61**: 76-88.
- Krüger, R., Kuhn, W., Müller, T., Voitalla, D., Graeber, M., Kösel, S., Przuntek, H., Epplen, J.T., Schöls, L., and Riess, O. (1998) Ala30Pro mutation in the gene encoding  $\alpha$ -synuclein in Parkinson's disease. *Nat Genet* **18**: 106-108.
- Kurepa, J., Walker, J.M., Smalle, J., Gosink, M.M., Davis, S.J., Durham, T.L., Sung, D.Y., and Vierstra, R.D. (2003) The small ubiquitin-like modifier (SUMO) protein modification system in *Arabidopsis*. Accumulation of SUMO1 and -2 conjugates is increased by stress. *J Biol Chem* **278**: 6862-6872.
- Kuzuhara, S., Mori, H., Izumiyama, N., Yoshimura, M., and Ihara, Y. (1988) Lewy bodies are ubiquitinated. A light and electron microscopic immunocytochemical study. *Acta Neuropathol* **75**: 345-353.
- Lansbury, P.T., Jr. (1999) Evolution of amyloid: what normal protein folding may tell us about fibrillogenesis and disease. *Proc Natl Acad Sci U S A* **96**: 3342-3344.
- Lashuel, H.A., Petre, B.M., Wall, J., Simon, M., Nowak, R.J., Walz, T., and Lansbury, P.T., Jr. (2002)  $\alpha$ -Synuclein, especially the Parkinson's disease-associated mutants, forms pore-like annular and tubular protofibrils. *J Mol Biol* **322**: 1089-1102.

- Lee, J.T., Wheeler, T.C., Li, L., and Chin, L.S. (2007) Ubiquitination of  $\alpha$ -synuclein by Siah-1 promotes  $\alpha$ -synuclein aggregation and apoptotic cell death. *Hum Mol Genet* **17**: 906-17.
- Li, S., Oakley, C.E., Chen, G., Han, X., Oakley, B.R., and Xiang, X. (2005a) Cytoplasmic dynein's mitotic spindle pole localization requires a functional anaphase-promoting complex,  $\gamma$ -tubulin, and NUDF/LIS1 in *Aspergillus nidulans*. *Mol Biol Cell* **16**: 3591-3605.
- Li, S.C., Goto, N.K., Williams, K.A., and Deber, C.M. (1996)  $\alpha$ -helical, but not  $\beta$ -sheet, propensity of proline is determined by peptide environment. *Proc Natl Acad Sci U S A* **93**: 6676-6681.
- Li, W., West, N., Colla, E., Pletnikova, O., Troncoso, J.C., Marsh, L., Dawson, T.M., Jäkälä, P., Hartmann, T., Price, D.L., and Lee, M.K. (2005b) Aggregation promoting C-terminal truncation of  $\alpha$ -synuclein is a normal cellular process and is enhanced by the familial Parkinson's disease-linked mutations. *Proc Natl Acad Sci U S A* **102**: 2162-2167.
- Liani, E., Eyal, A., Avraham, E., Shemer, R., Szargel, R., Berg, D., Bornemann, A., Riess, O., Ross, C.A., Rott, R., and Engelender, S. (2004) Ubiquitylation of synphilin-1 and  $\alpha$ -synuclein by SIAH and its presence in cellular inclusions and Lewy bodies imply a role in Parkinson's disease. *Proc Natl Acad Sci U S A* **101**: 5500-5505.
- Lippa, C.F., Schmidt, M.L., Lee, V.M., and Trojanowski, J.Q. (1999) Antibodies to  $\alpha$ -synuclein detect Lewy bodies in many Down's syndrome brains with Alzheimer's disease. *Ann Neurol* **45**: 353-357.
- Liu, C.W., Corboy, M.J., DeMartino, G.N., and Thomas, P.J. (2003) Endoproteolytic activity of the proteasome. *Science* **299**: 408-411.
- Lo Nigro, C., Chong, C.S., Smith, A.C., Dobyns, W.B., Carrozzo, R., and Ledbetter, D.H. (1997) Point mutations and an intragenic deletion in *LIS1*, the lissencephaly causative gene in isolated lissencephaly sequence and Miller-Dieker syndrome. *Hum Mol Genet* **6**: 157-164.
- Long, X., and Griffith, L.C. (2000) Identification and characterization of a SUMO-1 conjugation system that modifies neuronal calcium/calmodulin-dependent protein kinase II in *Drosophila melanogaster*. *J Biol Chem* **275**: 40765-40776.
- Lücking, C.B., Dürr, A., Bonifati, V., Vaughan, J., De Michele, G., Gasser, T., Harhangi, B.S., Meo, G., Denèfle, P., Wood, N.W., Agid, Y., and Brice, A. (2000) Association between early-onset Parkinson's disease and mutations in the parkin gene. *N Engl J Med* **342**: 1560-1567.
- Malatesta, P., Hack, M.A., Hartfuss, E., Kettenmann, H., Klinkert, W., Kirchhoff, F., and Gotz, M. (2003) Neuronal or glial progeny: regional differences in radial glia fate. *Neuron* **37**: 751-764.
- Maroteaux, L., and Scheller, R.H. (1991) The rat brain synucleins; family of proteins transiently associated with neuronal membrane. *Brain Res Mol Brain Res* **11**: 335-343.
- Martinez-Vicente, M., Tallozy, Z., Kaushik, S., Massey, A.C., Mazzulli, J., Mosharov, E.V., Hodara, R., Fredenburg, R., Wu, D.C., Follenzi, A., Dauer, W., Przedborski, S., Ischiropoulos, H., Lansbury, P.T., Sulzer, D., and Cuervo, A.M. (2008) Dopamine-modified  $\alpha$ -synuclein blocks chaperone-mediated autophagy. *J Clin Invest* **118**: 777-788.
- Marx, J. (2005) Cell biology. SUMO wrestles its way to prominence in the cell. *Science* **307**: 836-839.

- Mateja, A., Cierpicki, T., Paduch, M., Derewenda, Z.S., and Otlewski, J. (2006) The dimerization mechanism of LIS1 and its implication for proteins containing the LisH motif. *J Mol Biol* **357**: 621-631.
- Matsumoto, N., and Ledbetter, D.H. (1999) Molecular cloning and characterization of the human *nudC* gene. *Hum Genet* **104**: 498-504.
- Mayorga, M.E., and Timberlake, W.E. (1990) Isolation and molecular characterization of the *Aspergillus nidulans wa* gene. *Genetics* **126**: 73-79.
- Melchior, F. (2000) SUMO-nonclassical ubiquitin. *Annu Rev Cell Dev Biol* **16**: 591-626.
- Melchior, F., Schergaut, M., and Pichler, A. (2003) SUMO: ligases, isopeptidases and nuclear pores. *Trends Biochem Sci* **28**: 612-618.
- Meluh, P.B., and Koshland, D. (1995) Evidence that the MIF2 gene of *Saccharomyces cerevisiae* encodes a centromere protein with homology to the mammalian centromere protein CENP-C. *Mol Biol Cell* **6**: 793-807.
- Meulmeester, E., and Melchior, F. (2008) Cell biology: SUMO. *Nature* **452**: 709-711.
- Mooney, J.L., and Yager, L.N. (1990) Light is required for conidiation in *Aspergillus nidulans*. *Genes Dev* **4**: 1473-1482.
- Morris, N.R. (1975) Mitotic mutants of *Aspergillus nidulans*. *Genet Res* **26**: 237-254.
- Morris, N.R., Efimov, V.P., and Xiang, X. (1998a) Nuclear migration, nucleokinesis and lissencephaly. *Trends Cell Biol* **8**: 467-470.
- Morris, N.R. (2000) Nuclear migration. From fungi to the mammalian brain. *J Cell Biol* **148**: 1097-1101.
- Morris, S.M., Anaya, P., Xiang, X., Morris, N.R., May, G.S., and Yu-Lee, L. (1997) A prolactin-inducible T cell gene product is structurally similar to the *Aspergillus nidulans* nuclear movement protein NUDC. *Mol Endocrinol* **11**: 229-236.
- Morris, S.M., Albrecht, U., Reiner, O., Eichele, G., and Yu-Lee, L.Y. (1998b) The lissencephaly gene product Lis1, a protein involved in neuronal migration, interacts with a nuclear movement protein, NudC. *Curr Biol* **8**: 603-606.
- Morris, S.M., and Yu-Lee, L.Y. (1998) Expression of RNUDC, a potential nuclear movement protein, in mammalian cells: localization to the Golgi apparatus. *Exp Cell Res* **238**: 23-32.
- Motegi, A., Kuntz, K., Majeed, A., Smith, S., and Myung, K. (2006) Regulation of gross chromosomal rearrangements by ubiquitin and SUMO ligases in *Saccharomyces cerevisiae*. *Mol Cell Biol* **26**: 1424-1433.
- Mukhopadhyay, D., and Dasso, M. (2007) Modification in reverse: the SUMO proteases. *Trends Biochem Sci* **32**: 286-295.
- Murray, I.V., Giasson, B.I., Quinn, S.M., Koppaka, V., Axelsen, P.H., Ischiropoulos, H., Trojanowski, J.Q., and Lee, V.M. (2003) Role of  $\alpha$ -synuclein carboxy-terminus on fibril formation in vitro. *Biochemistry* **42**: 8530-8540.
- Nayak, T., Szewczyk, E., Oakley, C.E., Osmani, A., Ukil, L., Murray, S.L., Hynes, M.J., Osmani, S.A., and Oakley, B.R. (2006) A versatile and efficient gene-targeting system for *Aspergillus nidulans*. *Genetics* **172**: 1557-1566.
- Niethammer, M., Smith, D.S., Ayala, R., Peng, J., Ko, J., Lee, M.S., Morabito, M., and Tsai, L.H. (2000) NUDEL is a novel Cdk5 substrate that associates with LIS1 and cytoplasmic dynein. *Neuron* **28**: 697-711.
- Nishie, M., Mori, F., Fujiwara, H., Hasegawa, M., Yoshimoto, M., Iwatsubo, T., Takahashi, H., and Wakabayashi, K. (2004) Accumulation of phosphorylated  $\alpha$ -synuclein in the brain and peripheral ganglia of patients with multiple system atrophy. *Acta Neuropathol* **107**: 292-298.

- Nishino, M., Kurasawa, Y., Evans, R., Lin, S.H., Brinkley, B.R., and Yu-Lee, L.Y. (2006) NudC is required for Plk1 targeting to the kinetochore and chromosome congression. *Curr Biol* **16**: 1414-1421.
- Noctor, S.C., Flint, A.C., Weissman, T.A., Dammerman, R.S., and Kriegstein, A.R. (2001) Neurons derived from radial glial cells establish radial units in neocortex. *Nature* **409**: 714-720.
- Nogales, E., Whittaker, M., Milligan, R.A., and Downing, K.H. (1999) High-resolution model of the microtubule. *Cell* **96**: 79-88.
- Nonaka, T., Iwatsubo, T., and Hasegawa, M. (2005) Ubiquitination of  $\alpha$ -synuclein. *Biochemistry* **44**: 361-368.
- O'Hara, E.B., and Timberlake, W.E. (1989) Molecular characterization of the *Aspergillus nidulans* *yA* locus. *Genetics* **121**: 249-254.
- Oakley, B.R., and Morris, N.R. (1980) Nuclear movement is  $\beta$ -tubulin-dependent in *Aspergillus nidulans*. *Cell* **19**: 255-262.
- Oakley, B.R. (2004) Tubulins in *Aspergillus nidulans*. *Fungal Genet Biol* **41**: 420-427.
- Okuma, T., Honda, R., Ichikawa, G., Tsumagari, N., and Yasuda, H. (1999) In vitro SUMO-1 modification requires two enzymatic steps, E1 and E2. *Biochem Biophys Res Commun* **254**: 693-698.
- Osmani, A.H., Osmani, S.A., and Morris, N.R. (1990) The molecular cloning and identification of a gene product specifically required for nuclear movement in *Aspergillus nidulans*. *J Cell Biol* **111**: 543-551.
- Outeiro, T.F., and Lindquist, S. (2003) Yeast cells provide insight into  $\alpha$ -synuclein biology and pathobiology. *Science* **302**: 1772-1775.
- Paleologou, K.E., Schmid, A.W., Rospigliosi, C.C., Kim, H.Y., Lamberto, G.R., Fredenburg, R.A., Lansbury, P.T., Jr., Fernandez, C.O., Eliezer, D., Zweckstetter, M., and Lashuel, H.A. (2008) Phosphorylation at Ser-129 but not the phosphomimics S129E/D inhibits the fibrillation of  $\alpha$ -synuclein. *J Biol Chem* **283**: 16895-16905.
- Parkinson, J. (2002) An essay on the shaking palsy. 1817. *J Neuropsychiatry Clin Neurosci* **14**: 223-36; discussion 222.
- Paschal, B.M., and Vallee, R.B. (1987) Retrograde transport by the microtubule-associated protein MAP 1C. *Nature* **330**: 181-183.
- Percy, A.K., and Lane, J.B. (2005) Rett syndrome: model of neurodevelopmental disorders. *J Child Neurol* **20**: 718-721.
- Pichler, A., Gast, A., Seeler, J.S., Dejean, A., and Melchior, F. (2002) The nucleoporin RanBP2 has SUMO1 E3 ligase activity. *Cell* **108**: 109-120.
- Pickart, C.M. (2004) Back to the future with ubiquitin. *Cell* **116**: 181-190.
- Pöggeler, S., Nowrousian, M., and Kück, U. (2006) Fruiting-body development in ascomycetes. In *Mycota, vol. I* Kües, U. and Fischer, R. (eds). Berlin Heidelberg New York: Springer, pp. 325-355.
- Polymeropoulos, M.H., Lavedan, C., Leroy, E., Ide, S.E., Dehejia, A., Dutra, A., Pike, B., Root, H., Rubenstein, J., Boyer, R., Stenroos, E.S., Chandrasekharappa, S., Athanassiadou, A., Papapetropoulos, T., Johnson, W.G., Lazzarini, A.M., Duvoisin, R.C., Di Iorio, G., Golbe, L.I., and Nussbaum, R.L. (1997) Mutation in the  $\alpha$ -synuclein gene identified in families with Parkinson's disease. *Science* **276**: 2045-2047.
- Pontecorvo, G., Roper, J.A., Hemmons, L.M., Macdonald, K.D., and Bufton, A.W. (1953) The genetics of *Aspergillus nidulans*. *Adv Genet* **5**: 141-238.

- Pountney, D.L., Chegini, F., Shen, X., Blumbergs, P.C., and Gai, W.P. (2005) SUMO-1 marks subdomains within glial cytoplasmic inclusions of multiple system atrophy. *Neurosci Lett* **381**: 74-79.
- Probst-Cousin, S., Bergmann, M., Kuchelmeister, K., Schröder, R., and Schmid, K.W. (1996) Ubiquitin-positive inclusions in different types of multiple system atrophy: distribution and specificity. *Pathol Res Pract* **192**: 453-461.
- Punt, P.J., and van den Hondel, C.A. (1992) Transformation of filamentous fungi based on hygromycin B and phleomycin resistance markers. *Methods Enzymol* **216**: 447-457.
- Purschwitz, J., Muller, S., Kastner, C., Schoser, M., Haas, H., Espeso, E.A., Atoui, A., Calvo, A.M., and Fischer, R. (2008) Functional and physical interaction of blue- and red-light sensors in *Aspergillus nidulans*. *Curr Biol* **18**: 255-259.
- Rakic, P. (2003) Developmental and evolutionary adaptations of cortical radial glia. *Cereb Cortex* **13**: 541-549.
- Reiner, O., Carrozzo, R., Shen, Y., Wehnert, M., Faustinella, F., Dobyns, W.B., Caskey, C.T., and Ledbetter, D.H. (1993) Isolation of a Miller-Dieker lissencephaly gene containing G protein  $\beta$ -subunit-like repeats. *Nature* **364**: 717-721.
- Reiner, O., Albrecht, U., Gordon, M., Chianese, K.A., Wong, C., Gal-Gerber, O., Sapir, T., Siracusa, L.D., Buchberg, A.M., Caskey, C.T., and et al. (1995) Lissencephaly gene (*LIS1*) expression in the CNS suggests a role in neuronal migration. *J Neurosci* **15**: 3730-3738.
- Rodriguez, M.S., Desterro, J.M., Lain, S., Midgley, C.A., Lane, D.P., and Hay, R.T. (1999) SUMO-1 modification activates the transcriptional response of p53. *Embo J* **18**: 6455-6461.
- Rosenberger, R.F., and Kessel, M. (1967) Synchrony of nuclear replication in individual hyphae of *Aspergillus nidulans*. *J Bacteriol* **94**: 1464-1469.
- Roth, J., Bendayan, M., Carlemalm, E., Villiger, W., and Garavito, M. (1981) Enhancement of structural preservation and immunocytochemical staining in low temperature embedded pancreatic tissue. *J Histochem Cytochem* **29**: 663-671.
- Saito, Y., Kawashima, A., Ruberu, N.N., Fujiwara, H., Koyama, S., Sawabe, M., Arai, T., Nagura, H., Yamanouchi, H., Hasegawa, M., Iwatsubo, T., and Murayama, S. (2003) Accumulation of phosphorylated  $\alpha$ -synuclein in aging human brain. *J Neuropathol Exp Neurol* **62**: 644-654.
- Saitoh, H., and Hinchey, J. (2000) Functional heterogeneity of small ubiquitin-related protein modifiers SUMO-1 versus SUMO-2/3. *J Biol Chem* **275**: 6252-6258.
- Sambrook, J., Fritsch, E.F., and Maniatis, T. (1989) *Molecular Cloning: A Laboratory Manual*. New York: Cold Spring Harbor Laboratory Press.
- Santangelo, S.L., and Tsatsanis, K. (2005) What is known about autism: genes, brain, and behavior. *Am J Pharmacogenomics* **5**: 71-92.
- Sapir, T., Cahana, A., Seger, R., Nekhai, S., and Reiner, O. (1999) LIS1 is a microtubule-associated phosphoprotein. *Eur J Biochem* **265**: 181-188.
- Sasaki, S., Shionoya, A., Ishida, M., Gambello, M.J., Yingling, J., Wynshaw-Boris, A., and Hirotsune, S. (2000) A LIS1/NUDEL/cytoplasmic dynein heavy chain complex in the developing and adult nervous system. *Neuron* **28**: 681-696.
- Schafer, D.A., Gill, S.R., Cooper, J.A., Heuser, J.E., and Schroer, T.A. (1994) Ultrastructural analysis of the dynactin complex: an actin-related protein is a component of a filament that resembles F-actin. *J Cell Biol* **126**: 403-412.
- Schroer, T.A. (2004) Dynactin. *Annu Rev Cell Dev Biol* **20**: 759-779.

- Schwartz, D.C., and Hochstrasser, M. (2003) A superfamily of protein tags: ubiquitin, SUMO and related modifiers. *Trends Biochem Sci* **28**: 321-328.
- Schwechheimer, C., Serino, G., Callis, J., Crosby, W.L., Lyapina, S., Deshaies, R.J., Gray, W.M., Estelle, M., and Deng, X.W. (2001) Interactions of the COP9 signalosome with the E3 ubiquitin ligase SCFTIR1 in mediating auxin response. *Science* **292**: 1379-1382.
- Seiler, S., Vogt, N., Ziv, C., Gorovits, R., and Yarden, O. (2006) The STE20/germinal center kinase POD6 interacts with the NDR kinase COT1 and is involved in polar tip extension in *Neurospora crassa*. *Mol Biol Cell* **17**: 4080-4092.
- Shimura, H., Schlossmacher, M.G., Hattori, N., Frosch, M.P., Trockenbacher, A., Schneider, R., Mizuno, Y., Kosik, K.S., and Selkoe, D.J. (2001) Ubiquitination of a new form of  $\alpha$ -synuclein by parkin from human brain: implications for Parkinson's disease. *Science* **293**: 263-269.
- Singleton, A.B., Farrer, M., Johnson, J., Singleton, A., Hague, S., Kachergus, J., Hulihan, M., Peuralinna, T., Dutra, A., Nussbaum, R., Lincoln, S., Crawley, A., Hanson, M., Maraganore, D., Adler, C., Cookson, M.R., Muentner, M., Baptista, M., Miller, D., Blancato, J., Hardy, J., and Gwinn-Hardy, K. (2003)  $\alpha$ -Synuclein locus triplication causes Parkinson's disease. *Science* **302**: 841.
- Skromne, I., Sánchez, O., and Aguirre, J. (1995) Starvation stress modulates the expression of the *Aspergillus nidulans* *brlA* regulatory gene. *Microbiology* **141** ( Pt 1): 21-28.
- Smith, W.W., Margolis, R.L., Li, X., Troncoso, J.C., Lee, M.K., Dawson, V.L., Dawson, T.M., Iwatsubo, T., and Ross, C.A. (2005)  $\alpha$ -Synuclein phosphorylation enhances eosinophilic cytoplasmic inclusion formation in SH-SY5Y cells. *J Neurosci* **25**: 5544-5552.
- Southern, E.M. (1975) Detection of specific sequences among DNA fragments separated by gel electrophoresis. *J Mol Biol* **98**: 503-517.
- Spillantini, M.G., Schmidt, M.L., Lee, V.M., Trojanowski, J.Q., Jakes, R., and Goedert, M. (1997)  $\alpha$ -synuclein in Lewy bodies. *Nature* **388**: 839-840.
- Spillantini, M.G., Crowther, R.A., Jakes, R., Cairns, N.J., Lantos, P.L., and Goedert, M. (1998a) Filamentous  $\alpha$ -synuclein inclusions link multiple system atrophy with Parkinson's disease and dementia with Lewy bodies. *Neurosci Lett* **251**: 205-208.
- Spillantini, M.G., Crowther, R.A., Jakes, R., Hasegawa, M., and Goedert, M. (1998b)  $\alpha$ -Synuclein in filamentous inclusions of Lewy bodies from Parkinson's disease and dementia with Lewy bodies. *Proc Natl Acad Sci USA* **95**: 6469-6473.
- Stefanis, L., Larsen, K.E., Rideout, H.J., Sulzer, D., and Greene, L.A. (2001) Expression of A53T mutant but not wild-type  $\alpha$ -synuclein in PC12 cells induces alterations of the ubiquitin-dependent degradation system, loss of dopamine release, and autophagic cell death. *J Neurosci* **21**: 9549-9560.
- Stewart, R.M., Richman, D.P., and Caviness, V.S., Jr. (1975) Lissencephaly and Pachygyria: an architectonic and topographical analysis. *Acta Neuropathol* **31**: 1-12.
- Stinnett, S.M., Espeso, E.A., Cobeño, L., Araújo-Bazán, L., and Calvo, A.M. (2007) *Aspergillus nidulans* VeA subcellular localization is dependent on the importin  $\alpha$  carrier and on light. *Mol Microbiol* **63**: 242-255.
- Su, H.L., and Li, S.S. (2002) Molecular features of human ubiquitin-like SUMO genes and their encoded proteins. *Gene* **296**: 65-73.

- Suzuki, G., Yanagawa, Y., Kwok, S.F., Matsui, M., and Deng, X.W. (2002) *Arabidopsis* COP10 is a ubiquitin-conjugating enzyme variant that acts together with COP1 and the COP9 signalosome in repressing photomorphogenesis. *Genes Dev* **16**: 554-559.
- Swan, A., Nguyen, T., and Suter, B. (1999) *Drosophila* Lissencephaly-1 functions with Bic-D and dynein in oocyte determination and nuclear positioning. *Nat Cell Biol* **1**: 444-449.
- Sweeney, K.J., Prokscha, A., and Eichele, G. (2001) NudE-L, a novel Lis1-interacting protein, belongs to a family of vertebrate coiled-coil proteins. *Mech Dev* **101**: 21-33.
- Tanaka, K., Nishide, J., Okazaki, K., Kato, H., Niwa, O., Nakagawa, T., Matsuda, H., Kawamukai, M., and Murakami, Y. (1999) Characterization of a fission yeast SUMO-1 homologue, pmt3p, required for multiple nuclear events, including the control of telomere length and chromosome segregation. *Mol Cell Biol* **19**: 8660-8672.
- Tanaka, T., Serneo, F.F., Higgins, C., Gambello, M.J., Wynshaw-Boris, A., and Gleeson, J.G. (2004) Lis1 and doublecortin function with dynein to mediate coupling of the nucleus to the centrosome in neuronal migration. *J Cell Biol* **165**: 709-721.
- Tanaka, Y., Engelender, S., Igarashi, S., Rao, R.K., Wanner, T., Tanzi, R.E., Sawa, A., V, L.D., Dawson, T.M., and Ross, C.A. (2001) Inducible expression of mutant  $\alpha$ -synuclein decreases proteasome activity and increases sensitivity to mitochondria-dependent apoptosis. *Hum Mol Genet* **10**: 919-926.
- Tarricone, C., Perrina, F., Monzani, S., Massimiliano, L., Kim, M.H., Derewenda, Z.S., Knapp, S., Tsai, L.H., and Musacchio, A. (2004) Coupling PAF signaling to dynein regulation: structure of LIS1 in complex with PAF-acetylhydrolase. *Neuron* **44**: 809-821.
- Tatham, M.H., Jaffray, E., Vaughan, O.A., Desterro, J.M., Botting, C.H., Naismith, J.H., and Hay, R.T. (2001) Polymeric chains of SUMO-2 and SUMO-3 are conjugated to protein substrates by SAE1/SAE2 and Ubc9. *J Biol Chem* **276**: 35368-35374.
- Tesfagzi, J., Smith-Harrison, W., and Carlson, D.M. (1994) A simple method for reusing western blots on PVDF membranes. *Biotechniques* **17**: 268-269.
- Thomas, B., and Beal, M.F. (2007) Parkinson's disease. *Hum Mol Genet* **16 Spec No. 2**: R183-194.
- Timberlake, W.E. (1990) Molecular genetics of *Aspergillus* development. *Annu Rev Genet* **24**: 5-36.
- Tofaris, G.K., Layfield, R., and Spillantini, M.G. (2001)  $\alpha$ -Synuclein metabolism and aggregation is linked to ubiquitin-independent degradation by the proteasome. *FEBS Lett* **509**: 22-26.
- Tofaris, G.K., Razaq, A., Ghetti, B., Lilley, K.S., and Spillantini, M.G. (2003) Ubiquitination of  $\alpha$ -synuclein in Lewy bodies is a pathological event not associated with impairment of proteasome function. *J Biol Chem* **278**: 44405-44411.
- Tofaris, G.K., and Spillantini, M.G. (2005)  $\alpha$ -synuclein dysfunction in Lewy body diseases. *Mov Disord* **20 Suppl 12**: S37-44.
- Tofaris, G.K., Revesz, T., Jacques, T.S., Papacostas, S., and Chataway, J. (2007) Adult-onset neurodegeneration with brain iron accumulation and cortical  $\alpha$ -synuclein and tau pathology: a distinct clinicopathological entity. *Arch Neurol* **64**: 280-282.
- Tofaris, G.K., and Spillantini, M.G. (2007) Physiological and pathological properties of  $\alpha$ -synuclein. *Cell Mol Life Sci* **64**: 2194-2201.

- Trojanowski, J.Q., and Lee, V.M. (2003) Parkinson's disease and related  $\alpha$ -synucleinopathies are brain amyloidoses. *Ann N Y Acad Sci* **991**: 107-110.
- Tsigelny, I.F., Bar-On, P., Sharikov, Y., Crews, L., Hashimoto, M., Miller, M.A., Keller, S.H., Platoshyn, O., Yuan, J.X., and Masliah, E. (2007) Dynamics of  $\alpha$ -synuclein aggregation and inhibition of pore-like oligomer development by  $\beta$ -synuclein. *Febs J* **274**: 1862-1877.
- Ueda, K., Fukushima, H., Masliah, E., Xia, Y., Iwai, A., Yoshimoto, M., Otero, D.A., Kondo, J., Ihara, Y., and Saitoh, T. (1993) Molecular cloning of cDNA encoding an unrecognized component of amyloid in Alzheimer disease. *Proc Natl Acad Sci U S A* **90**: 11282-11286.
- Ugalde, U. (2006) Autoregulation signals in mycelial fungi. In *The Mycota*, Vol. I. Kues, U., and Fischer, R. (eds). Berlin Heidelberg New York: Springer, pp. 2035-2213.
- Ulmer, T.S., Bax, A., Cole, N.B., and Nussbaum, R.L. (2005) Structure and dynamics of micelle-bound human  $\alpha$ -synuclein. *J Biol Chem* **280**: 9595-9603.
- Uversky, V.N., Li, J., Souillac, P., Millett, I.S., Doniach, S., Jakes, R., Goedert, M., and Fink, A.L. (2002a) Biophysical properties of the synucleins and their propensities to fibrillate: inhibition of  $\alpha$ -synuclein assembly by  $\beta$ - and  $\gamma$ -synucleins. *J Biol Chem* **277**: 11970-11978.
- Uversky, V.N., Yamin, G., Souillac, P.O., Goers, J., Glaser, C.B., and Fink, A.L. (2002b) Methionine oxidation inhibits fibrillation of human  $\alpha$ -synuclein in vitro. *FEBS Lett* **517**: 239-244.
- Vallee, R.B., Wall, J.S., Paschal, B.M., and Shpetner, H.S. (1988) Microtubule-associated protein 1C from brain is a two-headed cytosolic dynein. *Nature* **332**: 561-563.
- Vallee, R.B., and Tsai, J.W. (2006) The cellular roles of the lissencephaly gene *LIS1*, and what they tell us about brain development. *Genes Dev* **20**: 1384-1393.
- Vallim, M.A., Miller, K.Y., and Miller, B.L. (2000) *Aspergillus* SteA (sterile12-like) is a homeodomain-C2/H2-Zn<sup>2+</sup> finger transcription factor required for sexual reproduction. *Mol Microbiol* **36**: 290-301.
- Veith, D., Scherr, N., Efimov, V.P., and Fischer, R. (2005) Role of the spindle-pole-body protein ApsB and the cortex protein ApsA in microtubule organization and nuclear migration in *Aspergillus nidulans*. *J Cell Sci* **118**: 3705-3716.
- Venkatraman, P., Wetzel, R., Tanaka, M., Nukina, N., and Goldberg, A.L. (2004) Eukaryotic proteasomes cannot digest polyglutamine sequences and release them during degradation of polyglutamine-containing proteins. *Mol Cell* **14**: 95-104.
- Verger, A., Perdomo, J., and Crossley, M. (2003) Modification with SUMO. A role in transcriptional regulation. *EMBO Rep* **4**: 137-142.
- Vertegaal, A.C., Ogg, S.C., Jaffray, E., Rodriguez, M.S., Hay, R.T., Andersen, J.S., Mann, M., and Lamond, A.I. (2004) A proteomic study of SUMO-2 target proteins. *J Biol Chem* **279**: 33791-33798.
- Volles, M.J., and Lansbury, P.T., Jr. (2002) Vesicle permeabilization by protofibrillar  $\alpha$ -synuclein is sensitive to Parkinson's disease-linked mutations and occurs by a pore-like mechanism. *Biochemistry* **41**: 4595-4602.
- Wakabayashi, K., Yoshimoto, M., Fukushima, T., Koide, R., Horikawa, Y., Morita, T., and Takahashi, H. (1999) Widespread occurrence of  $\alpha$ -synuclein/NACP-immunoreactive neuronal inclusions in juvenile and adult-onset Hallervorden-Spatz disease with Lewy bodies. *Neuropathol Appl Neurobiol* **25**: 363-368.

- Webb, J.L., Ravikumar, B., Atkins, J., Skepper, J.N., and Rubinsztein, D.C. (2003)  $\alpha$ -Synuclein is degraded by both autophagy and the proteasome. *J Biol Chem* **278**: 25009-25013.
- Welchman, R.L., Gordon, C., and Mayer, R.J. (2005) Ubiquitin and ubiquitin-like proteins as multifunctional signals. *Nat Rev Mol Cell Biol* **6**: 599-609.
- Willins, D.A., Liu, B., Xiang, X., and Morris, N.R. (1997) Mutations in the heavy chain of cytoplasmic dynein suppress the *nudF* nuclear migration mutation of *Aspergillus nidulans*. *Mol Gen Genet* **255**: 194-200.
- Wilson, C.A., Murphy, D.D., Giasson, B.I., Zhang, B., Trojanowski, J.Q., and Lee, V.M. (2004) Degradative organelles containing mislocalized  $\alpha$ - and  $\beta$ -synuclein proliferate in presenilin-1 null neurons. *J Cell Biol* **165**: 335-346.
- Wolkow, T.D., Harris, S.D., and Hamer, J.E. (1996) Cytokinesis in *Aspergillus nidulans* is controlled by cell size, nuclear positioning and mitosis. *J Cell Sci* **109 ( Pt 8)**: 2179-2188.
- Wong, K.H., Todd, R.B., Oakley, B.R., Oakley, C.E., Hynes, M.J., and Davis, M.A. (2008) Sumoylation in *Aspergillus nidulans*: *sumO* inactivation, overexpression and live-cell imaging. *Fungal Genet Biol* **45**: 728-737.
- Wood, S.J., Wypych, J., Steavenson, S., Louis, J.C., Citron, M., and Biere, A.L. (1999)  $\alpha$ -synuclein fibrillogenesis is nucleation-dependent. Implications for the pathogenesis of Parkinson's disease. *J Biol Chem* **274**: 19509-19512.
- Woodcock, D.M., Crowther, P.J., Doherty, J., Jefferson, S., DeCruz, E., Noyer-Weidner, M., Smith, S.S., Michael, M.Z., and Graham, M.W. (1989) Quantitative evaluation of *Escherichia coli* host strains for tolerance to cytosine methylation in plasmid and phage recombinants. *Nucleic Acids Res* **17**: 3469-3478.
- Wright, P.E., and Dyson, H.J. (1999) Intrinsically unstructured proteins: re-assessing the protein structure-function paradigm. *J Mol Biol* **293**: 321-331.
- Wynshaw-Boris, A., and Gambello, M.J. (2001) LIS1 and dynein motor function in neuronal migration and development. *Genes Dev* **15**: 639-651.
- Wynshaw-Boris, A. (2007) Lissencephaly and LIS1: insights into the molecular mechanisms of neuronal migration and development. *Clin Genet* **72**: 296-304.
- Xiang, X., Beckwith, S.M., and Morris, N.R. (1994) Cytoplasmic dynein is involved in nuclear migration in *Aspergillus nidulans*. *Proc Natl Acad Sci U S A* **91**: 2100-2104.
- Xiang, X., Osmani, A.H., Osmani, S.A., Xin, M., and Morris, N.R. (1995a) *NudF*, a nuclear migration gene in *Aspergillus nidulans*, is similar to the human *LIS-1* gene required for neuronal migration. *Mol Biol Cell* **6**: 297-310.
- Xiang, X., Roghi, C., and Morris, N.R. (1995b) Characterization and localization of the cytoplasmic dynein heavy chain in *Aspergillus nidulans*. *Proc Natl Acad Sci U S A* **92**: 9890-9894.
- Xiang, X., and Morris, N.R. (1999) Hyphal tip growth and nuclear migration. *Curr Opin Microbiol* **2**: 636-640.
- Xiang, X., Zuo, W., Efimov, V.P., and Morris, N.R. (1999) Isolation of a new set of *Aspergillus nidulans* mutants defective in nuclear migration. *Curr Genet* **35**: 626-630.
- Xiang, X., and Fischer, R. (2004) Nuclear migration and positioning in filamentous fungi. *Fungal Genet Biol* **41**: 411-419.
- Yager, L.N. (1992) Early developmental events during asexual and sexual sporulation in *Aspergillus nidulans*. *Biotechnology* **23**: 19-41.

- Yamamoto, A., and Hiraoka, Y. (2003) Cytoplasmic dynein in fungi: insights from nuclear migration. *J Cell Sci* **116**: 4501-4512.
- Yamazaki, M., Arai, Y., Baba, M., Iwatsubo, T., Mori, O., Katayama, Y., and Oyanagi, K. (2000)  $\alpha$ -synuclein inclusions in amygdala in the brains of patients with the parkinsonism-dementia complex of Guam. *J Neuropathol Exp Neurol* **59**: 585-591.
- Yeh, E., Yang, C., Chin, E., Maddox, P., Salmon, E.D., Lew, D.J., and Bloom, K. (2000) Dynamic positioning of mitotic spindles in yeast: role of microtubule motors and cortical determinants. *Mol Biol Cell* **11**: 3949-3961.
- Zarranz, J.J., Alegre, J., Gómez-Esteban, J.C., Lezcano, E., Ros, R., Ampuero, I., Vidal, L., Hoenicka, J., Rodriguez, O., Atarés, B., Llorens, V., Gomez Tortosa, E., del Ser, T., Muñoz, D.G., and de Yebenes, J.G. (2004) The new mutation, E46K, of  $\alpha$ -synuclein causes Parkinson and Lewy body dementia. *Ann Neurol* **55**: 164-173.
- Zhang, J., Han, G., and Xiang, X. (2002a) Cytoplasmic dynein intermediate chain and heavy chain are dependent upon each other for microtubule end localization in *Aspergillus nidulans*. *Mol Microbiol* **44**: 381-392.
- Zhang, J., Li, S., Fischer, R., and Xiang, X. (2003) Accumulation of cytoplasmic dynein and dynactin at microtubule plus ends in *Aspergillus nidulans* is kinesin dependent. *Mol Biol Cell* **14**: 1479-1488.
- Zhang, M.Y., Huang, N.N., Clawson, G.A., Osmani, S.A., Pan, W., Xin, P., Razzaque, M.S., and Miller, B.A. (2002b) Involvement of the fungal nuclear migration gene *nudC* human homolog in cell proliferation and mitotic spindle formation. *Exp Cell Res* **273**: 73-84.
- Zhao, Y., Kwon, S.W., Anselmo, A., Kaur, K., and White, M.A. (2004) Broad spectrum identification of cellular small ubiquitin-related modifier (SUMO) substrate proteins. *J Biol Chem* **279**: 20999-21002.
- Zhou, T., Aumais, J.P., Liu, X., Yu-Lee, L.Y., and Erikson, R.L. (2003) A role for Plk1 phosphorylation of NudC in cytokinesis. *Dev Cell* **5**: 127-138.
- Zhu, M., Li, J., and Fink, A.L. (2003) The association of  $\alpha$ -synuclein with membranes affects bilayer structure, stability, and fibril formation. *J Biol Chem* **278**: 40186-40197.
- Zonneveld, B.J. (1977) Biochemistry and ultrastructure of sexual development in *Aspergillus*. In *Genetics and physiology of Aspergillus*. Smith, J.E., and Pateman, J.A. (eds). London: Academic Press, pp. 59-80.





# *Curriculum vitae*

## **Personal details**

Karen Laubinger

born on December 19, 1975

in Rendsburg, Germany

## **Education**

**1982-1986: Primary education**, Grundschule Jevenstedt, Germany

**1986-1996: High School education**, Herderschule Gymnasium, Rendsburg, Germany

**1992-1993: Student exchange** in Llano, Texas, USA

**1997-1999: "Kaufmännische Ausbildung zur Schifffahrtskauffrau"**, Hamburg,  
Germany

## **Scientific background**

**Oct. 1997 – Nov. 2004:** Study of biology at the Georg-August-University Göttingen,  
Germany

**from Jan. 2005:** **Ph.D. student** in the Department of Molecular Microbiology  
and Genetics of Prof. Dr. G. H. Braus at the Institute of  
Microbiology and Genetics, Georg-August-University,  
Göttingen



